UNIVERSITAT POLITÈCNICA DE CATALUNYA
BARCELONATECH
Escola d'Enginyeria de Telecomunicació
i Aeroespacial de Castelldefels

TREBALL DE FI DE GRAU

TFG TITLE: A system to determine the inertia tensor of small satellites

DEGREE: Grau en Enginyeria de Sistemes Aeroespacials

AUTHOR: Marc Gabarró Olsina

ADVISORS: Pilar Gil Pons
Jordi Gutiérrez Cabello

DATE: July 17, 2019

Título: Un sistema para determinar el tensor de inercia de satélites pequeños

Autor: Marc Gabarró Olsina

Directores: Pilar Gil Pons
Jordi Gutiérrez Cabello

Fecha: 17 de julio de 2019

Resumen

Contexto: El control de actitud de un satélite se basa en una determinación precisa de su tensor de inercia, sin embargo, la determinación del tensor de inercia de un sistema complejo, como es el caso de los satélites, escapa por completo a los métodos analíticos. Aunque el tensor de inercia se puede obtener por medio de modelos *CAD*, este método está sujeto a un grado de incertidumbre debido a las aproximaciones requeridas en la definición de materiales y en la geometría de algunos de los dispositivos. Además, el cableado a menudo es difícil de integrar en los diseños *CAD*, e introduce una fuente de error adicional.
Objetivos: En este trabajo de final de grado, proponemos realizar el diseño y el análisis de las bases del funcionamiento de un péndulo de torsión que permite determinar todos los componentes del tensor de inercia de un objeto tipo *CubeSat*, con mayor eficiencia y precisión que la que nos permitiría un análisis de *CAD*.
Metodología: Partimos de una idea general de un péndulo, que incluye un conjunto de partes fijas con función principalmente estructural, y de partes que pueden rotar alrededor de una fibra de torsión, unida a una plataforma sobre la cual se puede situar el *CubeSat* cuyo tensor de inercia deseamos conocer. A partir de las medidas del periodo de rotación de la plataforma podemos determinar de manera sencilla el momento de inercia del conjunto de partes giratorias alrededor del eje de la fibra de torsión. Para realizar el diseño detallado del dispositivo utilizamos el *software* SOLIDWORKS. Para analizar las bases de su funcionamiento utilizamos conocimientos de Mecánica Clásica y Álgebra de matrices de rotación, así como el *software* MATLAB.
Resultados: Hemos diseñado, presentado los planos, y realizado un análisis numérico de estrés sobre el péndulo propuesto. Además hemos completado el desarrollo matemático que permite construir el tensor de inercia del *CubeSat*, a partir de valores individuales de momentos de inercia, derivados de las medidas del periodo de rotación del sistema con distintas orientaciones del *CubeSat*. Finalmente, nuestro cálculo de errores básico muestra que podemos obtener valores de las componentes del tensor de inercia con la precisión deseada, a partir de medidas de periodos factibles.

Title: A system to determine the inertia tensor of small satellites

Author: Marc Gabarró Olsina

Advisors: Pilar Gil Pons
Jordi Gutiérrez Cabello

Date: July 17, 2019

Overview

Context: Attitude control of a satellite relies upon a precise determination of its inertia tensor. However, the determination of the inertia tensor of a complex system, as is the case of satellites, completely escapes analytic methods. Even though the inertia tensor can be obtained by means of CAD models, this method is subject to a degree of uncertainties due to required approximations in the materials definition and the geometry of some components. Furthermore, cabling is often difficult to integrate into CAD designs, which may introduce an additional source of error.
Aims: In this Degree Thesis, we propose the design of a torsion pendulum which will allow us to determine all the components of the inertia tensor of a *CubeSat*-type object. We intend to achieve more efficiency and better accuracy than performing standard CAD simulations.
Methodology: Our starting point is a general idea of a pendulum, Our sketch involves a set of fixed parts, mostly with structural purposes, and a set of mobile parts. The latter must be able to rotate about the axis of a torsion fiber. Besides, it must connect to a platform on top of which the *CubeSat* whose tensor of inertia we intend to determine will be placed. By measuring the period of rotation of the mobile parts (which include the platform and *CubeSat*), it is easy to derive the inertia moment of rotating set about the axis given by the torsion fiber. The detailed design of the pendulum was executed with the *software* SOLIDWORKS. Foundations of Classical Mechanics and rotation matrix Algebra, as well as the *software* MATLAB were required to develop the operation analysis of the proposed pendulum. *Results*: We designed, obtained detailed maps, and developed stress analysis calculations of the pendulum. Besides, we completed the mathematical analysis which allows to build the inertia tensor of a *CubeSat*, by using individual inertia moments, derived from a set of period measurements obtained with different orientations of the *CubeSat*. Finally, we used basic error analysis to show that the components of the inertia tensor can be obtained with the desire precision by using feasible period measurements.

CONTENTS

LIST OF FIGURES

LIST OF TABLES

CHAPTER 1. INTRODUCTION

Nowadays, the inertia tensor of small satellites is often calculated by means of CAD models, as the determination of the tensor of inertia of such complex systems completely escapes analytic methods. However, these tensors are subjected to a small degree of uncertainty, as CAD simulations can not be precise enough to perfectly simulate the complex insides of the satellites, which include irregular elements such as electronic components, cables or batteries. Hence, we always get a small error in the inertia tensor calculation, which is one of the main inputs for the attitude control system. Along the present chapter we briefly estate the aims of this degree thesis, describe the different types of small satellites and the new technologies they use, and focus on a special type of picosatellites, the *CubeSats*.

1.1. *CubeSat* Standard

The *CubeSat* Standard was proposed in 1999 by Jordi Puig-Suari (California Polytechnic University) and Robert Twiggs (Stanford University) as a learning project devoted to the design and construction of satellites in shorter timescales and with lower budgets. As soon as 2001, students from Aalborg University (Denmark) started the first communication *CubeSat* satellite design (1). Later on, many universities from all around the world started similar projects to design and construct *CubeSats*. The number of these projects just kept growing with time: by 2015 more than one hundred *CubeSats* had been launched and the pace is increasing: the launches performed in the first 7 months of 2016 already outnumbered the total in 2015, and in 2018 the total number of *CubeSats* reached the 1,000 mark.

The development of *CubeSats* has not been restricted to academic usage but, instead, many have been designed and manufactured for commercial exploitation. Currently, several companies (including giants as Amazon and Space X) are planning the launch of constellations of *CubeSats* to provide Earth observation data and Internet of the Thing connectivity from remote locations.

Space agencies have also realized the importance of *CubeSats* in education; in 2010, National Aeronautics and Space Administration (NASA) started the *CubeSat* Launch Initiative (2) to launch, free of cost, *CubeSats* manufactured by educational and non-profit institutions. These launches were executed either as rocket's auxiliary payloads, or from the International Space Station. In 2015 NASA started an even more ambitious project: the Cube Quest Challenge (3), to encourage *CubeSat* missions beyond LEO Orbit and, eventually, near and beyond the Moon. The European Space Agency (ESA) also launched the Fly Your Satellite program (4), intended to provide students with assistance in the design, construction and launch of *CubeSats* as an auxiliary payload of the rocket *Vega*.

Additionally, June last 17th, 2019 three *CubeSats* were ejected from the International Space Station (ISS) for a mission called BIRDS-3, sponsored by the United Nations Office for Outer Space Affairs. These three 1U *CubeSats* were released into low Earth orbit as part of a program that helps developing countries to build and operate their first satellites. Its final goal is to open the advantages of space utilization to countries with no access to standard satellites, as well as to promote space education in these countries.

Figure 1.1: *Bird CubeSats* released in low Earth orbit. (Image credit: NASA).

CubeSats are satellites created as a simple but realistic basic design for students to adapt, construct, test and, eventually, launch into low Earth Orbit (LEO Orbit) and operate in space (5). The standard 1U (1 unit) *CubeSat* design consists of $10\times10\times11.35$ cm^3 box; if need arise, several of these units can be combined to form a larger satellite. Each unit has a mass of at most 1.33 kg, and its design specifications seek to fulfill many goals. Its simplified cubical structure allows *CubeSats* to be considered as a fully functional low cost satellite by its design and manufacturing. *CubeSats* from 1U (single unit) to 3U (three units) share a common base of 10×10 cm^2 and thus can be launched by a common deployment system, such as the Poly-Picosatellite Orbital Deployer (P-POD), which fits in almost every rocket as a secondary payload. This avoids the need to design –and qualify– a specific interface with the launcher, and then waives an expensive satellite procedure with its concomitant bureaucracy and mission inconveniences.

CubeSats often use commercial off-the-shelf (COTS) components for their electronics and internal design and structure. This fact allows *CubeSats* to use affordable and fully functional technologies which have been developed over these last years, for instance, *Arduino* open-source hardware, software and micro-controllers, which are reliable to be used in space missions. An open source *Arduino*-based *CubeSat*, christened *ArduSat*, containing a set of *Arduino* boards and sensors, has already been designed. It is intended to allow the general public to use data gathered in space for their own creative purposes. Besides this, a myriad of affordable components can be purchased off-the-self in order to create a tailored *CubeSat*, such as solar panels, communication devices, power and attitude control systems among many others.

As happens in many cases, CAD programs allow to draw most of the properties (mass, position, materials) of the different components, and ultimately provide the inertia tensor of the system. Nevertheless, when the satellite is built, some uncertainties on the positioning of the devices may result in small changes in the inertia tensor. An even more relevant situation is related with the cabling of the satellite, that is very often overlooked in CAD designs. This situation calls for an independent way to determine experimentally the inertia tensor.

1.2. Torsion pendulum

As we have seen, *CubeSats* are becoming very important space assets, and will be more so in the near future. Therefore, in this thesis we will focus our efforts in designing a tool that permits us to determine the inertia tensor of small satellites. After a revision of the different methods available for this purpose, we have chosen a torsion pendulum by its simplicity and low cost.

This torsion pendulum must ultimately allow to obtain the inertia tensor of a *CubeSat*. The tensor of inertia of the satellite must be determined with a very high accuracy because it is required to determine the torque needed for a desired angular acceleration about a rotational axis. In other words, the inertia tensor is a necessary ingredient of the attitude control of a rigid body.

The torsion pendulum and similar tools designed to calculate inertia tensors already exist. A good review can be found in Szöke and Horváth (6) were several such systems are discussed. Of course, there are other kinds of physical pendulums, like the five-wire torsion pendulum of Stanford University (7) or triple-wire torsional pendulum (8).

Prior to the design process, we make a theoretical analysis of the torsion pendulum on the bases of first principles of Classical Mechanics. Our actual design has been largely influenced by the torsion pendulum built and used at Samara University (Russia). To perform our design we use the SOLIDWORKS CAD software.

1.3. Project structure

This thesis is structured as follows. Chapter 2 summarizes all the theoretical analysis required to understand a damped torsion pendulum, the basics of rotation dynamics, and the procedures to determine all the components of the inertia tensor of a given rigid solid.

Once the theoretical background of the torsion pendulum is understood, in chapter 3 we describe the SOLIDWORKS CAD software and how it works. In the same chapter, we also describe the design process of the torsion pendulum using SOLIDWORKS. This kind of software allows users to perform a high number of trial and error tests prior to obtaining the desired design. This chapter, therefore, describes which criteria have been followed in order to get to the final pendulum design.

Of course, once the design for the torsion pendulum has been decided, we must test if that design is suitable for the environment in which the pendulum will eventually operate, as well as its resistance to the weight of the satellites whose inertia tensor we intend to determine. Hence, in Chapter 4 we check if the design of chapter 3 is correct or must be modified.

In Chapter 5 we theoretically determine the inertia tensor of the oscillatory components of the pendulum, which is necessary to find the inertia tensor of the satellite, as we will see during this degree thesis. Then, in Chapter 6 we show how to calculate the inertia tensor of the satellite, and how this aforementioned inertia tensor of the oscillatory components of the pendulum affect the inertia tensor calculation of the satellite. We also make a simple error analysis of the results to determine, to first approximation, the required accuracy in the determination of the period of oscillation.

To sum up, in chapter 7 we discuss the main results of this thesis, as well as possible improvements to the pendulum and future tasks that would be required for an efficient use of this facility.

CHAPTER 2. THEORETICAL ANALYSIS

A *torsion pendulum* undergoes an oscillatory motion caused by the restoring force provided by a torsion fiber. In this Chapter we describe the properties of the oscillation and present the relation between the oscillation period and the characteristics of the device. We also give an overview of the physical meaning and the calculation of the tensor of inertia, as well as a summary of Euler equations, critical for the understanding of 3-dimensional rotation. The information we present here was compiled from Classical Mechanics textbooks, (9), (10).

2.1. The torsion pendulum

Besides a restoring torque proportional to the rotated angle (-$b\,\theta$), real torsion fibers experience the effect of friction proportional to the time variation of the angle (-$b_f\dot{\theta}$). Therefore, the equation of motion for an extended object of moment of inertia I along the axis of the torsion fiber ($\sum \tau^{ext} = I\,\ddot{\theta}$), with both τ and I given with respect to the same point, is:

$$-b\theta - b_f\,\dot{\theta} = I\,\ddot{\theta} \implies \ddot{\theta} + \frac{b_f}{I}\,\dot{\theta} + \frac{b}{I}\,\theta = 0$$

Rewriting $\gamma = \frac{b_f}{I}$ (the friction constant of the oscillator), $\omega_0 = \sqrt{\frac{b}{I}}$ (its natural frequency), and solving the above differential equation for the case $\gamma < \omega_0$, we get the solution for the motion of underdamped oscillators:

$$\theta = \theta_0\, e^{-\gamma t}\cos(\omega t + \zeta) \tag{2.1}$$

Where: $\omega = \sqrt{\omega_0^2 - \gamma^2}$ is the actual angular frequency of the system, t is the time, θ_0 is the maximum amplitude of the oscillation, and ζ is its phase. θ_0 and ζ are to be determined as functions of the initial conditions in each case. Note that the condition $\gamma < \omega_0$ can be easily achieved by choosing a torsion fiber with suitable properties. We impose it because we are interested in pendulums able to undergo many oscillations before their amplitude decreases significantly. An example of underdamped oscillator is shown in Figure 2.1.

The result above shows that the angular frequency of oscillation ω is constant, and will only depend on the properties of the device. This means that by adequately measuring oscillations periods ($T = \frac{\omega}{2\pi}$), we can obtain properties of the system under study and, in particular, information leading to the tensor of inertia. Besides, the amplitude of the oscillation will exponentially decrease with time ($\propto e^{-\gamma t}$). Therefore we are interested in devices with relatively low γ.

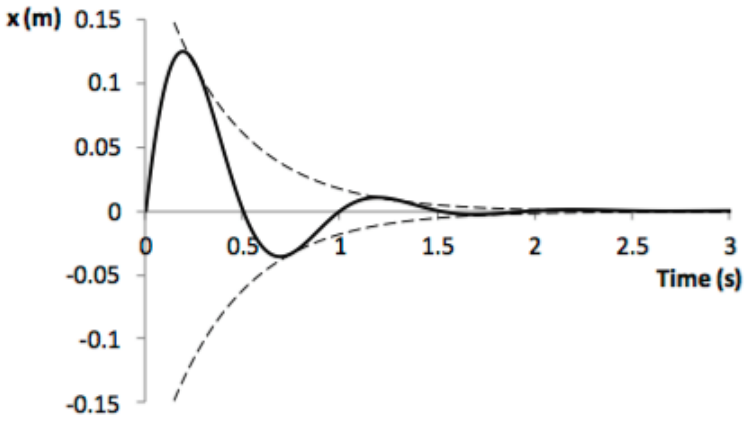

Figure 2.1: Example of an underdamped system graph

2.2. Fundamentals of rotation in 3 dimensions

2.2.1. Concept of rigid body

A *rigid body* consists of an arbitrary number of particles such that their relative distances remain constant. Therefore, the entire mass distribution in space of a solid rigid will remain constant.

A rigid body can be composed of a finite number *N* of individual particles of mass $(m_i,\ i = 1,\ldots,N)$. In such case, we refer to the rigid body as a *discrete mass distribution*, and its total mass M can be expressed as:

$$M = \sum_{i=1}^{N} m_i \tag{2.2}$$

Alternatively, a rigid body can consist of continuous medium composed of infinitesimal mass elements, dm occupying infinitesimal volumes dV, so that we can define a density function ρ (not necessarily constant throughout the body), that follows the relation $\rho = \frac{dm}{dV}$. in this case we will refer to a *continuous mass distribution*, and its total mass can be expressed as:

$$M = \int \rho \, dV \tag{2.3}$$

2.2.2. Angular momentum and tensor of inertia for a system of particles

The angular momentum is a physical magnitude which represents the rotational momentum of a rotating body. It plays a role in rotating systems analogous to that of linear momentum in systems undergoing translations.

Angular momentum must always be referred to a certain point O in space (typically, the origin of a frame of reference, or the centre of mass of the system). If a particle of mass m_i

has velocity $\vec{v}_i$, its linear momentum will of course be $\vec{p}_i = m_i\vec{v}_i$. If the position of m_i with respect to O is $\vec{r}$, , the angular momentum of m_i will be the cross product:

$$\vec{L}_i = \vec{r}_i \wedge \vec{p}_i = m_i\, \vec{r}_i \wedge \vec{v}_i \tag{2.4}$$

The angular momentum of an entire system composed of N point-like masses will be:

$$\vec{L} = \sum_{i=1}^{N} m_i\, \vec{r}_i \wedge \vec{v}_i = \sum_{i=1}^{N} m_i\, \vec{r}_i \wedge (\vec{\omega} \wedge \vec{r}_i) \tag{2.5}$$

where $\omega\ (rad/s)$ is the angular velocity of the system in the considered frame of reference.

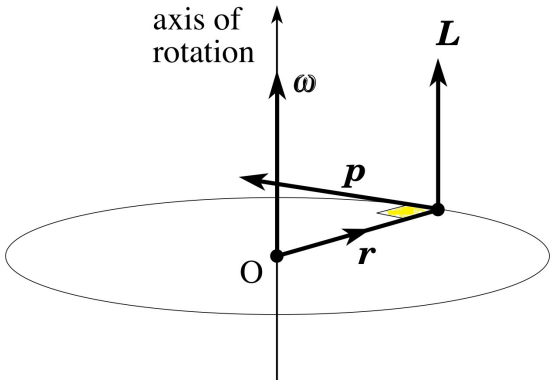

Figure 2.2: Relation between angular momentum ($\vec{L}$), position vector of the particle ($\vec{r}$), and linear momentum, ($\vec{p}$). Note that, in general, $\vec{L}$ will not always be parallel to the angular velocity of the particle $\vec{\omega}$.

Using the relation: $\vec{A} \wedge (\vec{B} \wedge \vec{A}) = (\vec{A} \cdot \vec{A})\, \vec{B} - (\vec{A} \cdot \vec{B})\, \vec{A}$, we can rewrite:

$$\vec{L} = \sum_{i=1}^{N} m_i \left[(\vec{r}_i \cdot \vec{r}_i)\, \vec{\omega} - (\vec{\omega} \cdot \vec{r}_i)\, \vec{r}_i \right] \tag{2.6}$$

The angular momentum vector for the system in Cartesian coordinates (L_x, L_y, L_z) is expressed as:

$$\vec{L} = L_x\, \vec{i} + L_y\, \vec{j} + L_z\, \vec{k}$$

Using that:

$$\vec{r} = x\, \vec{i} + y\, \vec{j} + z\, \vec{k}$$

$$\vec{\omega} = \omega_x\, \vec{i} + \omega_y\, \vec{j} + \omega_z\, \vec{k}$$

$$\Longrightarrow \vec{r} \cdot \vec{r} = x_i^2 + y_i^2 + z_i^2 \quad ; \quad \vec{\omega} \cdot \vec{r} = \omega_x\, x_i + \omega_y\, y_i + \omega_z\, z_i$$

The general expression for the angular momentum for the axis x is:

$$L_x = \sum_{i=1}^{N} m_i \left[(x_i^2 + y_i^2 + z_i^2)\, \omega_x - (\omega_x x_i + \omega_y y_i + \omega_z z_i)\, x_i) \right]$$

$$\Longrightarrow \sum_{i=1}^{N} m_i \left[(y_i^2 + z_i^2)\, \omega_x - x_i\, t\, y_i\, \omega_y - x_i\, z_i\, \omega_z \right]$$

Analogously:

$$L_y = \sum_{i=1}^{N} m_i \left[(x_i^2 + z_i^2)\, \omega_y - x_i\, y_i\, \omega_x - y_i\, z_i\, \omega_z \right]$$

$$L_z = \sum_{i=1}^{N} m_i \left[(x_i^2 + y_i^2)\, \omega_z - y_i\, z_i\, \omega_y - x_i\, z_i\, \omega_x \right]$$

Which can be written as:

$$\begin{bmatrix} L_x \\ L_y \\ L_z \end{bmatrix} = \underbrace{\begin{bmatrix} \sum_{i=1}^{N} m_i (y_i^2 + z_i^2) & -\sum_{i=1}^{N} m_i x_i\, y_i & -\sum_{i=1}^{N} m_i x_i y_i \\ -\sum_{i=1}^{N} m_i x_i y_i & \sum_{i=1}^{N} m_i (x_i^2 + z_i^2) & -\sum_{i=1}^{N} m_i y_i z_i \\ -\sum_{i=1}^{N} m_i x_i z_i & -\sum_{i=1}^{N} m_i y_i z_i & \sum_{i=1}^{N} m_i (x_i^2 + y_i^2) \end{bmatrix}}_{\{I\}} \begin{bmatrix} \omega_x \\ \omega_y \\ \omega_z \end{bmatrix} \tag{2.7}$$

Where the matrix $\{I\}$ is the tensor of inertia. It is a generalized version of the moment of inertia, and therefore it represents the resistance (or inertia) of systems to change its state of rotation. Note that:

(i) The diagonal elements of the tensor of inertia (I_{ii}) are the moments of inertia

(ii) The off-diagonal elements of the tensor of inertia, I_{ij} with $i \neq j$ are the products of inertia

If we now consider a continuous distribution instead of a discrete distribution, we can rewrite by analogy:

$$m_i \longrightarrow dm$$

$$\sum_{i=1}^{N} \longrightarrow \int_M$$

Therefore, the moments of inertia will be:

$$I_{xx} = \textstyle\sum_{i=1}^{N} m_i\, (y_i^2 + z_i^2) \Longrightarrow I_{xx} = \int (y^2 + z^2)\, dm$$
$$I_{yy} = \textstyle\sum_{i=1}^{N} m_i\, (x_i^2 + z_i^2) \Longrightarrow I_{yy} = \int (x^2 + z^2)\, dm$$
$$I_{zz} = \textstyle\sum_{i=1}^{N} m_i\, (x_i^2 + y_i^2) \Longrightarrow I_{zz} = \int (x^2 + y^2)\, dm$$

And the products of inertia will be:

$$I_{xy} = -\textstyle\sum_{i=1}^{N} m_i\, x_i y_i = I_{y,x} \Longrightarrow I_{x,y} = -\int xy\, dm = I_{yx}$$
$$I_{xz} = -\textstyle\sum_{i=1}^{N} m_i\, x_i z_i = I_{zx} \Longrightarrow I_{xz} = -\int xz\, dm = I_{zx}$$
$$I_{yz} = -\textstyle\sum_{i=1}^{N} m_i\, y_i z_i = I_{zy} \Longrightarrow I_{yz} = -\int yz\, dm = I_{zy}$$

The kinetic energy due to the rotation of an object expressed in terms of the tensor of inertia is given by:

$$K_{\text{rotation}} = \frac{1}{2}\,\vec{\omega}^{T}\,\underbrace{I\,\vec{\omega}}_{\vec{L}} \Longrightarrow K_{\text{rotation}} = \frac{1}{2}\,\vec{\omega}\,\vec{L} \tag{2.8}$$

Note that, just as the moment of inertia relevant for rotation about a fixed axis, was given for a specific object and a specific axis, the tensor of inertia is given for a specific object and for a specific frame of reference (origin and set of Cartesian axes which follow the right hand's rule).

By construction, the tensor of inertia is real and symmetric ($I_{ij} = I_{ji}$), and thus it can always be diagonalized. Mathematically, the results of the diagonalization of a 3×3 matrix is a set of *3 eigenvalues* and *3 eigenvectors*. From the physical point of view, it means that we can always find a set of perpendicular axes (with directions given by the *eigenvectors*) such that the tensor of inertia in that set of axes will be diagonal. The corresponding moments of inertia of the new diagonal tensor will be the *eigenvalues*. Note that, after the diagonalization process, the origin of the frame of reference remains constant, and the set of axes which makes a tensor of inertia diagonal is referred to as a set of *Principal Axes of inertia*. It can be naturally inferred that for an arbitrary object and an arbitrary point in space, we can always find a set of *3 principal axes of inertia* with origin at the given arbitrary point, and such that the object will be able to rotate with constant ω around any of these axis without the need of external torques. Actually, in such case, the angular momentum vector will be parallel to the angular velocity: $\vec{\omega} \parallel \vec{L}$.

2.2.3. Steiner's (parallel axis) theorem in matrix form

The theorem in its 1-dimensional formulation proves that, given an axis which passes through the center of mass of a solid, and another axis parallel to the first one, the moment of inertia of both axes are related as as follows:

$$I_{\text{P}} = I_{\text{G}} + m\,d^2 \qquad \text{(1D)} \tag{2.9}$$

Where I_{G} Is the moment of inertia of the solid given for an axis going through the center of mass, I_{P} is the moment of inertia of the solid given for the parallel axis, m is the solid mass and d is the perpendicular distance between the two axes.

Steiner's theorem in its 3-dimensional version can be written as:

$$\{I_{\text{P}}\} = \{I_{\text{G}}\} + m \begin{bmatrix} y^2+z^2 & -x\,y & -x\,z \\ -y\,x & x^2+z^2 & -y\,z \\ -z\,x & -z\,y & x^2+y^2 \end{bmatrix} \qquad \text{(3D)} \tag{2.10}$$

Where:

(i) I_{G} is the tensor of inertia of the solid given for a frame of reference centred at the center of mass of a solid, $FRCM$.

(ii) I_{P} is the tensor of inertia of the solid given for a frame of reference parallel to the $FRCM$, FRP.

(iii) m is the mass of the solid.

(iv) x, y and z are the coordinates of the origin of FRP with respect to $FRCM$.

2.2.4. Rotation matrices:

Rotation matrices can be active (as below), or passive (inverting the matrices below). An active matrix transform a vector by rotating it. A passive matrix leaves the vector unchanged and, instead, rotates the frame of reference accordingly.

A rotation matrix of an angle θ about the X axis is:

$$\text{About x axis:} \qquad R_x(\theta) = \begin{bmatrix} 1 & 0 & 0 \\ 0 & \cos\theta & -\sin\theta \\ 0 & \sin\theta & \cos\theta \end{bmatrix} \tag{2.11}$$

A rotation matrix of an angle θ about the Y axis is:

$$\text{About y axis:} \qquad R_y(\theta) = \begin{bmatrix} \cos\theta & 0 & \sin\theta \\ 0 & 1 & 0 \\ -\sin\theta & 0 & \cos\theta \end{bmatrix} \tag{2.12}$$

A rotation matrix of an angle θ about the Z axis is:

$$\text{About z axis:} \qquad R_z(\theta) = \begin{bmatrix} \cos\theta & -\sin\theta & 0 \\ \sin\theta & \cos\theta & 0 \\ 0 & 0 & 1 \end{bmatrix} \tag{2.13}$$

We can apply a rotation matrix R on a vector $\vec{v}$ as follows:

$$\vec{v}_{rotated} = R\,\vec{v}$$

We can apply two consecutive rotations (first rotation R_1 and then R_2) as follows:

$$\vec{v}_{rotated} = R_2\,R_1\,\vec{v}$$

Rotation matrices are orthogonal, and thus their inverse is equal to their transposed form: $R^{-1} = R^T$. Matrices form a non-Abelian group with the product, therefore the product of matrices is non-commutative. This means that the order in which we apply matrix rotations does matter.

$$\vec{v}_{rotated} = R_2\,R_1\,\vec{v} \neq R_1\,R_2\,\vec{v}$$

Just as with vectors, rotation matrices can be applied on other matrices and, specifically, can be applied to the tensor of inertia $\{I\}$:

$$\{I\} = R\,\{I\}\,R^T$$

2.2.5. Euler's equations

Let us recall that the tensor of inertia of a body depends on the mass distribution of the body itself with respect to the system of reference with which tensor of inertia has been calculated. If we choose a fixed frame of reference, as the body moves, its tensor of inertia will change. However, if we consider a system of reference which is attached to the body, the tensor of inertia will remain constant, regardless the motion of the body.

We can use this fact and the relation between the time variation of the angular momentum $\vec{L}$ (in fixed system of reference SR) and the time variation of the angular momentum $\vec{L}^*$ (in the rotating system of reference SR):

$$\underbrace{\frac{d\vec{L}}{dt}}_{\text{Time variation in non-rotating SR}} = \underbrace{\frac{d^*\vec{L}}{dt}}_{\text{Time variation in rotating SR}} + \vec{\omega}\wedge\vec{L} \tag{2.14}$$

According to Newton's second law for rotating objects:

$$\frac{d\vec{L}}{dt} = \underbrace{\vec{\tau}}_{\text{sum of all external torques}} = \begin{bmatrix} \tau_1 \\ \tau_2 \\ \tau_3 \end{bmatrix} \tag{2.15}$$

We also know that $\vec{L} = \{I\}\ \vec{\omega}$ because $\{I\}$ is constant in the system of reference that rotates with the body. Besides, it is clever to chose a frame of reference attached to the body which is also a system of principal axes of inertia, so that the associated tensor of inertia will be diagonal. The unitary vectors associated to this frame of reference will be $\{\vec{e_1}, \vec{e_2}, \vec{e_3}\}$), and we will use the standard notation x$\Longleftrightarrow$1, y$\Longleftrightarrow$2, z$\Longleftrightarrow$3. Then we can express:

$$\frac{d^*\vec{L}}{dt} = \{I\}\ \dot{\vec{\omega}} = \begin{bmatrix} I_1\,\dot{\omega}_1 \\ I_1\,\dot{\omega}_2 \\ I_3\,\dot{\omega}_3 \end{bmatrix} \tag{2.16}$$

Therefore we can write:

$$\vec{\tau} = \frac{d\vec{L}}{dt} = \{I\}\ \dot{\vec{\omega}} + \vec{\omega}\wedge(\{I\}\ \vec{\omega}), \tag{2.17}$$

with:

$$\vec{\omega}\wedge(\{I\}\ \vec{\omega}) = \begin{bmatrix} \vec{i} & \vec{j} & \vec{k} \\ \omega_1 & \omega_2 & \omega_3 \\ I_1\,\omega_1 & I_2\,\omega_2 & I_3\,\omega_3 \end{bmatrix} =$$

$$= (I_3 - I_2)\,\omega_2\,\omega_3\,\vec{i} + (I_1 - I_3)\,\omega_1\,\omega_3\,\vec{j} + (I_2 - I_1)\,\omega_1\,\omega_2\,\vec{k}$$

Therefore:

$$\begin{aligned} \tau_1 &= I_1\,\dot{\omega}_1 + (I_3 - I_2)\,\omega_3\,\omega_2 \\ \tau_2 &= I_2\,\dot{\omega}_2 + (I_1 - I_3)\,\omega_1\,\omega_2 \\ \tau_3 &= I_3\,\dot{\omega}_3 + (I_2 - I_1)\,\omega_2\,\omega_1 \end{aligned} \tag{2.18}$$

The former are the so-called Euler equations for rotation, and are the key to understand 3-dimensional rotation. Usually, if the body rotates about a fixed point $\Longrightarrow$ The origin of the SR' is at that point. If the body is unconstrained can move freely $\Longrightarrow$ The origin of the SR' is taken at the center of mass of the body.

It is easy to prove that, unless external torques are applied, the body can only rotate with constant ω about a principal axis of inertia.

Proof:

$\vec{\tau} = \{I\}\ \dot{\vec{\omega}} + \vec{\omega} \wedge (\{I\}\ \vec{\omega}) \Longrightarrow$ Therefore, if $\vec{\omega}$ is constant $\Longrightarrow \vec{\tau} = \vec{\omega} \wedge (\{I\}\ \vec{\omega})$

Under these conditions $\vec{\tau} = \vec{0} \Longleftrightarrow \vec{\omega} \wedge (\{I\}\ \vec{\omega}) = 0 \Longleftrightarrow \vec{\omega}\ ||\ \{I\}\ \vec{\omega} = \vec{L}$

This will only happen when $\vec{\omega}$ goes along a principal axis of inertia, as we wanted to prove.

CHAPTER 3. SOLIDWORKS AND PENDULUM DESIGN

This Chapter describes the design of the torsion pendulum. In the first section we outline the most relevant aspects of the design software we use, SOLIDWORKS. The second section is devoted to present and justify the characteristics of the pendulum components.

For the sake of clarity, we firstly present the preliminary concept design for our physical torsion pendulum. We divide its components in two different parts, the **oscillatory components**, which oscillate together with the torsion fiber, and the non-oscillatory **fixed components**. Figure 3.1 shows the initial sketch we proposed. Red-colored parts correspond to the fixed and white-colored parts correspond to the oscillatory components. A laser emitter is to be placed in the arm (c') attached to the *CubeSat* platform (f). The laser beam must point exactly to the detector placed in the arm (c) of the fixed column (b) when the pendulum is at rest. Once the device is set in motion, the platform (f) together with the arm (c') will rotate with period T about the axis given by the torsion fiber (d). Every time the laser beam points to the detector half a period $T/2$ will be measured.

Once the pendulum design is completed with SOLIDWORKS, it can be eventually built (some components could be 3D printed), calibrated and used to obtain the tensor of inertia of *CubeSat*-like objects. We defer the construction process to a future work.

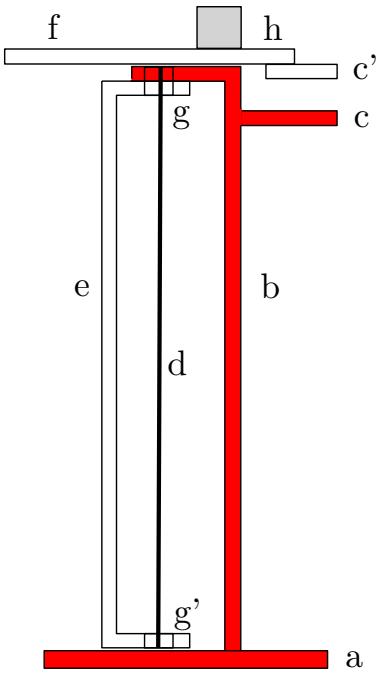

Figure 3.1: Preliminary sketch of the torsion pendulum: Supporting base (**a**); fixed support column (**b**); fixed arm aimed to hold sensor (**c**); torsion fiber (**d**); oscillatory support column (**e**); oscillatory satellite platform (**f**); arm attached to platform, aimed to hold laser (**c'**); bearings (**g and g'**); *CubeSat* whose tensor of inertia we intend to measure (not part of the pendulum itself, **h**). The oscillatory part of the system is supposed to rotate about the axis of the torsion fiber.

3.1. SOLIDWORKS CAD Software

SOLIDWORKS is a solid modeling software; it works by means of parametric feature-based approaches to create models which can be assembled in more complex shapes and 3D bodies.

Solid modeling is based on a consistent set of principles for analytical and numerical modelling of 3D solids. The most salient advantage that solid modeling presents in front of related areas such as geometric modeling and computer graphics is the emphasis that can be obtained on physical fidelity. The use of solid modeling techniques allows to perform complex engineering calculations automatically during the design process. Simulation, planning and verification of the processes such as machining and assembly are some of the multiple advantages this technology presents. Moreover, solid modeling covers a wide range of manufacturing applications such as sheet metal manufacturing, injection molding, welding and, more recently, additive manufacturing or 3D printing.

Apart from manufacturing, solid modeling techniques allow rapid prototyping, digital data archival, reverse engineering and mechanical analysis using finite elements, motion planning and kinematic and dynamic analysis of structures and mechanisms. These features are the most interesting aspects for us in order to choose SOLIDWORKS as our CAD model software.

3.1.1. Bases of 3D design

SOLIDWORKS allows users to create 2D sketches in a plane or in space. It can be composed of any kind of 2D shapes (composed of arcs, lines or points in the plane). Then, in order to completely define our shape in the plane we can add relations to define attributes such as dimensions in the International System of Units, tangency, parallelism, perpendicularity and concentricity can be added to completely define the sketch.

2D sketches can be transformed into 3D solids by means of different operations. The most commonly used features are to *extrude* (add material to) or *cut* (remove material from), the shape of the designed sketch. Moreover, non-sketch based features can also be performed, such as *fillets, chamfers, shells*, material definitions, etc. which are tools provided by the software itself. Solids can also be emptied in order to reduce component masses. By means of an *assembly* we can impose relations which will allow to unite a number of 3D elements into one single composed solid.

3.1.2. Simulations

SOLIDWORKS also provides a simulation package licensed by the labs of the EETAC. It provides structural analysis tools which, by means of the Finite Element Analysis (FEA) method, is able to simulate the realistic physical behavior of an object by virtually testing CAD models. This package provides us with linear, non-linear static and dynamic analysis capabilities that will be used to test our pendulum.

The most interesting simulations for this project will be related to frequency and dynamic analysis, aimed to check the conditions in which the pendulum will operate and to obtain its tensor of inertia.

3.2. Pendulum design

We now describe each of the different solid components we designed with SOLIDWORKS. Once assembled, they compose the final shape of the torsion pendulum. The dimensions of the different solids will be provided in 3D Cartesian coordinates (x,y,z) and, unless otherwise indicated, in centimeters.

The material chosen for the pendulum is 1060 aluminium alloy because of its good relation between mechanical properties and density (2700 kg/m^3), which makes it one of the most interesting materials we can use. Note that both resistance and lightness are critical for the good performance of our system.

The final design of the pendulum looks actually very similar to our initial idea (see Figure 3.1). However, along the design process, and as described in the following sections, we made decisions intended to optimize the final result. Note that both design particularities such as specific dimensions are chosen arbitrarily; therefore, there are many reasonable alternatives to our proposed design.

3.2.1. Supporting Base

The base of our pendulum is intended to fulfill two purposes: first, it must be a firm support for our system, and second, it must perform as well as possible in neutralizing environmental vibrations (such as steps, traffic,...) which might cause undesired oscillations. Vibrations can actually be an important source of noise which might compromise the validity of our measurements, and thus we must try and limit their effects as much as possible.

We chose a square shape both because of its good vibration resistance, and because it is very easy to build, from the constructive point of view. It consists of a 50×50 cm slab which is extruded 5 cm, so that the final dimensions of the solid are [50, 50, 5] cm. We added 4 drill holes to the 3D extrude in order to allow anchoring of the pendulum onto the ground. Holes are ISO M20 margin and were placed close to each corner of the platform in order to provide a reasonable stress distribution. This holes will be done at a 5 cm distance in both axis x and y from the corners. We also used the *shell* feature, with uniform thickness, in order to empty the base and make it lighter and easier to transport, in case we desire to move the pendulum. Its mass after being emptied is of 15.05 kg and the final design can be seen in the Figure 3.2.

The chosen dimensions for the supporting base can also be seen in Figure A.2 of Appendix A, together with the multi-view projection and the detailed blueprints for the component.

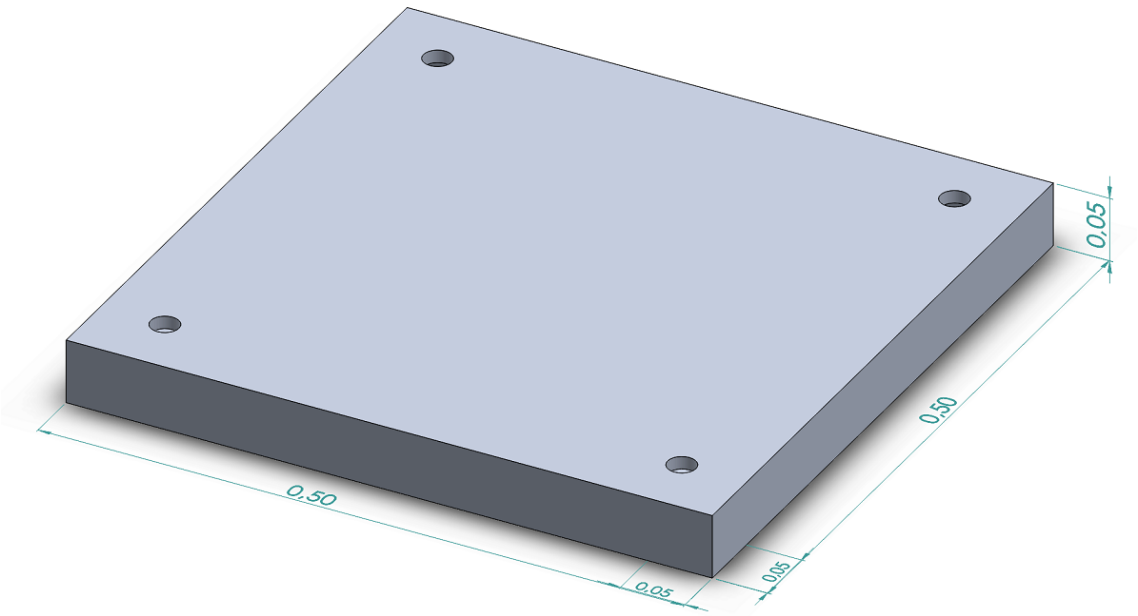

Figure 3.2: Floor Supporting Base (dimensions in meters)

3.2.2. Oscillatory Satellite Platform and oscillatory arm with laser

The *CubeSat* platform is aimed to hold *CubeSats* from 1U (approximately, cubes of side 10 cm) to 3U (dimension $10\times10\times33$ cm), and thus we opted for a flattened cuboid of dimensions (50 cm, 50 cm, 1 cm). It is completely free to rotate around the axis of rotation given by the torsion fiber axis. Besides, we tried to minimize friction with the other parts of the pendulum.

The mass of the *CubeSat* platform is 6.58 kg, and just as the rest of oscillating components, it is aimed to be as light as possible, while keeping the required structural properties. As we will see in Chapter 4, keeping the oscillating components as light as possible is relevant in order to achieve the required accuracy in tensor of inertia component determination.

The platform must be able to hold the *CubeSats* in many different positions with respect to the rotation axis given by the torsion fiber. In this way, additional period measurements (and thus more accurate determinations of the tensor of inertia) can be made. Therefore, we introduced a 9×9 mesh of holes with 5 cm separation between their centres. 79 holes are circular, with 1 cm diameter and the 2 remaining holes are hexagonal. The circular holes are aimed to screw the *CubeSat* onto the platform, whereas the 2 remaining hexagonal holes allow two screw positions of the platform with respect to the oscillating column. The hexagonal shape ensures that the platform will not be unscrewed from the oscillating column during rotations. One of the hexagonal holes is located at the center of the plate and the other one at a 10 cm distance, as can be seen in Figure 3.3, and in further detail in Figure 3.4. The chosen dimensions for the oscillatory satellite platform can also be seen in Figure A.2 of Appendix A, together with the multi-view projection and the detailed blueprints for the component.

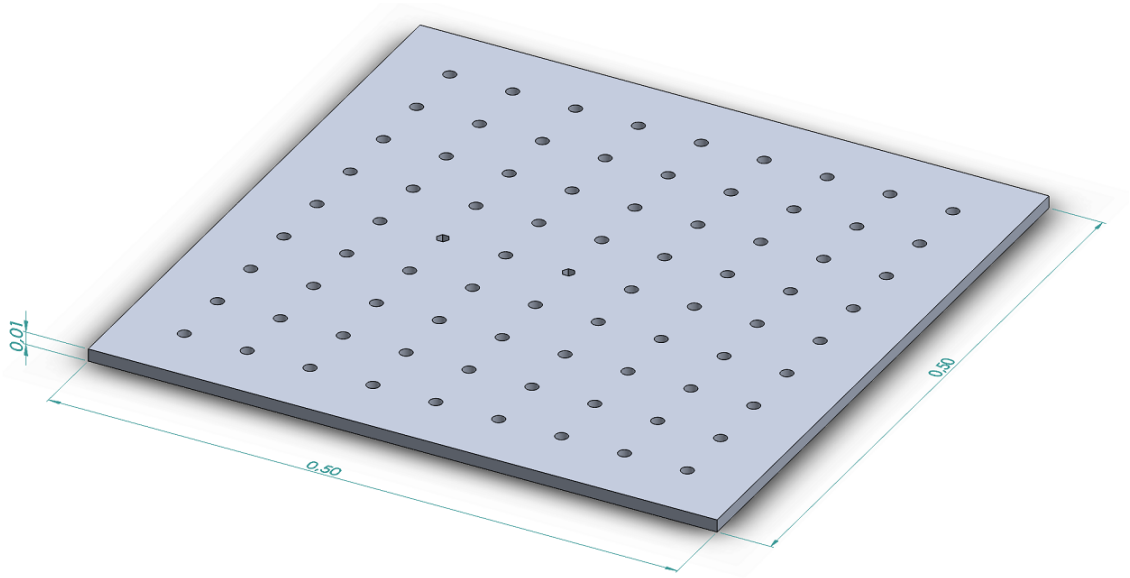

Figure 3.3: Oscillatory Satellite Platform (dimensions in m).

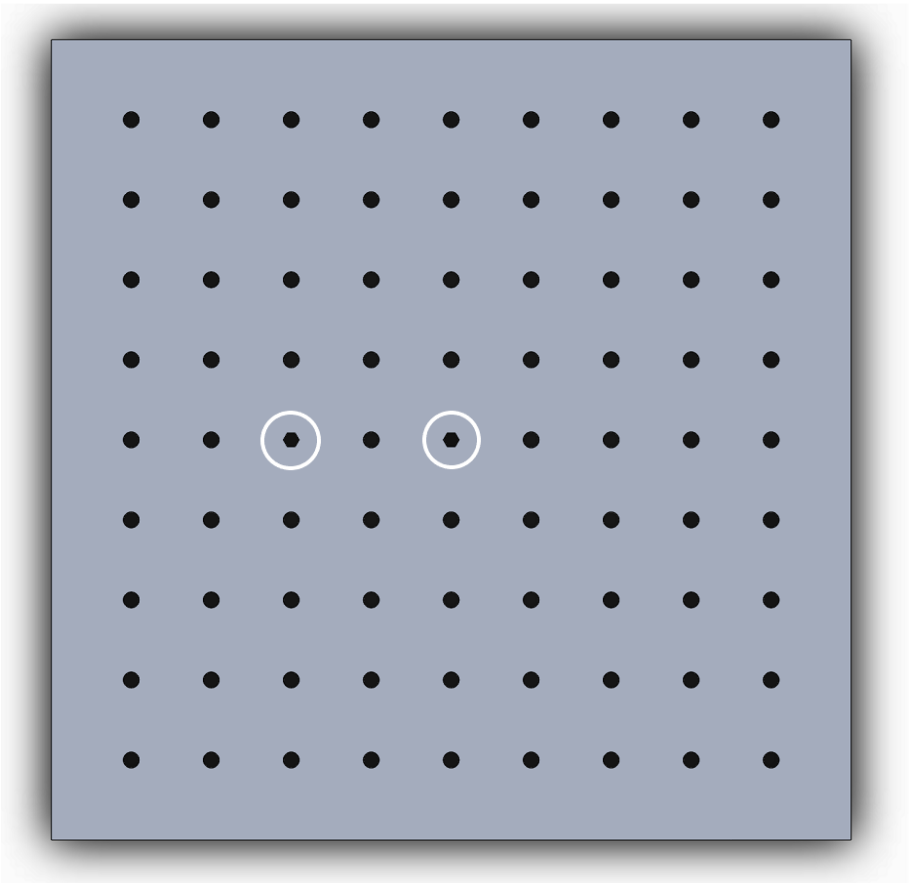

Figure 3.4: Oscillatory Satellite Platform. Hexagonal holes are highlighted with white circles.

An arm must be attached to the *CubeSat* platform in order to hold a laser emitter. The arm will be screwed to the oscillatory satellite platform through the upper cylinder that can be

seen in Figure 3.5, and the laser will be fixed to the arm through the lower cylinder shown in the same figure. The beam will aim directly to the laser sensor held by the fixed support column when the pendulum is at rest. Once the pendulum is oscillating, every time the beam is directly over the sensor, half a period ($T/2$) will be measured by the detector.

Once more, as this arm is one of the oscillatory parts, it is important to design it as light as possible. Therefore, even though its mass is very low, we can further reduce it by applying the *shell* feature with uniform thickness, so that the mass of material used is reduced. In this way, the final mass becomes about 0.14 kg. The chosen dimensions for the oscillatory arm with laser can also be seen in Figure A.3 in Appendix A together with the multi-view projection and the detailed blueprints for the component.

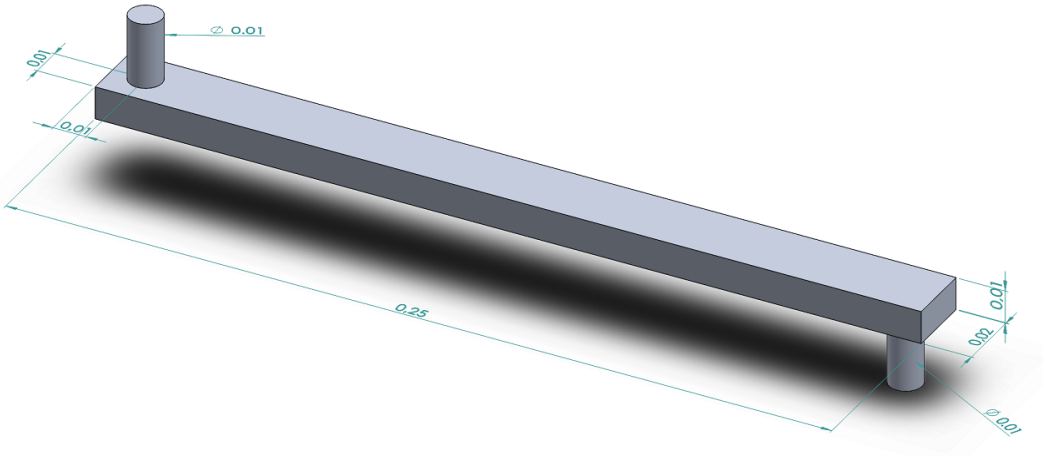

Figure 3.5: Oscillatory Arm With Laser

3.2.3. Torsion Fiber

The torsion fiber is a critical component in the torsion pendulum because it is the one that excites the oscillatory motion which will allow us to calculate the inertia tensors of the satellites. This motion will be transmitted to the oscillatory components of the pendulum, such as the satellite platform and the oscillatory support column (see Section 3.2.5.). The dimensions of the torsion fiber will be of 2 mm of diameter and 1.21 m height, and it will be made of steel, thus its resulting mass will be 10.26 g. The chosen dimensions for the torsion fiber can also be seen in Figure A.4 and in Appendix A together with the multi-view projection and the detailed blueprints for the component. For the sake of clarity, in the different Figures we have exaggerated the diameter by a factor of 5.

The upper end of the fiber will be solidly attached to the oscillating support platform, and the lower part of the fiber will be fixed directly to the supporting base of the pendulum (so at rest). Torsion will be produced by rotating the *CubeSat* support platform perpendicularly to the axis of the fiber. The purpose of the two supporting columns described hereunder is to liberate the torsion fiber from any compression effort, because it has a very bad resistance to compression.

Figure 3.6: Torsion Fiber (dimensions in cm); for the sake of clarity we have exaggerated the diameter by a factor 5.

3.2.4. Fixed Support Column and sensor holder

The main purposes of the fixed column, (b, see Figure 3.1), is to release the torsion fiber from any compression caused by the masses placed above it, namely, the oscillatory satellite platform (f), the arm with the laser (c'), and the *CubeSat* itself (h). We also intended to make it both resistant and as light as possible, so the SOLIDWORKS *shell* feature was applied. For the sake of design simplicity, this fixed column (b) was assembled to the sensor arm (c).

The fixed column, to be welded to the ground platform (a), has a C-shape with an additional arm (c) aimed to hold a sensor (see Figure 3.7). It has a 4 cm diameter hole in each of the short parts of the C-shape. The fixed parts of the bearings (see Section 3.2.6.) are to be welded to these holes, whereas the mobile part of the bearings are to be connected to the oscillating column (e). The two small holes (drill ISO M10) in the arm allow two positions for the sensor, which provide flexibility regarding the position of the *CubeSat's* platform (h) during measurements. Data from the sensor can be transmitted to a PC or laptop, for instance, through a standard USB cable.

The total mass of the column is 15.16 kg. The different plans that describe the solid and the dimensions chosen for the fixed support column of the pendulum can be seen in Figure A.5 in Appendix A, together with the multi-view projection and the detailed blueprints for

the component.

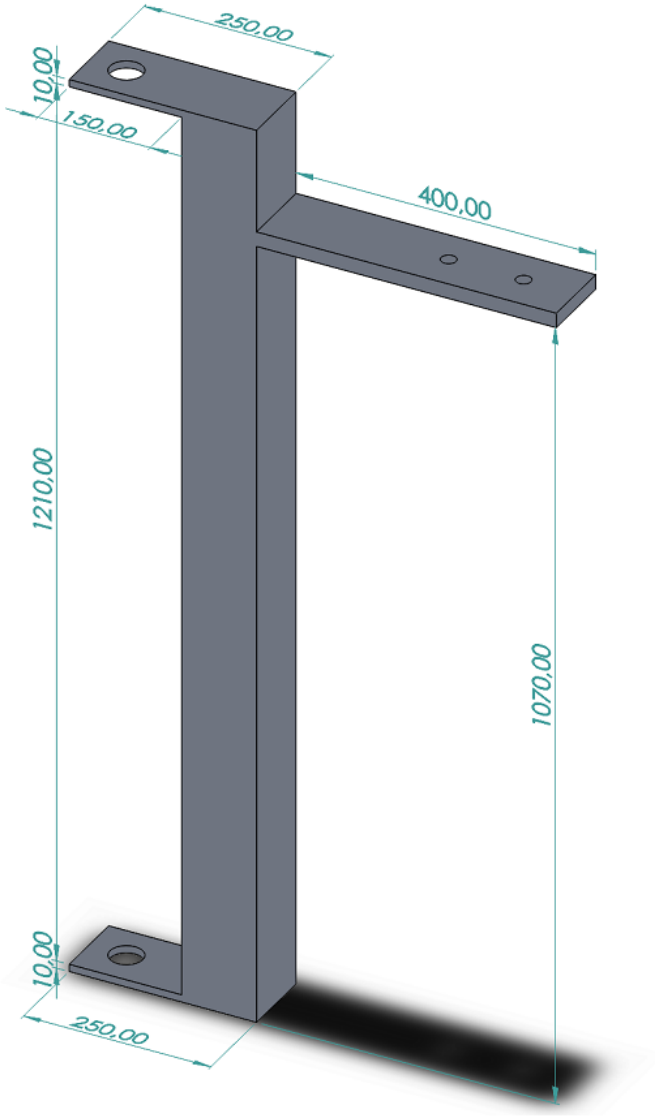

Figure 3.7: Fixed Support Column and sensor holder (dimensions in mm)

3.2.5. Oscillatory Support Column

The oscillatory support column has the same purpose as the fixed support column, which is to release the torsion fiber from compression. Besides, it must hold to the satellite platform and allow its rotation about the axis given by the torsion fiber. As this is an oscillating component, it must be as light as possible. Therefore, it has a C-shape, as the fixed column, but with cylindrical section (see Figure 3.8). It was designed to be hollow, by using the *shell* feature in SOLIDWORKS. Its final mass is of 4.75 kg, and its dimensions are shown in Figure A.6 of Appendix A, together with the multi-view projection and the detailed blueprints for the component.

This support column will be screwed by the top to the oscillatory satellite platform through the upper cylindrical piece shown in Figure 3.8. This cylindrical piece has an hexagonal

hole which will allow to screw the column to the *CubeSat* platform, and avoid unscrewing during rotation. It will also be united to the mobile inner part of the top bearing and to the torsion fiber. The torsion fiber will go through the small circular hole at the lower part of the oscillating column, to be ultimately attached to the ground platform. A cylindrical piece identical to the one at the top, can be found at the lower end of this column, and is to be welded to the inner part of lower bearing.

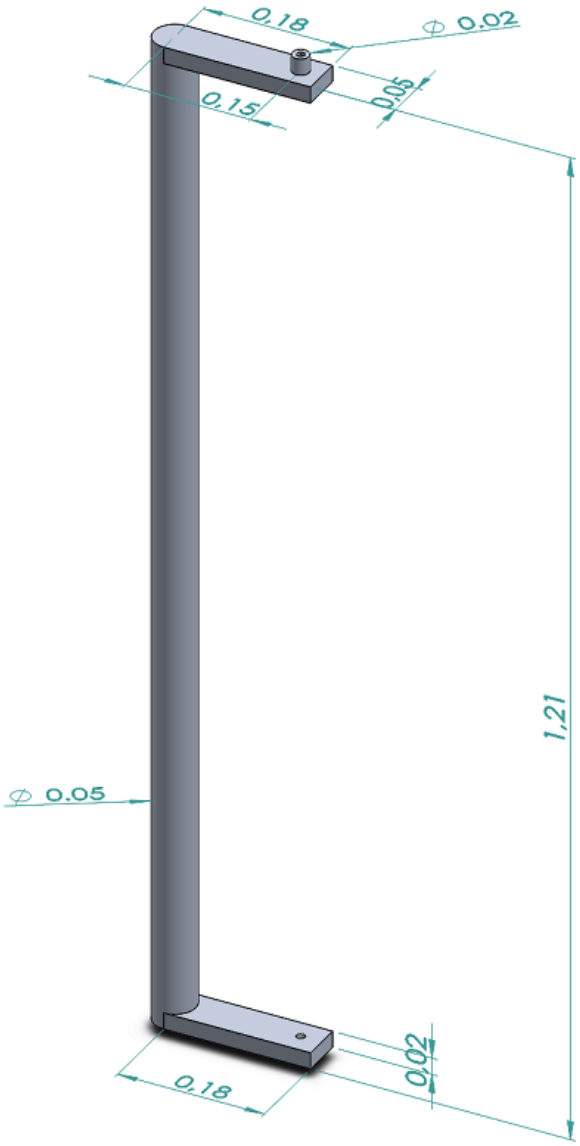

Figure 3.8: Oscillatory Support Column (dimensions in m)

3.2.6. Lower and Upper Bearings

The bearings (g, g') play a key role in this design, as they transmit the oscillatory motion produced by the torsion fiber to the satellite platform with the lowest possible friction. From the structural point of view, they connect the oscillatory parts of the pendulum to the fixed ones.

Two identical bearings, as in Figure 3.9, are required: both will be attached to the fixed column by its outer cylinder, one will be placed under the satellite platform (f). The other bearing will be placed on the top of the supporting base (a). These bearings together with the torsion fiber will be the only pendulum components made of steel. The dimensions chosen for both bearings can be seen in Figure A.7 of Appendix A together with the multi-view projection and the detailed blueprints for the component.

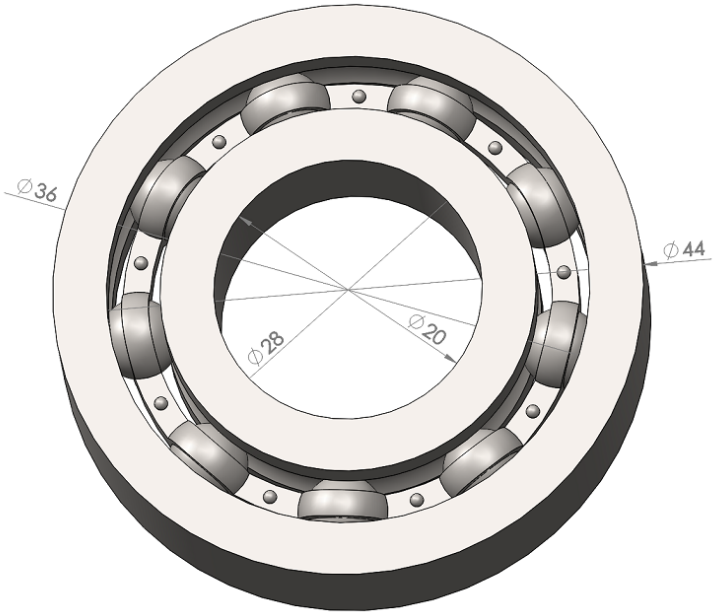

Figure 3.9: Bearing (dimensions in cm)

The bearings are composed of an outer cylindrical ring, which will be welded to the fixed column, and an inner part, composed of an inner cylindrical ring and 9 small spheres. This inner part is aimed to rotate jointly with the oscillating part of the pendulum. Therefore, both bearings are simultaneously both fixed components and oscillatory. The total mass of one bearing is about 64.12 g.

3.3. Complete pendulum assembly

At this point we summarize the relations between the different parts of the torsion pendulum, described in the previous subsections, and present the general aspect of the assembled device (see Figures 3.10). As explained in section 3.2.2., we will be able to place the oscillatory satellite platform in two different positions. The general view of the complete pendulum assembly depending on the position of the oscillatory satellite platform is shown in Figure 3.11. Table 3.1 compiles the physical properties of the different solids which compose the pendulum.

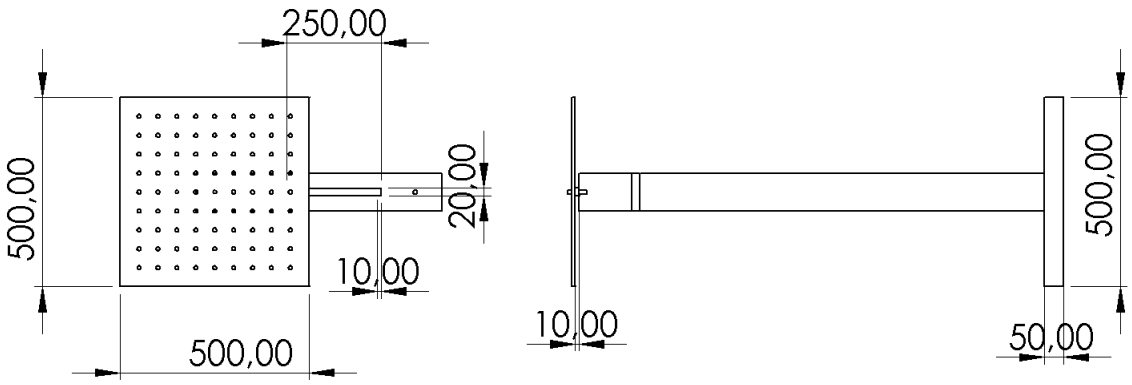

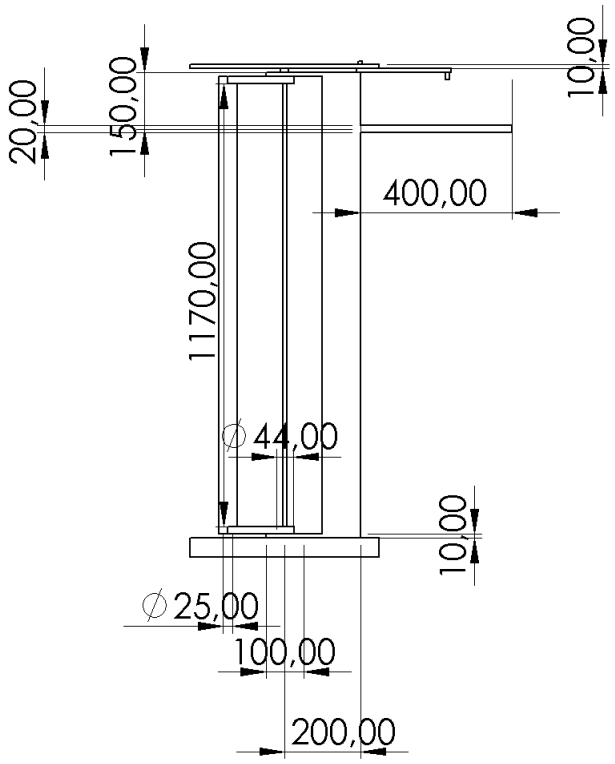

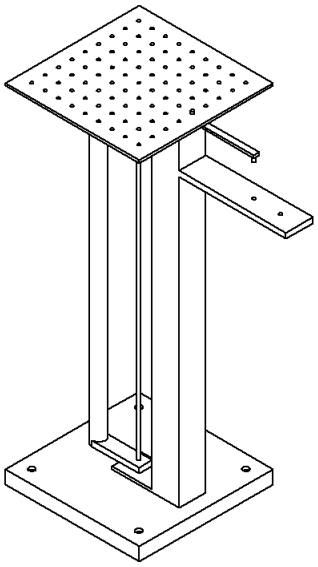

DO NOT SCALE DRAWING | REVISION

DEBURR AND
BREAK SHARP
EDGES

UNLESS OTHERWISE SPECIFIED:
DIMENSIONS ARE IN MILLIMETRES

TITLE:

Physical Pendulum

MATERIAL:
1060 Aluminium Alloy & Steel

DWG NO.
8

A4

MASS: 42.5 kg

SCALE:1:20

SHEET 1 OF 1

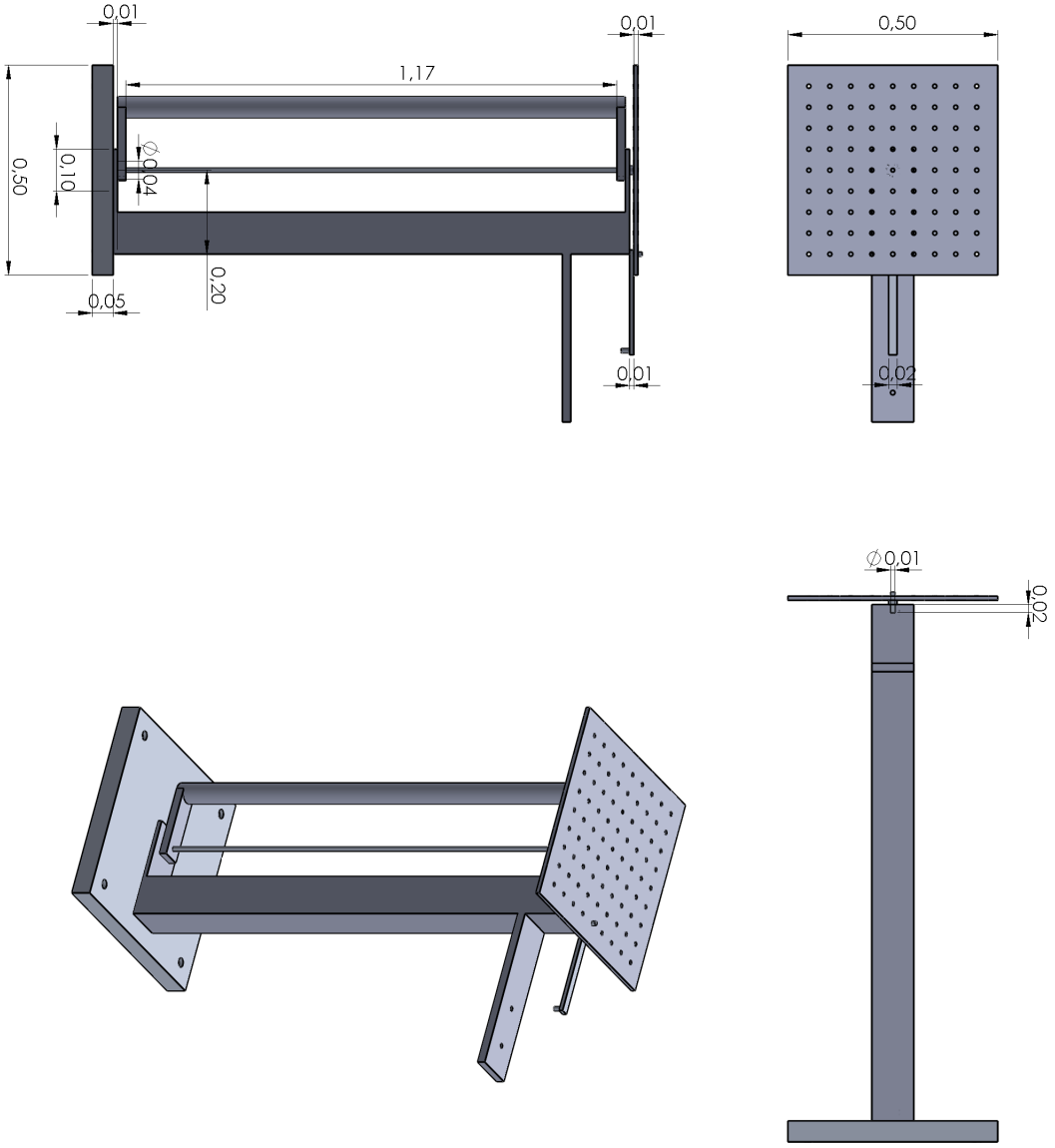

Figure 3.10: **torsion pendulum [m]**

Table 3.1: Complete Pendulum Physical Properties

Component	**Mass [kg]**	**Volume [cm^3]**
Base	15.05	5572.79
Fixed Support Column	15.16	5613.13
Bearings [2 of them]	0.06·2	8.78·2
Satellite Platform	6.58	2436.65
Torsion Fiber	0.01	3.8
Oscillatory Support Column	4.75	1759.54
Oscillatory Arm With Laser	0.14	53.14
Complete Pendulum	**42.50**	**15547.75**

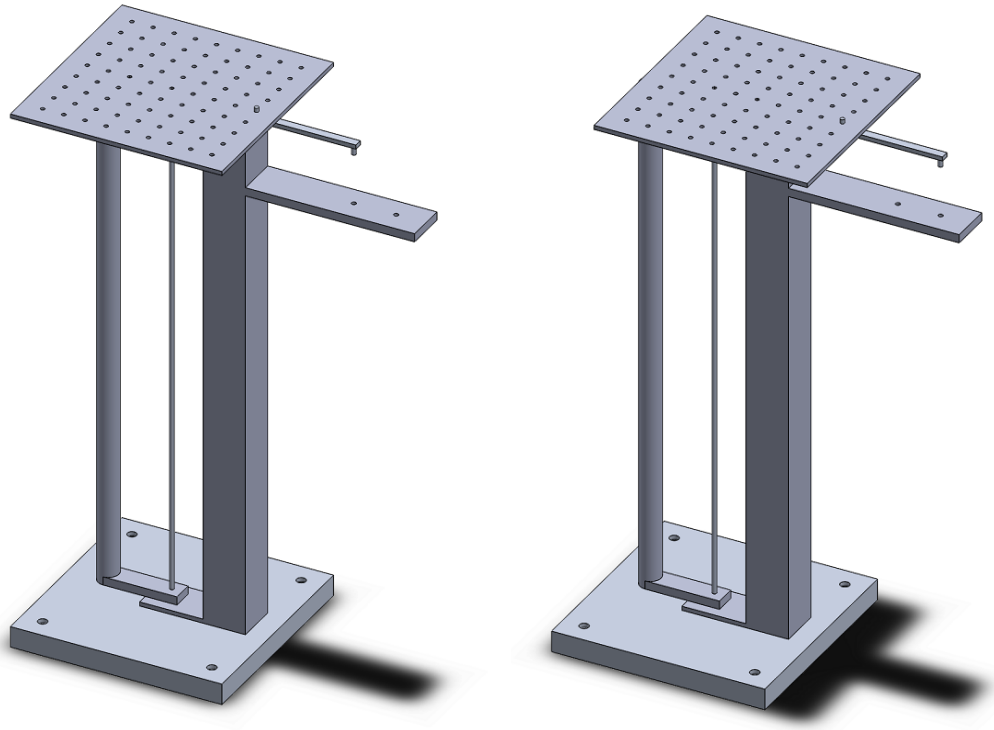

(a) Position 1 (b) Position 2

Figure 3.11: Complete pendulum assembly; (a) Oscillatory satellite platform screwed with the central hexagonal hole; (b) Oscillatory satellite platform screwed with the non-central hexagonal hole

We can also differentiate the oscillatory components from the fixed components in our final design by using the color code in Figure 3.1 (red are fixed and grey are oscillatory components). The result is shown in Figure 3.12.

Figure 3.12: Complete pendulum assembly; Grey-colored: Oscillatory components of the torsion pendulum; Red-colored: Fixed components of the torsion pendulum

Additionally, we can also set some of the parts in transparent mode so that we can see how the bearings interact with the other parts of the pendulum. In Figure 3.13 both support columns and the satellite support platform are shown as transparent. It is interesting to observe the *shell* features, introduced to reduce the amount of material and mass, and how the upper part of the torsion fiber is fixed to the oscillatory support column. Also, we can now easily distinguish the two different hexagonal holes of the oscillatory satellite platform, see section 3.2.2., and how is it connected by the central one to the rest of the torsion pendulum. Moreover, we can also observe how the bearing is connected by the outer part to the fixed support column and with the inner part to the small upper cylinder of the oscillating support column.

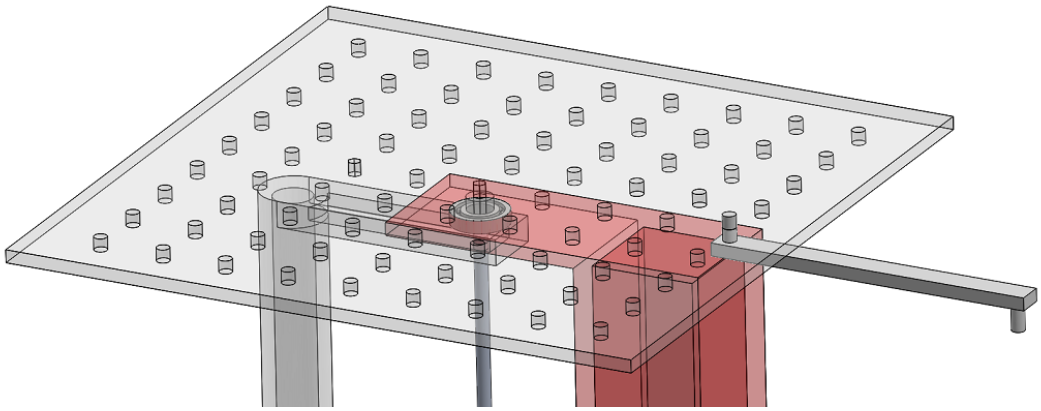

Figure 3.13: Upper Bearing Detail (Painted and Transparent)

Analogously, the same can be seen in Figure 3.14, where we can observe the lower bearing in detail, with the support columns transparent, and how the torsion fiber connects directly to the floor supporting base. As already explained, the bearing is connected by the outer part to the fixed support column and with the inner part to the small lower cylinder of the oscillatory support column, so that it works as the connection between the oscillating components and the fixed ones.

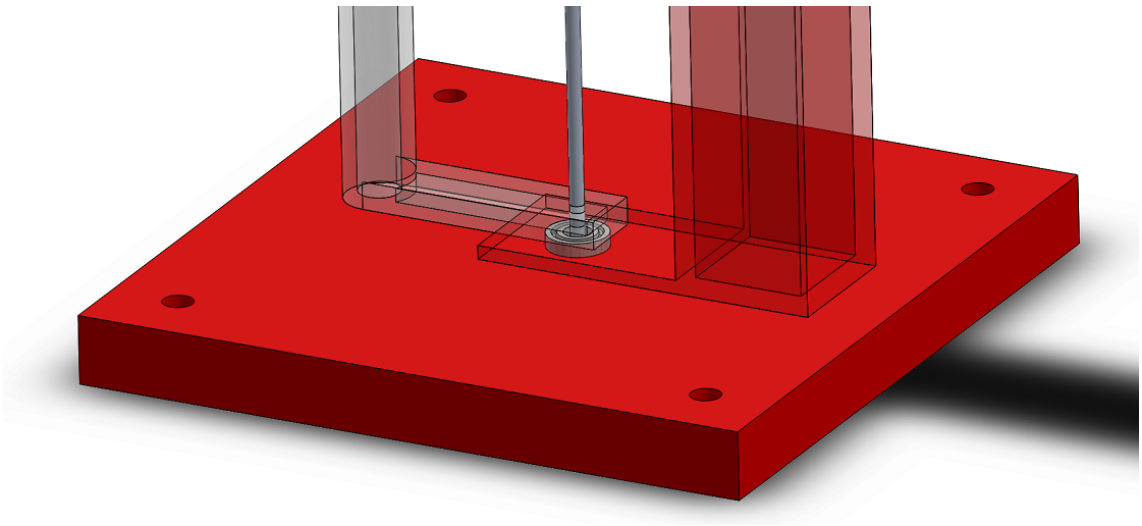

Figure 3.14: Lower Bearing Detail (Painted and Transparent)

CHAPTER 4. SIMULATIONS

Once the design of the torsion pendulum is completed, we must analyze whether the device is suitable to perform according to our requirements. In this Chapter we study the effects of applying external forces and pressures. Specifically, we consider the effects on the oscillatory satellite platform (3.2.2.), and on the complete pendulum assembly (3.3.).

We performed several analyses, using forces and pressures ranging from expected standard to extreme conditions (like punctual masses of maximum accepted weight in the borders of the oscillating plate). A maximum deformation displacement higher than 1 mm, or a maximum stress higher than the yield strength of aluminum alloy 1060 (28 MPa), was considered unacceptable for our requirements, as would result in plastic deformations.

We used the simulation analysis packages of SOLIDWORKS software to perform the following simulation tests:

- Stress simulation: SOLIDWORKS calculates the normal stress components (principal stresses), and the Von Mises, or Equivalent Stresses, which is used to assess failure of ductile materials and maximum stresses for an external load application.
- Displacement simulation: SOLIDWORKS calculates the maximum expected deformations in a solid for a certain external load application, and plots the URES (Resultant displacement).
- Strain simulation: SOLIDWORKS calculates the equivalent strain (ESTRN) in a solid when a certain external load is applied.

For each simulation we must enter some inputs, the part of the torsion pendulum which will be considered in the simulation as fixed in space, the external load (and where is it applied) and the mesh, which must always cover the full solid in which the simulation is performed.

We divide the present Chapter in the following sections: firstly, we study the oscillatory support platform, as a standalone, checking if the material and the dimensions of the oscillating plate are correctly chosen, and if it doesn't experience significant deformations due to the simulated applied force. Secondly, we perform the same studies with the complete pendulum assembly, with the goal of checking if the torsion fiber receives any kind of compression. Finally, we interpret the simulation results and draw our main conclusions.

4.1. Oscillatory Satellite Platform Analysis

As previously mentioned, we will perform different studies to check if the design and the selection of material (aluminum alloy 1060) done in the previous chapter are suitable.

Our first design for the oscillatory support platform assumed 3 mm height, and then, according to our initial pendulum design, its dimensions were (50 cm, 50 cm, 3 mm). Nevertheless, this dimensions proved to be unsuitable, as in some of the simulations the platform broke and produced unacceptable deformations.

So the first measure we took was to increase the thickness of the oscillating plate by 1 mm and retry the simulations, as the vertical thickness to horizontal area ratio was clearly

our main problem when performing the simulation. We repeated this step (increasing the thickness in steps of 1 mm) until the thickness was 1 cm, where we got suitable simulation results. It is important to recall that the thickness of the plate must be minimum, as it is directly related to the plate's mass and we need our oscillatory components with the smallest possible weight.

Hence, in order to simulate a worst case scenario, we simulate the effects of a satellite with a weight of 80 N, much larger than the largest ones we plan to analyze (3U *CubeSat*). If these simulations show that the torsion pendulum can operate under this weight, it will be even safer in operational conditions. Furthermore, as we have designed two different hexagonal holes in which we can screw the platform to the pendulum, we perform the corresponding analysis to the plate tighten in any of these two holes, so that we can test all possible scenarios in which the pendulum can be operated. The figures showing the results of these simulations can be found in Appendix B, section B.1.

4.2. Complete Pendulum Assembly Analysis

The goal of these simulations is to check the critical issue that the torsion fiber will not receive any kind of compression while the pendulum is operative, regardless the specific situation. Therefore, the aim of this section is to place the oscillatory satellite platform on the top of the pendulum and perform the same analysis we had studied in the previous section, this time with the complete torsion pendulum. Again, the different simulations are performed, positioning the oscillating platform in the two different possible arrangements.

Again, we use the same 80 N point weight as our input, and check if the torsion fiber receives any kind of compression. The first and second simulation, subsections B.2.1. and B.2.2. respectively, correspond to the oscillatory support platform 3.2.2. screwed by its central hexagonal hole. Whereas the third and fourth simulation, subsections B.2.3. and **??** respectively, are simulated with the oscillatory satellite platform screwed by its out-of-centre hexagonal hole.

The complete set of simulation figures can be seen in Section B.2. of Appendix B.

4.3. Simulation results and conclusions

In this section, we compile the eight simulations performed and discuss the obtained results. Tables 4.1 and 4.2 show the maximum von Mises stress, the resultant displacement, and the strain values on our solids. The von Mises stress is a magnitude proportional to the deformation energy. Once a certain value of the von Mises stress is surpassed, the object will undergo elastic failure. URES refers to the resultant displacement of a section of an object. If the displacement about axes X, Y and Z is, respectively, U_X, U_Y and U_Z, then the corresponding URES is $|\vec{U}| = \sqrt{U_X^2 + U_Y^2 + U_Z^2}$. ESTRN represents the strain, which corresponds to the quotient of the change in length of an object due to an applied force, to its original length.

Table 4.1: Oscillatory Satellite Platform Simulation Results

	von Mises stress [N/m^2]	**URES [mm]**	**ESTRN strain [-]**
1st Simulation	$3.861 \cdot 10^{2}$	$6.726 \cdot 10^{-8}$	$4.193 \cdot 10^{-9}$
2nd Simulation	$1.626 \cdot 10^{6}$	$4.446 \cdot 10^{-2}$	$1.725 \cdot 10^{-5}$
3rd Simulation	$8.386 \cdot 10^{6}$	$2.081 \cdot 10^{-1}$	$9.161 \cdot 10^{-5}$
4th Simulation	$3.647 \cdot 10^{7}$	$1.398 \cdot 10^{0}$	$2.684 \cdot 10^{-4}$

Table 4.1: **Oscillatory Satellite Platform Simulations:** stress and deformation analysis for the case in which the oscillatory satellite platform is considered. **1st Simulation** corresponds to the case of an homogeneous 80 N load on the isolated platform; **2nd Simulation** corresponds to the case of an homogeneous 80 N load on the platform fixed at the central hexagonal hole; **3rd Simulation** corresponds to the case of an homogeneous 80 N load fixed at the off-center hexagonal hole; **4th Simulation** corresponds to the case of a point 80 N load on an extreme point of the platform, which is fixed by the off-center hexagonal hole.

Table 4.2: Pendulum Simulation Results

	von Mises stress [N/m^2]	**URES [mm]**	**ESTRN strain [-]**
1st Simulation	$2.101 \cdot 10^{6}$	$9.268 \cdot 10^{-2}$	$2.221 \cdot 10^{-5}$
2nd Simulation	$1.657 \cdot 10^{7}$	$4.806 \cdot 10^{-1}$	$1.379 \cdot 10^{-4}$
3rd Simulation	$1.144 \cdot 10^{7}$	$5.022 \cdot 10^{-1}$	$1.066 \cdot 10^{-4}$
4th Simulation	$4.565 \cdot 10^{7}$	$2.139 \cdot 10^{0}$	$4.396 \cdot 10^{-4}$

Table 4.2: **Pendulum Simulations:** stress and deformation analysis for the case in which the entire device is considered. **1st Simulation** corresponds to the case of an homogeneous 80 N load on the isolated platform; **2nd Simulation** corresponds to the case of a punctual 80 N load on an extreme point of the platform, which is fixed by the central hexagonal hole; **3rd Simulation** corresponds to the case of an homogeneous 80 N load fixed at the off-center hexagonal hole; **4th Simulation** corresponds to the case of a punctual 80 N load on an extreme point of the platform, which is fixed by the off-center hexagonal hole.

As we can see in tables 4.1 and 4.2, the most extreme simulations performed with point masses in extreme positions (both 4th simulations), are the ones which surpass the yield strength and then the maximum allowed deformation of 1 mm. These simulations are the 4th simulation in table 4.1 and the 2nd and 4th simulation in table 4.2. In the rest of simulations, in which the mass of the satellite is distributed along the oscillatory satellite platform (not punctual) have acceptable values of stress and displacement which are complying our design requirements.

We must also take into account that the mass of the satellite that we have simulated is of about 8 kg, which is a worst case scenario, as the largest satellites we plan to study are of 4 kg (3U *CubeSat*s). Anyway, we will set the maximum permitted mass for the pendulum operation to be 8 kg (corresponding to a 6U *CubeSat*). In other words, the 8 kg satellite will be the upper mass operational limit for the pendulum.

Even in the most extreme simulations of the pendulum analysis, section 4.2., the torsion fiber does not receive any kind of compression as it is absorbed by the oscillatory support column and the fixed support column. Therefore, we are also achieving our design

requirements in this regard and we are checking that our design is suitable for its propose.

CHAPTER 5. SOFTWARE TOOLS AND INERTIA TENSOR CALCULATION

Our main objective in the present Chapter is to completely determine the inertia tensor of the oscillating components of the torsion pendulum. Note that the fixed components are irrelevant from the point of view of oscillation period measurements. Eventually, the operational pendulum will also include the *CubeSat*, and thus our actual period measurements will be determined by the sum of both the inertia tensor of this *CubeSat* ($\{I_{CS}\}$), and the inertia tensor of the oscillating elements of the pendulum ($\{I_P\}$). Thus, and as we describe in Chapter 6, the desired inertia tensor values of the *CubeSat* will be obtained as a subtraction $\{I_{\mathrm{CS}}\} = \{I_{\mathrm{measured}}\} - \{I_{\mathrm{P}}\}$.

As we also explain in Chapter 6, the most important component of the inertia tensor of the torsion pendulum is I_{zz}, as it is the on which we can measure, whereas the rest is to be obtained after additional measurements and rotation matrix algebra. Hence, for each of the oscillatory components of the pendulum, we will consider the following parameters in SOLIDWORKS:

- Mass [kg].
- Center of mass given in [x,y,z] coordinates [m].
- Component I_{zz} of the inertia tensor [kg·m^2].

In order to simplify the inertia tensor determination, we chose a new coordinate system, according to which the centre of mass and I_{zz} of the oscillatory components can be be obtained. The X_O and Y_O components of the origin of this new coordinate system are at the center of the oscillatory satellite platform, and the Z_O component is 5 cm above the upper surface of the platform. This way, if we place a 1U *CubeSat* centered in the platform, its centre of mass will coincide with the origin of our frame of reference, within the limits of reasonable approximation. Note at this point that the *CubeSat* standard requires that the center of mass shall be located at less than 2 cm of the geometric center of the satellite. Naturally, the X and Y axes of our frame of reference will be parallel to each side of the platform. The Z axis will be perpendicular to the platform, and thus along the axis of the torsion fiber. Defined in this way, the system will only experience rotation about the Z axis. A sketch of our frame of reference together with the oscillating parts of the pendulum is shown in Figure 5.1.

We now present the complete inertia tensors of the oscillating components, using the new coordinate system described above. Recall that the components studied are the oscillatory ones, that is, the ones which rotate about the torsion fiber when an external torque is applied to the platform. We must take into account that, even though the upper and lower bearings are identical, and thus their description was not duplicated in the previous chapter, we must now consider them separately, as they are placed in different positions in reference to the chosen frame of reference. Note however, that because of their identical mass distribution about the Z axis, their I_{ZZ} components will be, again, identical. Recall also that the bearings are composed of an oscillating part and a fixed part; therefore, we only take into account the oscillating parts, as they are the only relevant ones for our calculations of the inertia tensor.

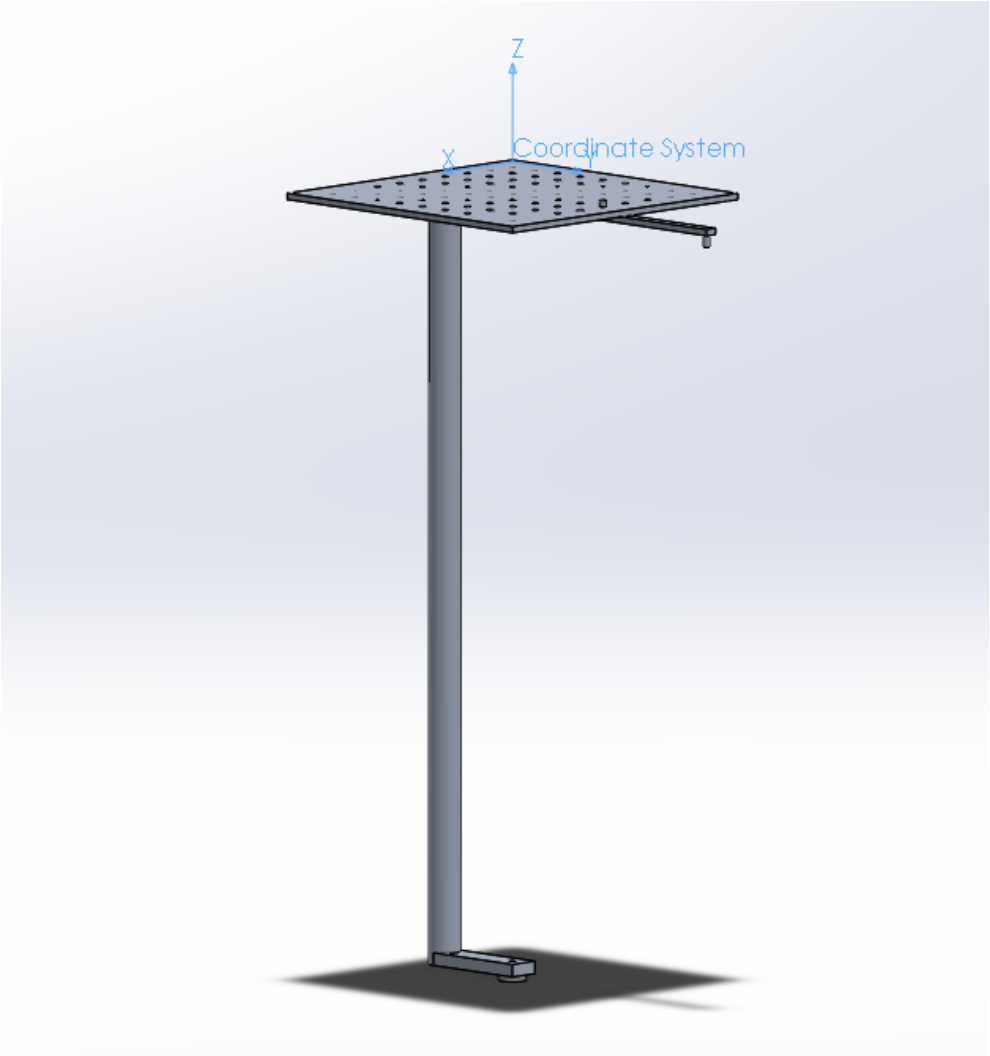

Figure 5.1: Oscillatory components of the pendulum and frame of reference used for the calculations of the centre of mass and the Z-component of the inertia tensor I_{ZZ} of the system. Components shown in the Figure are the oscillatory support column, the oscillatory arm with laser, the oscillatory satellite platform, and the lower and upper bearings (inner or mobile cylinder).

In order to calculate the inertia tensors of the different components we used the software tool known as *Physical properties*, provided by SOLIDWORKS, and the results for the different oscillatory components of the pendulum are shown below. Note that, because all the inertia tensors are given with respect to the same frame of reference, the total inertia tensor is the matrix sum of the individual tensors. Note also that the torsion fiber was not included either in Figure 5.1, or in the inertia tensor calculations. The reason is that, given its geometry (very narrowly close to the axis of rotation) its I_{zz} component is expected to be negligible.

$$\text{Upper Bearing} \Longrightarrow \{I_{UB}\} = \begin{bmatrix} 0.00017 & 0 & 0 \\ 0 & 0.00017 & 0 \\ 0 & 0 & 0.00001 \end{bmatrix} [kg \cdot m^2]$$

$$\text{Lower Bearing} \Longrightarrow \{I_{LB}\} = \begin{bmatrix} 0.05038 & 0 & 0 \\ 0 & 0.05038 & 0 \\ 0 & 0 & 0.00001 \end{bmatrix} \text{[kg}\cdot \text{m}^2\text{]}$$

$$\text{Oscillatory Satellite Platform} \Longrightarrow \{I_{OP}\} = \begin{bmatrix} 0.15772 & 0 & 0 \\ 0 & 0.15772 & 0 \\ 0 & 0 & 0.27553 \end{bmatrix} \text{[kg}\cdot \text{m}^2\text{]}$$

$$\text{Oscillatory Support Column} \Longrightarrow \{I_{OSP}\} = \begin{bmatrix} 3.04889 & 0 & 0 \\ 0 & 2.95331 & 0.44536 \\ 0 & 0.44536 & 0.09765 \end{bmatrix} \text{[kg}\cdot \text{m}^2\text{]}$$

$$\text{Oscillatory Arm With Laser} \Longrightarrow \{I_{OAL}\} = \begin{bmatrix} 0.01506 & 0 & 0 \\ 0 & 0.00061 & -0.00295 \\ 0 & -0.00295 & 0.01506 \end{bmatrix} \text{[kg}\cdot \text{m}^2\text{]}$$

Table 5.1 summarizes the relevant parameters for the different oscillating components in new coordinate system.

Table 5.1: Table of components

Component	**Mass [kg]**	**Center of mass [m]**	I_{zz} **[kg**$\cdot$ **m^2]**
Upper Bearing	0.06	[0, 0, -0.075]	0.00001
Lower Bearing	0.06	[0, 0, -1.295]	0.00001
Oscillatory Satellite Platform	6.58	[0, 0, -0.055]	0.27553
Oscillatory Support Column	4.75	[0, -0.14, -0.68]	0.09765
Oscillatory Arm With Laser	0.14	[0, 0.32, -0.06]	0.01506
Oscillatory Components	**11.5**	**[0,-0.05,-0.317]**	**0.38825**

We must also take into account that these calculations are done with the oscillatory satellite platform being screwed at its central hexagonal hole. In order to account for the alternative platform position, either these calculations should be repeated using SOLIDWORKS with the off-center configuration, or applying Steiner's theorem to the inertia tensors of the displaced components.

CHAPTER 6. SATELLITE INERTIA TENSOR CALCULATION

In the present chapter we will apply the analysis developed in Chapter 2 and use the inertia tensor calculated in Chapter 5, to finally determine the inertia tensor of our satellite as a standalone.

First, we must remember from Chapter 2 the main equation for the dynamics of rotation:

$$\vec{\tau} = \frac{d\overline{L}}{dt} = \frac{d}{dt}\left\{\left\{I\right\}\overline{\omega}\right\} = \frac{d}{dt}\begin{bmatrix} I_{xx} & I_{xy} & I_{xz} \\ I_{xy} & I_{yy} & I_{yz} \\ I_{xz} & I_{yz} & I_{zz} \end{bmatrix}\begin{bmatrix} \omega_x \\ \omega_y \\ \omega_z \end{bmatrix} \Longrightarrow$$

$$\begin{bmatrix} \dot{L}_x \\ \dot{L}_y \\ \dot{L}_z \end{bmatrix} = \frac{d}{dt}\begin{bmatrix} I_{xx}\omega_x & I_{xy}\omega_y & I_{xz}\omega_z \\ I_{xy}\omega_x & I_{yy}\omega_y & I_{yz}\omega_z \\ I_{xz}\omega_x & I_{yz}\omega_y & I_{zz}\omega_z \end{bmatrix} \tag{6.1}$$

Because rotation is about the Z axis, we can simply focus on L_z. Besides, taking into account that I_{zz} is constant, and that the torque due to a torsion fiber is $\tau_z = -b\theta_z$, where b is constant and θ_z is the rotation angle about the Z axis:

$$\frac{dL_z}{dt} = I_{zz}\omega_z \Longrightarrow -b\theta_z = I_{zz}\ddot{\theta}_z \Longrightarrow -b\theta_z = I_{zz}\ddot{\theta}_z$$

Therefore:

$$\ddot{\theta}_z + \frac{b}{I_{zz}}\theta_z = 0 \tag{6.2}$$

The former is, of course, the equation for a simple harmonic oscillator of frequency $\omega_0 = \sqrt{\frac{I}{b}}$, and its solution is the well-known expression $\theta = \theta_0\cos(\omega t + \phi)$, where θ_0 is the amplitude and ϕ is the initial phase. Therefore, the period of the oscillations is:

$$T_0 = \frac{2\pi}{\omega_0} = 2\pi\sqrt{\frac{I_{zz}}{b}}$$

Or, equivalently:

$$I_{zz} = \left(\frac{T_0}{2\pi}\right)^2 b \tag{6.3}$$

Note that a more realistic approach would include, as in Chapter 2, the effects of friction. However, given the geometry of our device, we expect the friction coefficient (in the air) to be $\gamma \sim 10^{-4}\,s^{-1}$, and thus much smaller than $\omega_0 \sim 0.1\,s^{-1}$. In order to calculate ω_0 we took I_{zz} from Chapter 5, and the torsion fiber constant b$\sim$ 0.01 Nm^2, characteristic of torsion fibers similar to the one we would use for an eventual construction of our pendulum. Therefore we are in the regime of a good quality factor oscillator and thus we can safely assume that $\omega \approx \omega_0$, that is, that the frequency of the realistic damped oscillator is very similar to the frequency of a harmonic oscillator.

Summarizing, we know now how to fully determine the I_{zz} component of the inertia tensor of a our pendulum (with or without an attached *CubeSat*) by using measurements of its period. Recall that our analysis is referenced to the coordinate system described in Chapter 5, that is, with origin coincident with the geometrical center of a *CubeSat* placed at the center of the oscillatory satellite platform.

We also know that the complete inertia tensor is:

$$\{I_{\text{TOTAL}}\} = \{I_{\text{P}}\} + \{I_{\text{CS}}\},$$

where $\{I_P\}$ is the moment of inertia of the mobile parts of the pendulum, and $\{I_{CS}\}$ is the moment of inertia of the *CubeSat*, both given with respect to the axis of rotation of the system. Focusing on the zz component we can determine, after measuring the period of the pendulum alone, $I_{zz,P}$ for the pendulum. From equation 6.3, $I_{zz,P} = \left(\frac{T_{0,P}}{2\pi}\right)^2 b$. Analogously, after measuring periods of the oscillation of the system pendulum plus *CubeSat*, we can obtain $I_{zz,TOTAL} = \left(\frac{T_{0,TOTAL}}{2\pi}\right)^2 b$. Therefore:

$$I_{CS,zz} = I_{\text{TOTAL},zz} - I_{\text{P},zz} \tag{6.4}$$

In the next section we describe how we can use I_{zz} values and rotation matrix algebra in order to obtain the remaining components of the tensor of inertia of a *CubeSat*.

6.1. Complete determination of the inertia tensor

The key to determine additional components of the inertia tensor is to rotate the *CubeSat*, in order to place it in additional positions with respect to our frame of reference, and measure the corresponding periods. Mathematically, we can simulate a rotation of the inertia tensor by using the expression $I_{\text{ROTATED}} = R\{I\}R^T$, and the rotation matrices about the X, Y and Z axes given in Chapter 2. For the sake of efficiency we wrote a MATLAB program to automatically calculate the rotations. Note that because MATLAB calculates by defect passive rotations and we intend to rotate the *CubeSat*, the equivalent real rotations in the constructed pendulum should be performed clockwise. In this section $\{I\}$ may refer either to the tensor of inertia of the mobile parts of the pendulum or to the set mobile parts plus *CubeSat*, depending on the chosen configuration.

As the *CubeSat* has a cubic shape, it is actually very easy to rotate it by 90° about any of its main axes. The resulting inertia tensor rotated 90° about its X axis, according to our MATLAB program is as follows:

$$I_{\text{ROTATED}} = R_x(90)\{I\}R_x(90)^{\mathsf{T}} = \begin{bmatrix} I_{xx} & I_{xz} & -I_{xy} \\ I_{xz} & I_{zz} & -I_{yz} \\ -I_{xy} & -I_{yz} & I_{yy} \end{bmatrix}$$

It allows us to obtain the I_{yy} component.

Analogously, if we implement a 90° rotation about the Y axis:

$$I_{\text{ROTATED}} = R_y(90)\{I\}R_y(90)^T = \begin{bmatrix} I_{zz} & -I_{yz} & -I_{xz} \\ -I_{yz} & I_{yy} & I_{xy} \\ -I_{xz} & I_{xy} & I_{xx} \end{bmatrix}$$

So that, we can obtain the I_{xx} component.

At this point we have obtained the three moments of inertia, I_{xx}, I_{yy}, I_{zz} of the tensor, but we still need information of the products of inertia. More 90 $^\circ$ rotations do not provide us with additional components. However, we can still implement on the *CubeSat* rotations of 45°, These rotations are easy to apply, either if they are performed about the axis of the torsion fiber itself, or about another axis parallel to it. Alternatively, we can also adapt the *CubeSat* box so that it can sit (and be fixed to the platform) on its edges.

Then, if we apply a 45° rotation about the X axis:

$$I_{\text{ROTATED}} = R_x(45)\left\{I\right\}R_x(45)^{\mathsf{T}}$$

We get the following expression for the I'_{zz} component of the new inertia tensor, which is to be derived from the new measured period:

$$I'_{zz} = \frac{1}{2}(I_{yy} - 2I_{yz} + I_{zz})$$

As we have already determined I_{yy} and I_{zz}, we can infer from the expression above the missing component I_{yz}.

If we apply a 45° rotation about axis Y:

$$I_{\text{ROTATED}} = R_y(45)\left\{I\right\}R_y(45)^{\mathsf{T}}$$

We get the following expression for the I'_{zz} component of the inertia tensor:

$$I'_{zz} = \frac{1}{2}(I_{xx} + 2I_{xz} + I_{zz})$$

Again, as we have already know I_{xx} and I_{zz} we can easily calculate I_{xz} .

If we apply the same rotation of 45° about the Z axis we don't get any further information. Therefore, in order to calculate the I_{xy} component, we need to apply two consecutive rotations. For instance, we can apply a 90° rotation about the X axis and an additional 45° rotation about the Y axis, as follows:

$$\begin{aligned} I_{\text{ROTATED}} &= R_x(90)\left\{I\right\}R_x(90)^{\mathsf{T}} \\ I_{\text{ROTATED,TWICE}} &= R_y(45)\left\{I_{\text{ROTATED}}\right\}R_y(45)^{\mathsf{T}} \end{aligned}$$

We get the following expression for the new I'_{zz} component of the new inertia tensor:

$$I'_{zz} = \frac{1}{2}(I_{xx} - 2I_{xy} + I_{yy})$$

Now, we can see that we are in the same situation as before, were we know the components I_{xx} and I_{yy} and can calculate the missing component I_{xy}.

After these simple rotations, and using Equation 6.4, we can completely determine all the moments and products of inertia of the inertia tensor of the satellite. From this equation

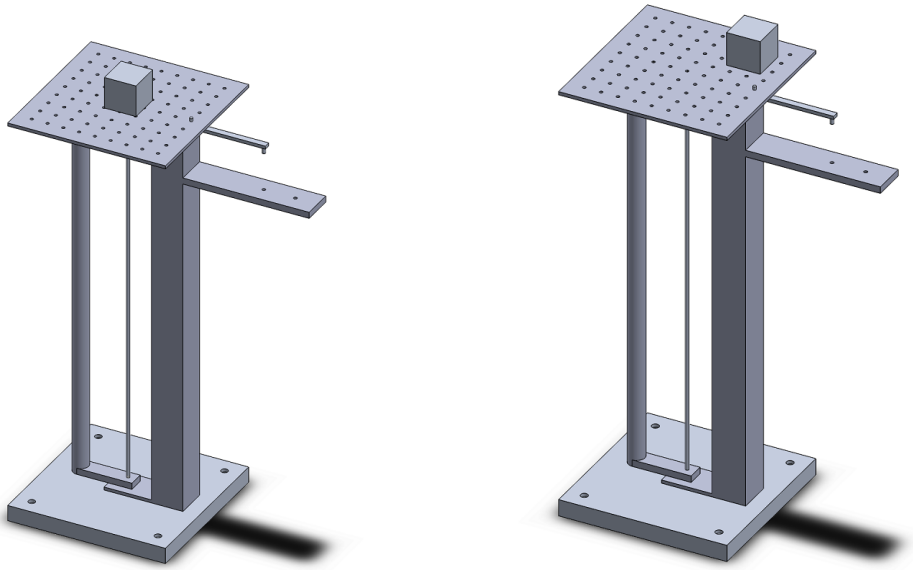

(a) Centered (b) Random Position

Figure 6.1: Complete pendulum assembly with *CubeSat* located in two different positions on the supporting plate.

we can also see that, as mentioned above, it is important to keep the tensor of inertia of the oscillating components of the pendulum $I_{\mathrm{P,zz}}$ as low as possible, as it may affect the proper determination of the tensor of inertia of the *CubeSat*, $I_{\mathrm{CS,zz}}$.

We must also remember that in the previous Chapter 5 we indicated that this value of $I_{\mathrm{P,zz}}$ is calculated with the oscillatory satellite platform being screwed by its central hexagonal hole (see Figure 6.1); therefore, if we want to screw it by its off-center hexagonal hole, in order to be able to perform more calculations, and obtain more accurate results, we would need to recalculate the value of $I_{\mathrm{P,zz}}$. We defer this calculations to future work.

6.2. *CubeSat* inertia tensor calculation

In the present section we show the results of a simple numerical experiment with SOLIDWORKS, aimed to calculate the inertia tensor of a simple model of *CubeSat*. We know that a *CubeSat* must be a cube of 10 cm side, and therefore, we consider a solid homogeneous cube of 1000 cm^3 volume. This design is not intended to be a good approximation for a *CubeSat*, as we are not considering the internal distribution of the satellite. However, this simulation will give us an idea of the order of magnitude of the moment of inertia values which we may expect, and ultimately, determine the approximate precision with which oscillation periods are to be measured. For the sake of comparison we also calculate analytically the inertia tensor of our simple *CubeSat* model as a standalone in reference to its center of mass, we get the following tensor of inertia:

$$[I] = \begin{bmatrix} 0.0045 & 0 & 0 \\ 0 & 0.0045 & 0 \\ 0 & 0 & 0.0045 \end{bmatrix} [kgm^2]$$

This inertia tensor is the one we are supposed to find using our torsion pendulum, and thus it can be used as a reference for calibration.

Regarding the simulation, we will use as our reference the coordinate system we created in the previous chapter (see Figure 5.1). Of course, we get the same result as in the analytic calculation.

Of course, by placing the *CubeSat* in the central position of the oscillatory satellite platform, we are considering the worst case scenario in terms of resolution needs. Because we are approximately making the center of mass of our *CubeSat* coincide with the origin of our coordinate system, we get the smallest possible values for the moments of inertia, and thus force the highest resolution in our device. If we want to operate at somewhat lower resolution and still get moment of inertia values with two significant figures, we can place the *CubeSat* at a known distance from the origin of our coordinate system. We know from Steiner's theorem (see section 2.2.3. in Chapter 2), that the new moment of inertia will be larger than that calculated along an axis passing through the centre of mass of the cube.

6.3. Considerations on period measurement resolution

For the sake of simplicity in the equation, we drop in this section the subscript zz for the considered moments of inertia. Note however that we always refer to the moments og inertia along this axis.

We know from Equation 6 how the pendulum period relates to the moment of inertia values:

$$\frac{T^2}{4\pi^2}b = I_{\mathrm{P}} + I_{\mathrm{CS}} \Rightarrow$$

$$T = 2\pi\sqrt{\frac{I_{\mathrm{P}} + I_{\mathrm{CS}}}{b}} \tag{6.5}$$

Where T is the measured period we get from the sensor, b is the torsion constant for the fiber, and I_{P} and I_{CS} are, respectively, the moments of inertia for the pendulum and the *CubeSat*, both given with respect to the z axis.

The constant b should be properly calibrated once the pendulum is built, but we can expect typical values for torsion fibers between 10^{-3} and 10^{-2} N m^2. From our former calculations I_{P}=0.3885 kg m^2, and $I_{\mathrm{CS}} \sim 10^{-3}$ kg m^2.

We can now use the standard equation for error propagation in order to obtain the required resolution for the measurements of T, assuming that the precision required for I_{P} and I_{CS} is $\sim 10^{-4}$.

$$dT = \sqrt{\left(\frac{\partial T}{\partial I_{\mathrm{P}}} dI_{\mathrm{P}}\right)^2 + \left(\frac{\partial T}{\partial I_{\mathrm{CS}}} dI_{\mathrm{CS}}\right)^2} \tag{6.6}$$

Plugging Equation 6.5 into 6.6, we get:

$$dT = \pi \sqrt{\frac{1}{b} \frac{dI_{\mathrm{P}}^2 + dI_{\mathrm{CS}}^2}{I_{\mathrm{P}} + I_{\mathrm{CS}}}} \tag{6.7}$$

Substituting the above values, and choosing $b = 0.01$ Nm^2 we get a dT $\sim$1ms, which is a reasonable value. If a precision of $\delta I/I = 10^{-6}$ is expected for the moments of inertia, our device should be able to measure down to values $\sim$0.1ms, also within feasible ranges. Note that, additionally, noise analysis should be made, but we defer this to a future work.

CHAPTER 7. CONCLUSIONS AND FUTURE IMPROVEMENTS

In this chapter we present the conclusions derived from our work, and propose possible future improvements, to be implemented prior to the eventual manufacturing of the described pendulum design.

7.1. Conclusions

Our main conclusions may be summarized as follows:

- We designed a torsion pendulum able to hold in different positions and orientations a *CubeSat* of up to 3 units. The pendulum is to hold a laser emitter and a detector, which will allow to measure and transmit oscillation period data. This design is simple enough to allow its construction with a relatively reduced budget. The detailed blueprints for the components of our pendulum, obtained with SOLIDWORKS, are presented in Appendix A. Connection elements such as screws are standard, so they were not designed in this work. However, the different types of standards required were referred to when necessary.

- Stress analysis has been performed through numerical simulations with SOLIDWORKS. Our results indicate that the design is robust enough to resist the solicitations found during normal operations. Once the pendulum is constructed, this analysis can be useful to outline the conditions of real laboratory stress tests.

- Using classical dynamics theory, we showed that the measured period can be related to the moment of inertia of the *CubeSat* around the axis of rotation of the pendulum. Furthermore, rotation matrix algebra allows to build the complete tensor of inertia, using the moments of inertia obtained from a series of periods measured with the *CubeSat* placed in different orientations. The detailed procedure was thoroughly described and justified, and can be the basis for an eventual instruction manual of the constructed pendulum.

- A basic error analysis has been presented. This error analysis shows that the pendulum designed allows to obtain experimental data, which will lead to the determination of accurate inertia tensors. This will be a significant improvement with respect to results obtained with standard simulations, which are unable to account for the complexity of real *CubeSats*.

Therefore, we achieved the main goals of our project. Our results are of interest for *CubeSat* developers, because the proposed design, once implemented, will allow to obtain accurate inertia tensors of these satellites, which are a fundamental input for attitude control, and thus to ensure a good performance during their operation stage.

Figure 7.1: New oscillatory components of the pendulum

7.2. Future improvements and developments

During advanced stages of the design process, some possible improvements of our design became apparent. We draw some future actions along these lines.

i) **Displacement of the oscillating column:** As already stated, minimizing the value of the pendulum's moment of inertia allows higher accuracy in the satellite's inertia tensor determination. We found a possible alternative design which could prove fruitful in this regard, that is, to locate the oscillating column with its axis coincident with the torsion fiber. In this way, the fiber would be inside the oscillating column, and the part of the pendulum's inertia tensor stemming from the column would be greatly reduced. As this design change is very promising, we will discuss it at some length.

   Actually, our new design merely implies a displacement of the oscillating column, and the design of the other components would remain unchanged. The new oscillatory support column is shown in Figure 7.1, together with the other oscillatory components of the pendulum and the coordinate system described in chapter 5. The design consists of a hollow cylinder whose axis coincides with the torsion fiber and provides support to the structure and avoids deformations of the fiber. The torsion fiber will be fixed to the supporting platform (on its upper end), and to the floor base support (in its lower end). Therefore, the new column will serve the same purposes as the previous one for the design of our torsion pendulum. Note that additional stress analysis simulations should be performed for the new design. The

Table 7.1: Table of rotating components with the displaced oscillating column design.

Component	Mass [kg]	Center of mass [m]	I_{zz} [kg· m^2]
Upper Bearing	0.06	[0, 0, -0.075]	0.00001
Lower Bearing	0.06	[0, 0, -1.295]	0.00001
Oscillatory Satellite Platform	6.58	[0, 0, -0.055]	0.27553
Oscillatory Support Column	5.21	[0, 0, -0.68]	0.00335
Oscillatory Arm With Laser	0.14	[0, 0.32, -0.06]	0.01506
Oscillating Components	**12.07**	**[0, 0.003, -0.333]**	**0.29409**

main benefit of this new design is the reduction of its impact in the component I_{zz} of the pendulum inertia tensor (see table 5.1). Note that it is reduced almost a factor 30 with respect to the original design. Additional information for the the entire oscillating set and its separate components is shown in Table 7.1. By comparison with Table 5.1 of Chapter 5, we realize that the total reduction in I_{zz} for the entire set is of about 25%. The final reduction is relatively modest because of the huge effect of the moment of inertia of the oscillating platform, which is not altered with our new design.

ii) **Supporting base:** The design of the floor supporting base could be improved by altering its shape. We thought three alternative shapes to compare with our square base. The new proposed shapes were circular, hexagonal and triangular. In order to check which design is the most suitable we performed simulations using SOLIDWORKS CAD software. The performed simulations are shown in Appendix C, where we can observe that the optimal shape is the triangular one. However, this kind of shape is constructively more complicated that the square shape we chose for our physic pendulum. Therefore, and given that the original square served our purpose, we should compromise when definite construction decisions are made.

iii) ***CubeSat* support structure design:** We must design proper support structures to which we can attach 0.5U, 1U, 1.5U, 2U and 3U *CubeSats*. These structures will be able to be screwed to the oscillatory satellite platform 3.2.2. in both the 90^o position and the 45^o position, so that we can easily perform the rotations described in Chapter 6. At the same time, we must know the inertia tensors of the structures we design, as they will be oscillating with the rest of the pendulum components, and therefore, influencing in the inertia tensor calculation of the satellite.

iv) **Fine adjustment of the *CubeSats* position:** We intend to implement a way to adjust either the *CubeSats* or both the platform and the *CubeSats* location, in order to keep the position of the centre of mass of the system constant during the successive re-orientations of the satellite.

v) **Alternative materials:** We have seen that the highest contribution to the moment of inertia of the oscillating set is given by the oscillating platform. Alternative materials, both lighter and as resistant as Aluminum 1060 should be considered prior to an eventual construction of the pendulum. One of the most promising options is 3D printing with high strength, low density thermoplastics.

vi) **Laser source, detector and communications:** These components must be carefully chosen, so that they meet our resolution purposes and low-budget specifications. The laser source must be light enough so that its moment of inertia with respect to the axis of rotation does not compromise the performance of our device. An alternative disposition, placing the sensor at the rotating platform and the laser emitter at the arm of the fixed column might be considered. However, the latter option would force the use of wireless communication of the sensor data.

vii) **Noise and errors:** Further error and noise analysis for our pendulum design should be performed. Additionally, a detailed calibration process should be described.

viii) **Preparation for construction:** Finally, we should also outline a practical implementation plan, including detailed costs of out-of-the-self components, material and manufacturing of the real torsion pendulum.

BIBLIOGRAPHY

[1] Educational value and lessons learned from the aau-cubesat project, institute of electrical and electronics engineers, isbn 0-7803-8142-4. 2003.

[2] NASA˙ Cubesat launch. URL: http://www.nasa.gov/directorates/heo/home/CubeSats_initiative.

[3] NASA. Nasa, cube quest challenge. URL: http://www.nasa.gov/cubequest/details.

[4] ESA. Launch your satellite. URL: http://www.esa.int/Education/CubeSats_-_Fly_Your_Satellite.

[5] Jordi Puig-Suari, Scott Williams, and Roland Coelho. Cubesat design specification rev. 13. *The CubeSat Program, Cal Poly SLO*, 2014.

[6] Dezsö Szöke and Norbert Horváth. Measurement of tensor of inertia with tetrahedron method. URL: https://pp.bme.hu/tr/article/viewFile/6589/5694.

[7] Ke-Xun Sun Dan B. DeBra Aaron J. Swank, Corwin Hardham. Moment of inertia measurement using a five-wire torsion pendulum and optical sensing. URL: https://pdfs.semanticscholar.org/a664/d3e1a3d03c75ba192fe5e36c173fd5b74ef1.pdf.

[8] An improved pendulum method for the determination of the center of gravity and inertia tensor for irregular-shaped bodies. URL: https://www.researchgate.net/publication/251542288_An_improved_pendulum_method_for_the_determination_of_the_center_of_gravity_and_inertia_tensor_for_irregular-shaped_bodies.

[9] David Morin. *Classical Mechanics*. Cambridge University Press, 2007.

[10] Jerry B. Marion. *Dynamics of Systems and Particles*. Academic Press, 1965.

APPENDICES

APPENDIX A. TORSION PENDULUM COMPONENTS

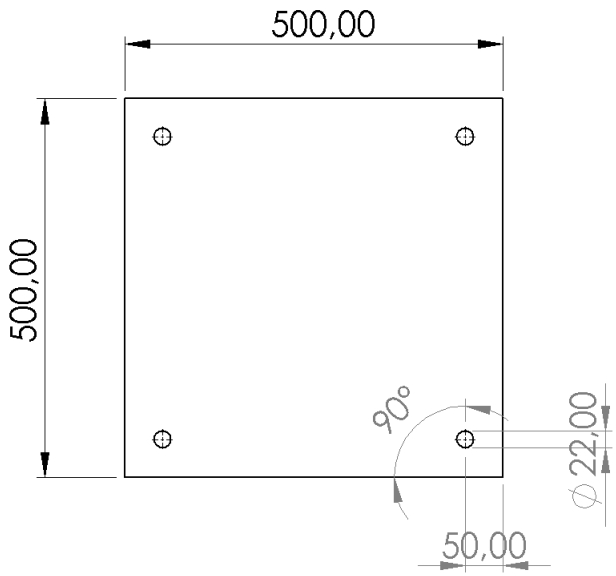

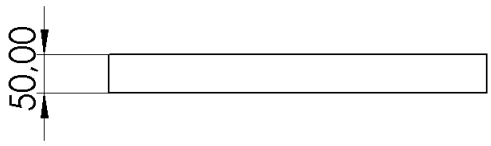

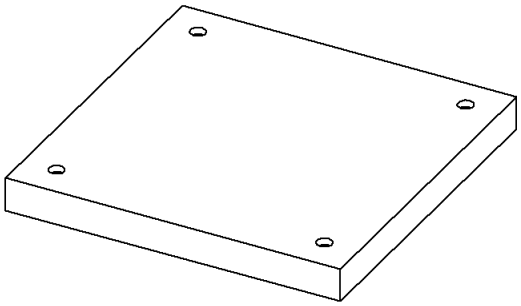

DO NOT SCALE DRAWING | REVISION

DEBURR AND
BREAK SHARP
EDGES

UNLESS OTHERWISE SPECIFIED:
DIMENSIONS ARE IN CENTIMETRES

TITLE:

Supporting Base

MATERIAL:
1060 Aluminium Alloy

DWG NO.
1

A4

MASS: 15.01 kg

SCALE:1:10

SHEET 1 OF 1

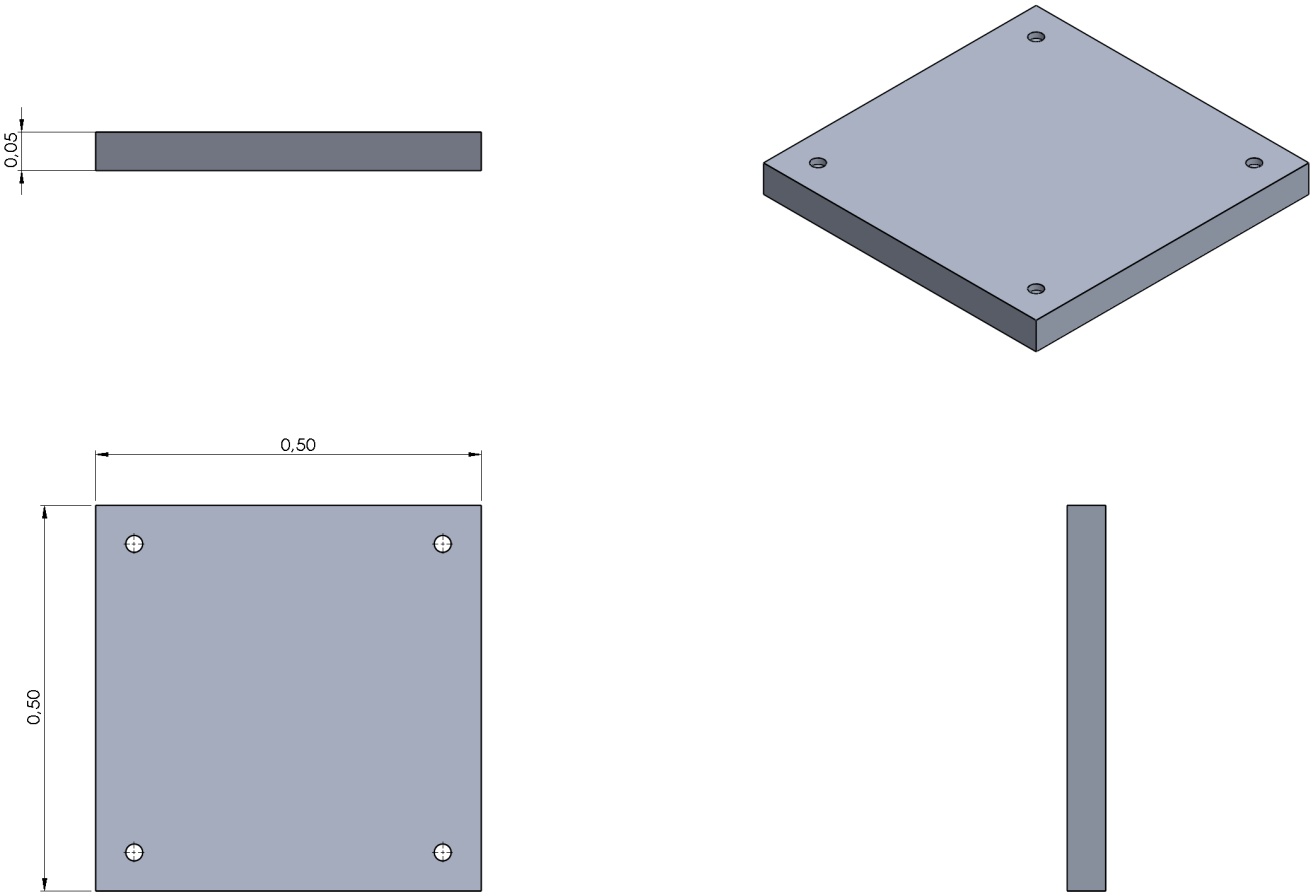

Figure A.1: **Supporting Base [m]**

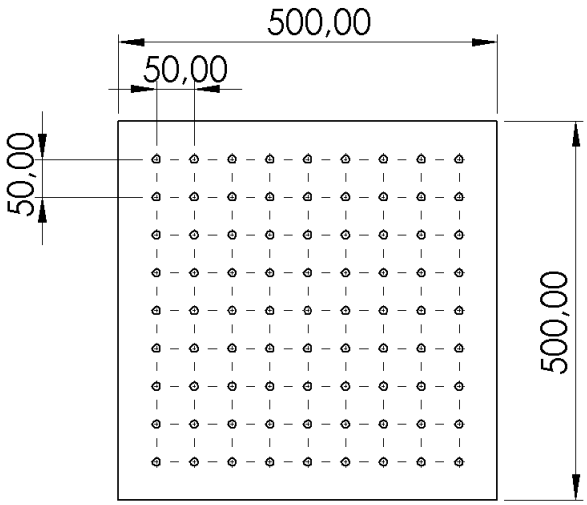

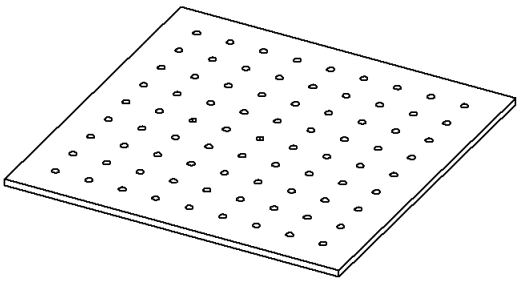

DO NOT SCALE DRAWING | REVISION

DEBURR AND
BREAK SHARP
EDGES

UNLESS OTHERWISE SPECIFIED:
DIMENSIONS ARE IN MILLIMETRES

TITLE:

Oscillatory Satellite Platform

MATERIAL:
1060 Aluminium Alloy

DWG NO.
2

A4

MASS: 6.58 kg

SCALE:1:10

SHEET 1 OF 1

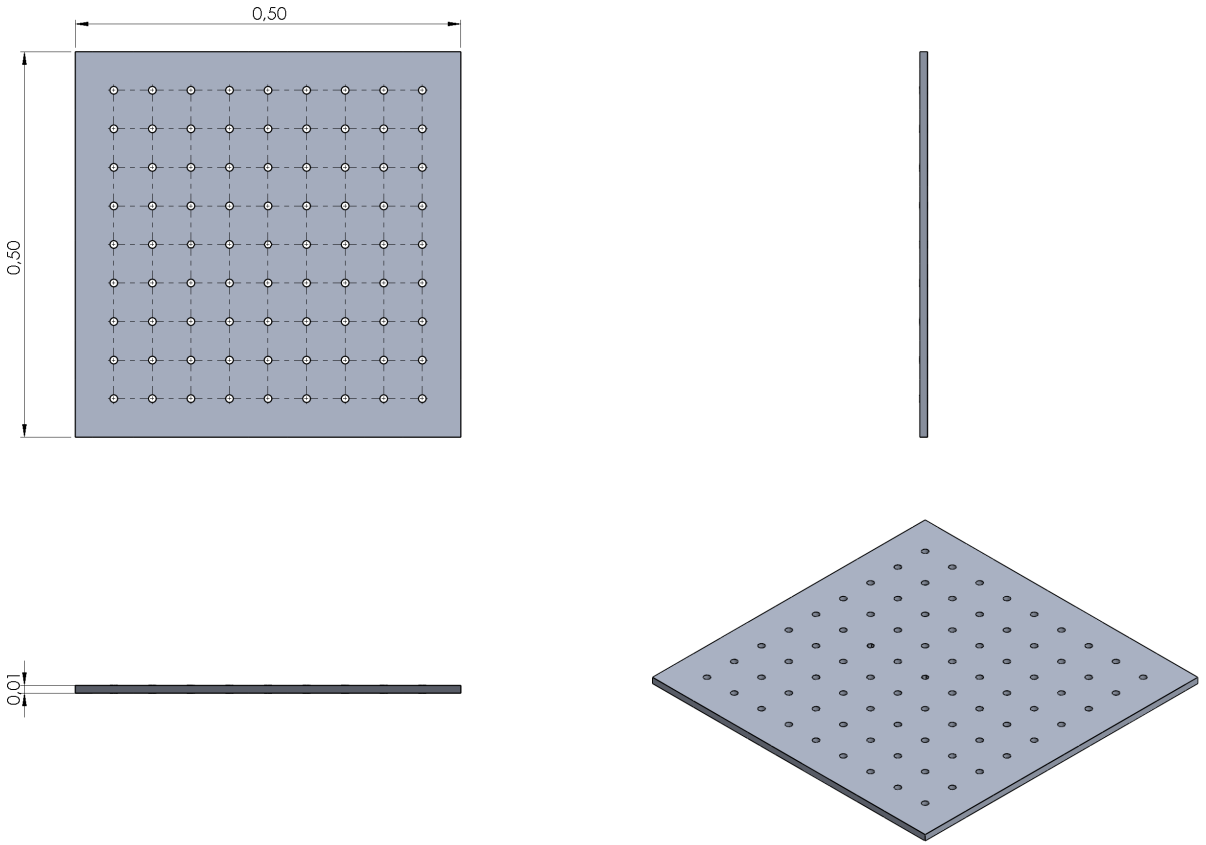

Figure A.2: **Oscillatory Satellite Platform [m]**

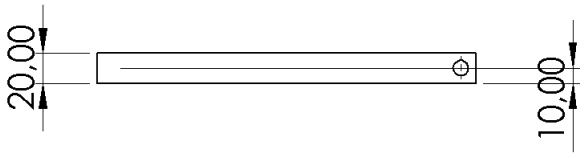

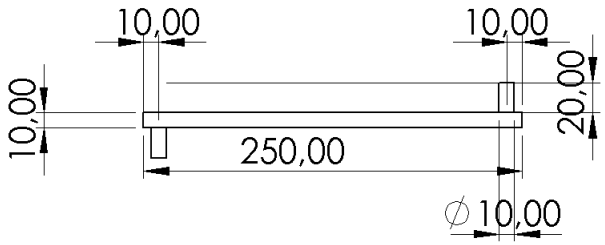

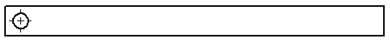

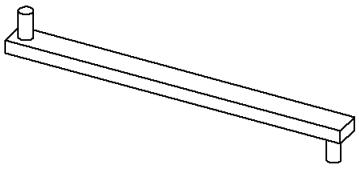

DO NOT SCALE DRAWING | REVISION

DEBURR AND
BREAK SHARP
EDGES

UNLESS OTHERWISE SPECIFIED:
DIMENSIONS ARE IN MILLIMETRES

TITLE:

Oscillatory Arm with Laser

MATERIAL:
1060 Aluminium Alloy

DWG NO.
3

A4

MASS: 0.14 kg

SCALE:1:5

SHEET 1 OF 1

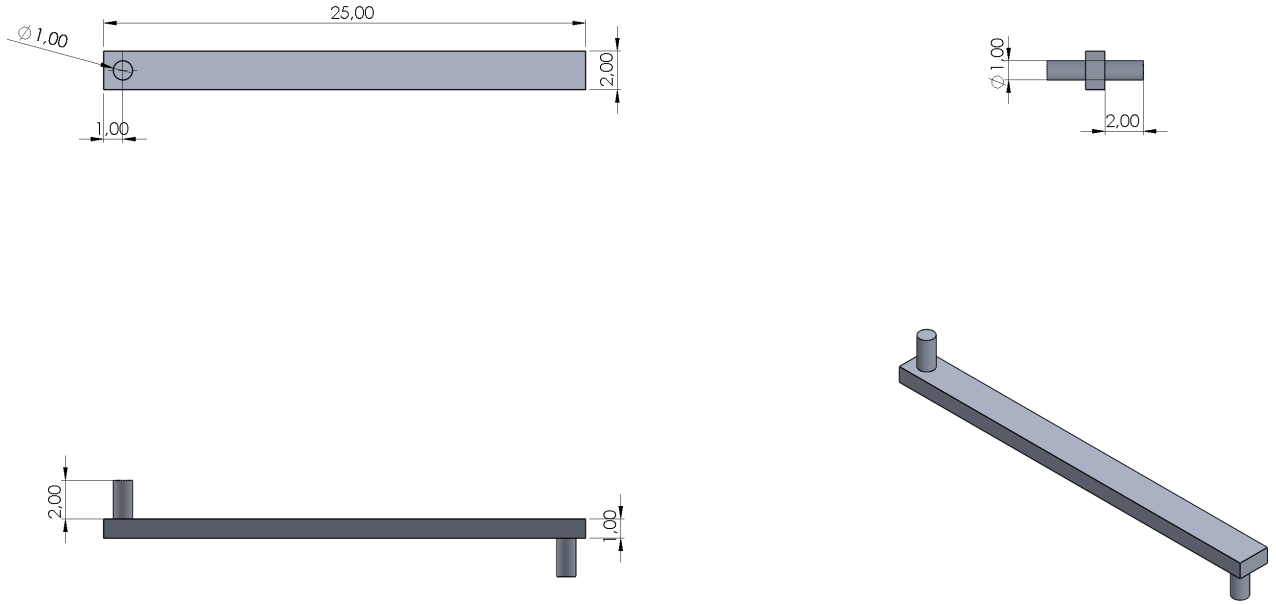

Figure A.3: **Oscillatory Arm With Laser [cm]**

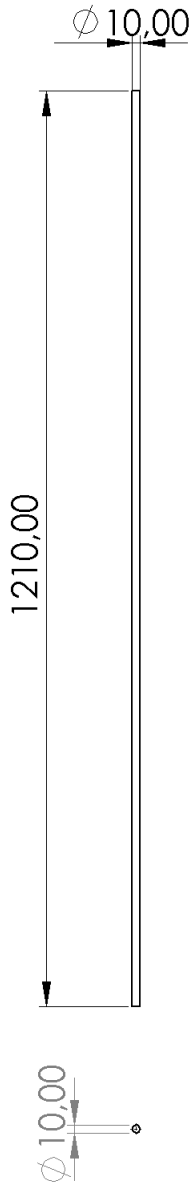

DO NOT SCALE DRAWING | REVISION

DEBURR AND
BREAK SHARP
EDGES

UNLESS OTHERWISE SPECIFIED:
DIMENSIONS ARE IN MILLIMETRES

TITLE:

Torsion Fiber

MATERIAL:
Steel

DWG NO.
4

A4

MASS: 10.26 g

SCALE:1:10

SHEET 1 OF 1

Figure A.4: **Torsion Fiber [mm]; for the sake of clarity we have exaggerated the diameter by a factor of 5**

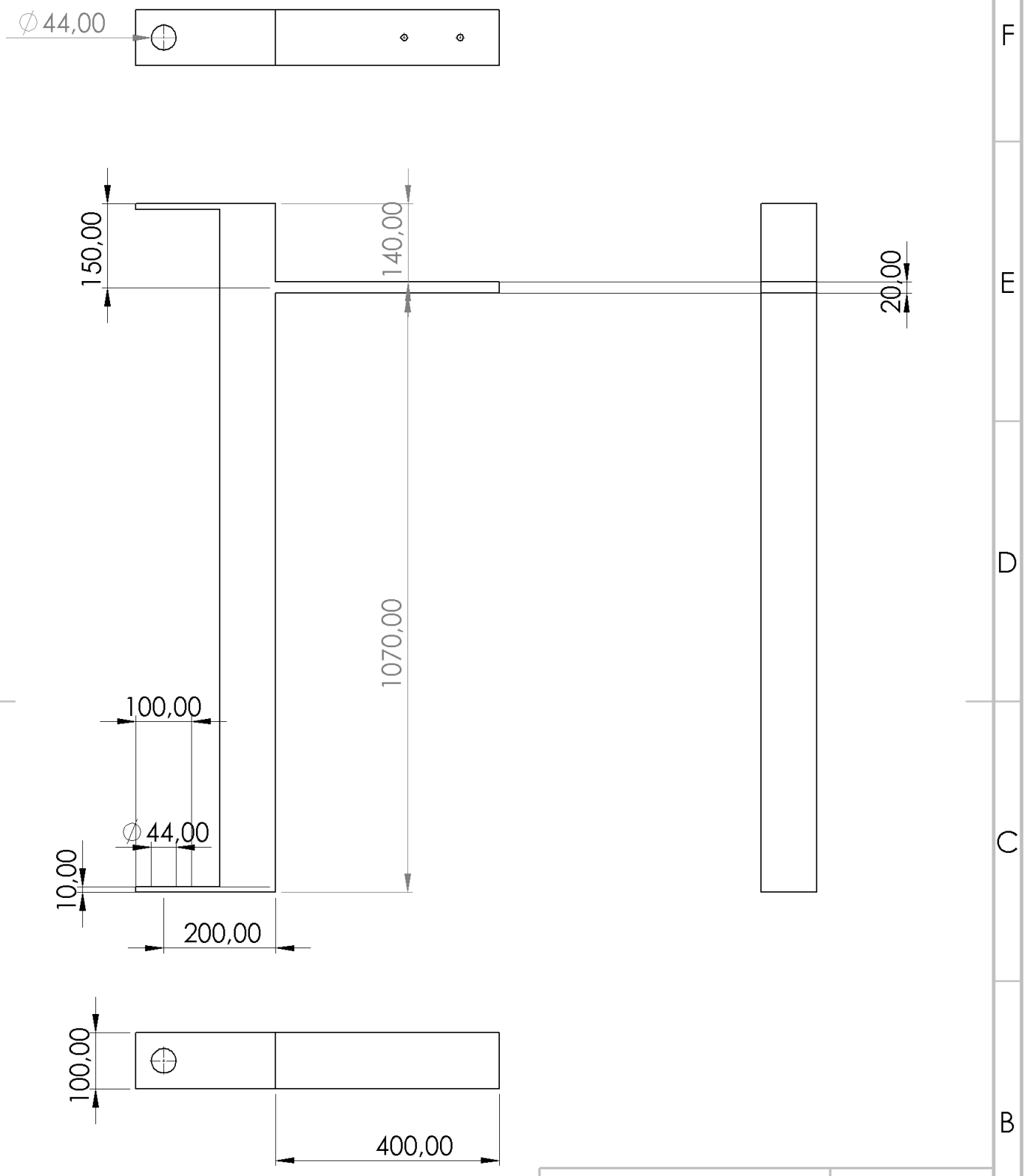

DO NOT SCALE DRAWING | REVISION

DEBURR AND
BREAK SHARP
EDGES

UNLESS OTHERWISE SPECIFIED:
DIMENSIONS ARE IN MILLIMETRES

TITLE:

Fixed Support Column

MATERIAL:
1060 Aluminium Alloy

DWG NO.
5

A4

MASS: 15.16 kg

SCALE:1:10

SHEET 1 OF 1

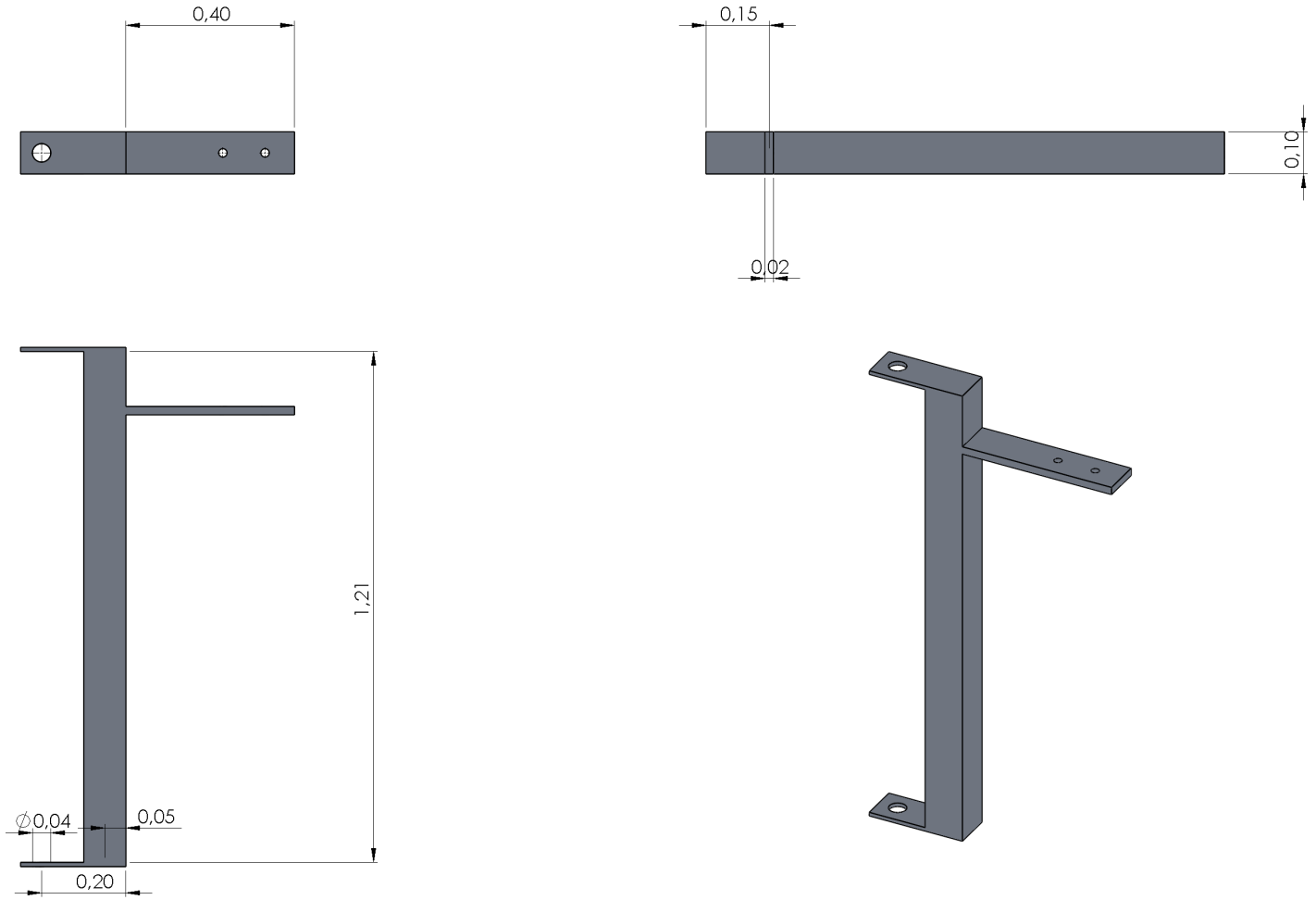

Figure A.5: **Fixed Support Column [m]**

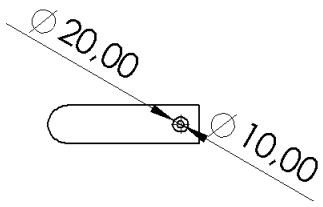

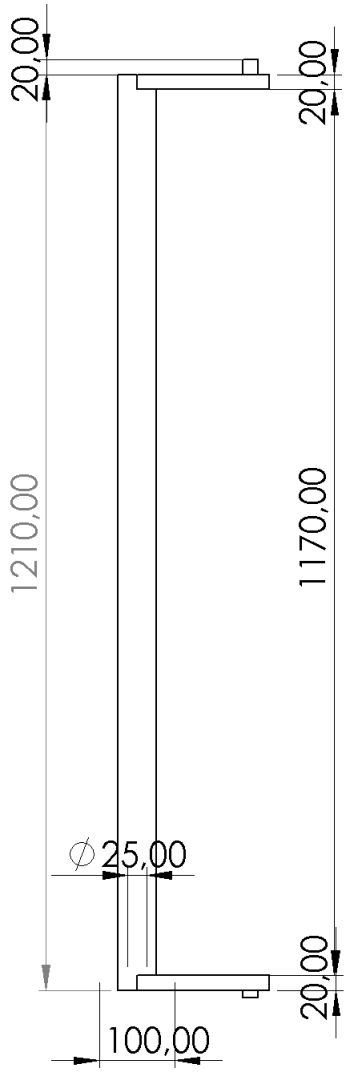

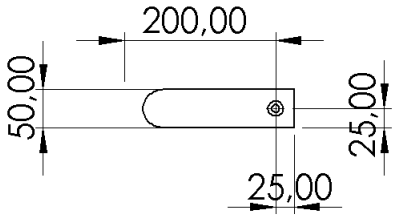

DO NOT SCALE DRAWING	REVISION
DEBURR AND BREAK SHARP EDGES	
UNLESS OTHERWISE SPECIFIED: DIMENSIONS ARE IN MILLIMETRES	TITLE: Oscillatory Support Column
MATERIAL: 1060 Aluminium Alloy	DWG NO. 6
	A4
MASS: 4.75 kg	SCALE:1:10
	SHEET 1 OF 1

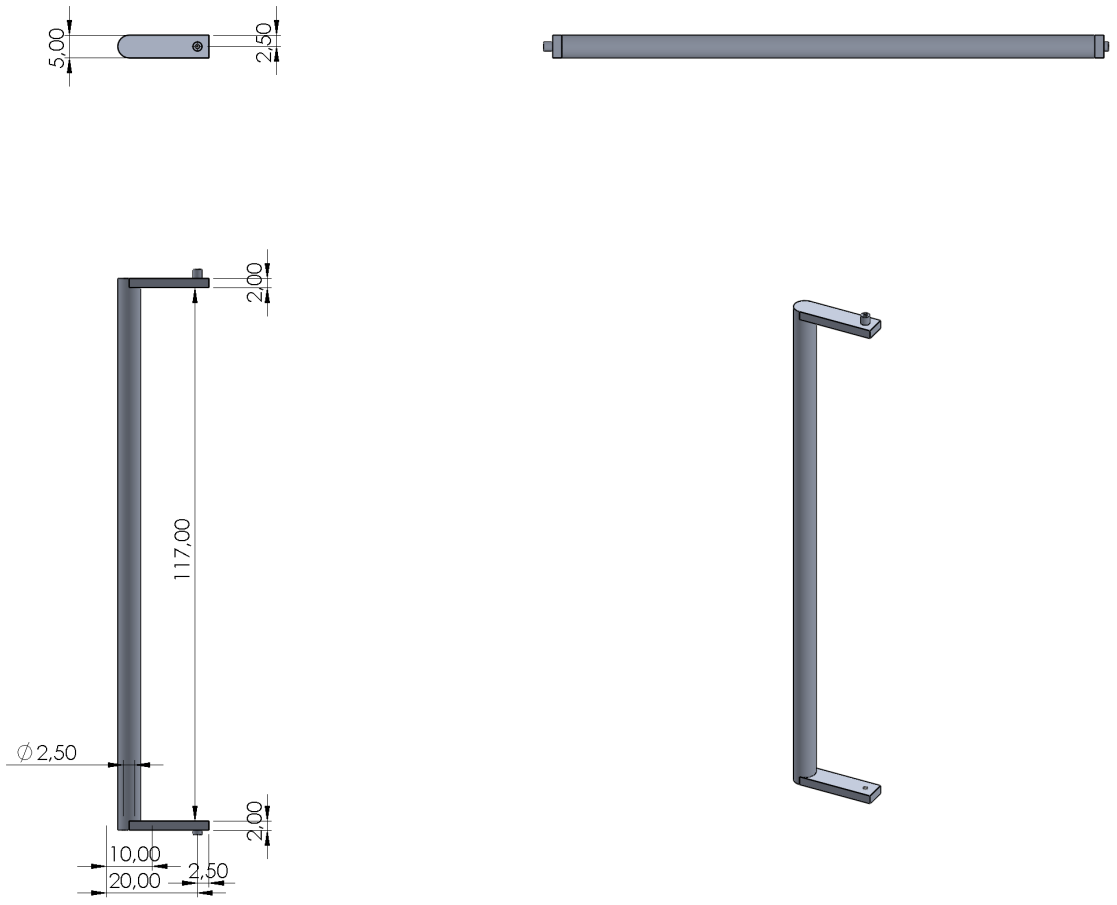

Figure A.6: **Oscillatory Support Column [cm]**

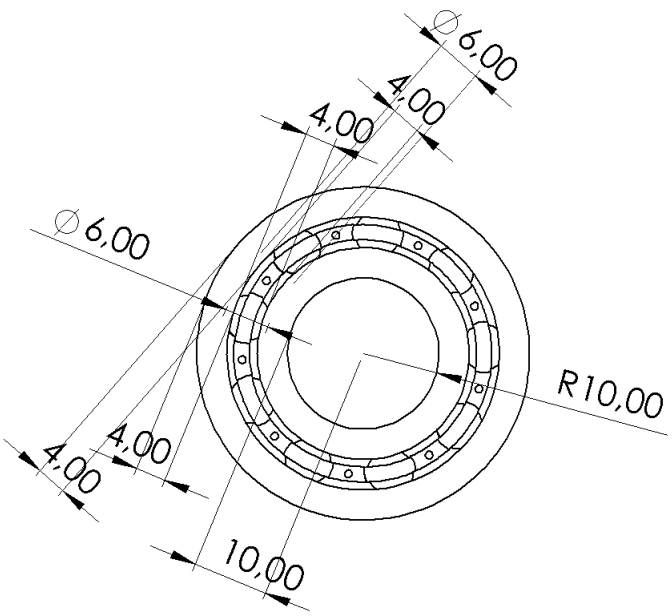

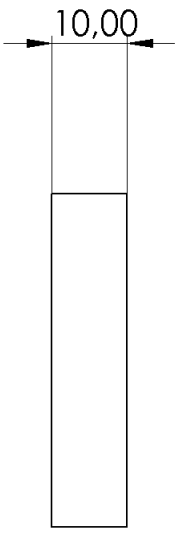

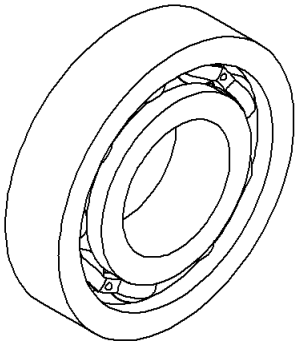

DO NOT SCALE DRAWING | REVISION

DEBURR AND
BREAK SHARP
EDGES

UNLESS OTHERWISE SPECIFIED:
DIMENSIONS ARE IN MILLIMETRES

TITLE:

Bearings

MATERIAL:
Steel

DWG NO.
7

A4

MASS: 64.12 g

SCALE:1:1

SHEET 1 OF 1

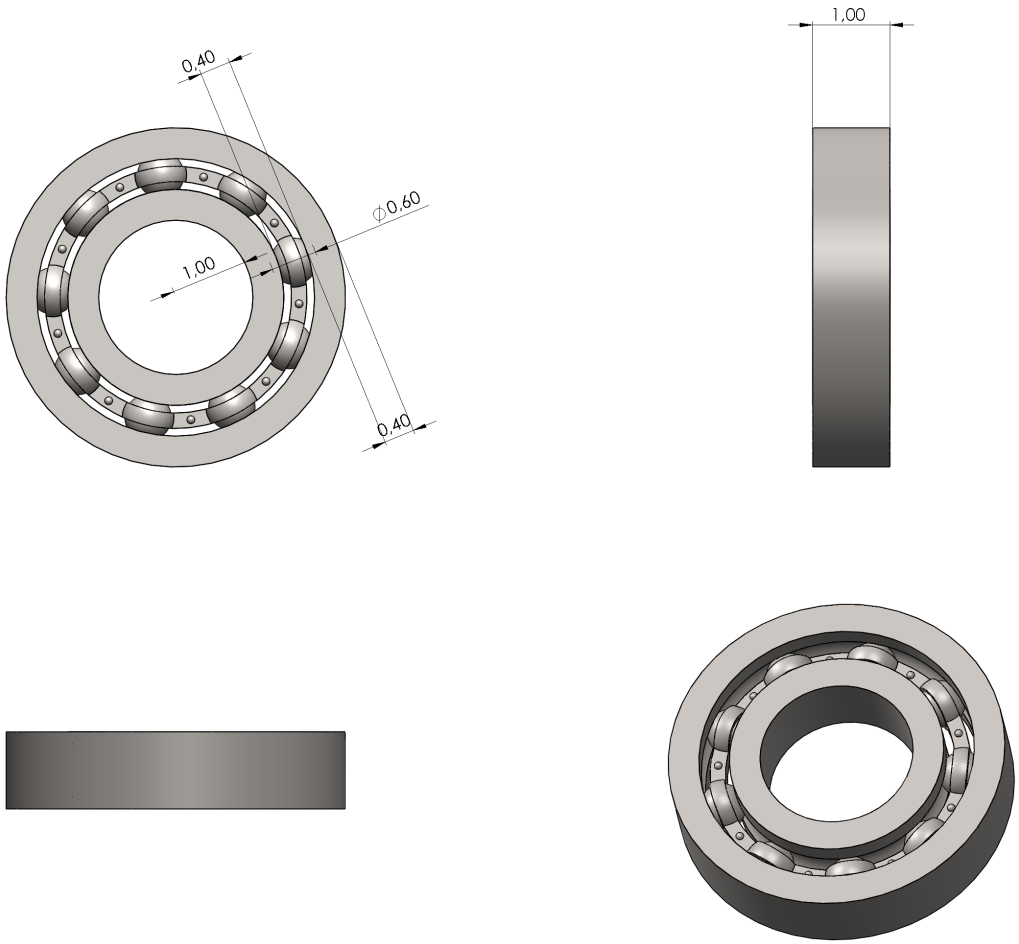

Figure A.7: **Bearing [cm]**

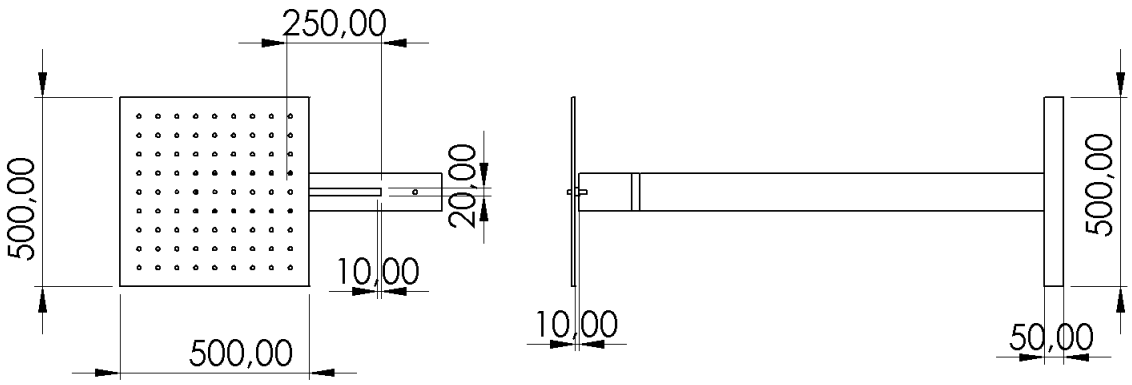

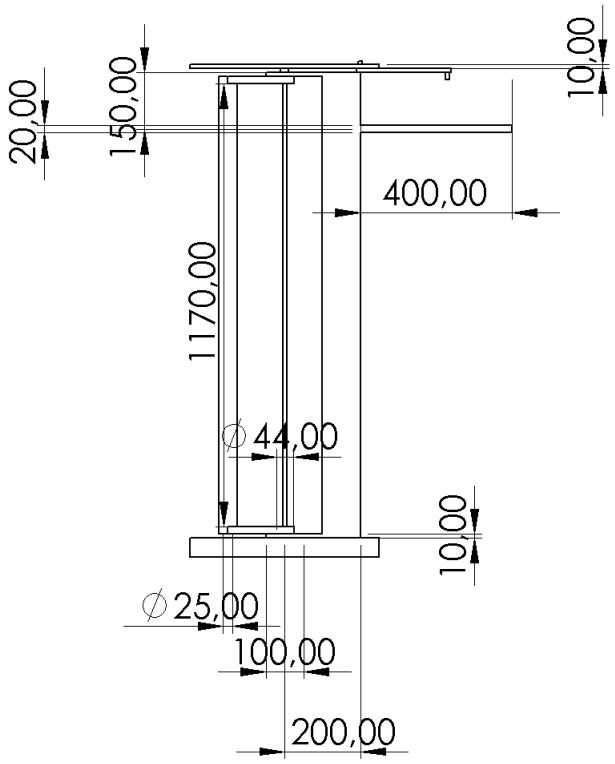

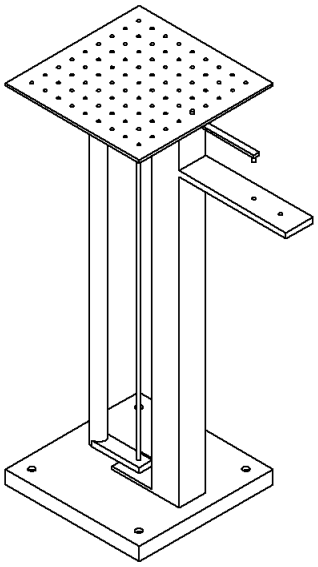

DO NOT SCALE DRAWING | REVISION

DEBURR AND
BREAK SHARP
EDGES

UNLESS OTHERWISE SPECIFIED:
DIMENSIONS ARE IN MILLIMETRES

TITLE:

Physical Pendulum

MATERIAL:
1060 Aluminium Alloy & Steel

DWG NO.
8

A4

MASS: 42.5 kg

SCALE:1:20

SHEET 1 OF 1

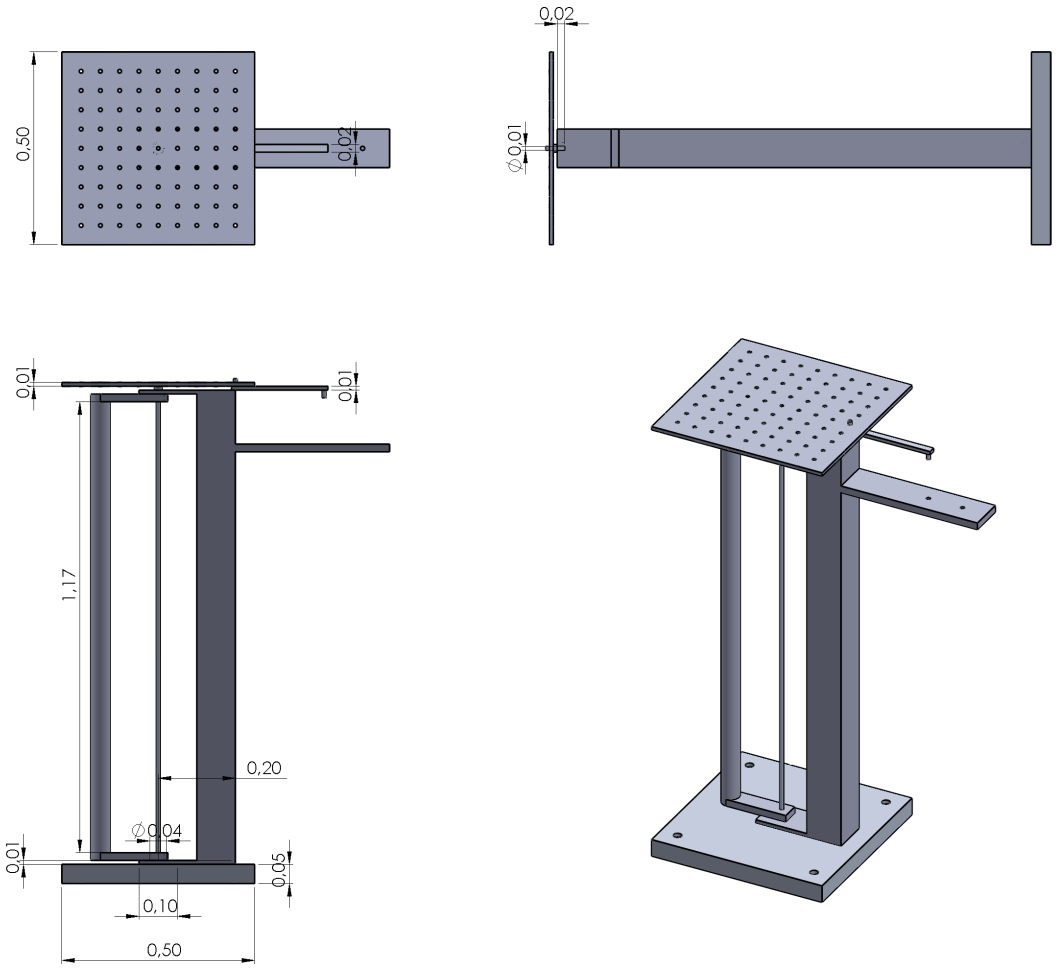

Figure A.8: **Physical Pendulum [m]**

APPENDIX B. SIMULATIONS

The present appendix shows the simulations performed for the study of Chapter 4. We divide the aforementioned simulations into two different sections:

B.1. Oscillatory Satellite Platform Analysis

B.1.1. First Simulation

In this first simulation we choose as the fixture the full base of the oscillating platform (as if it was directly weld to the floor) and we apply an external load of constant 80 N evenly distributed throughout the base, as can be seen in Figure B.1.

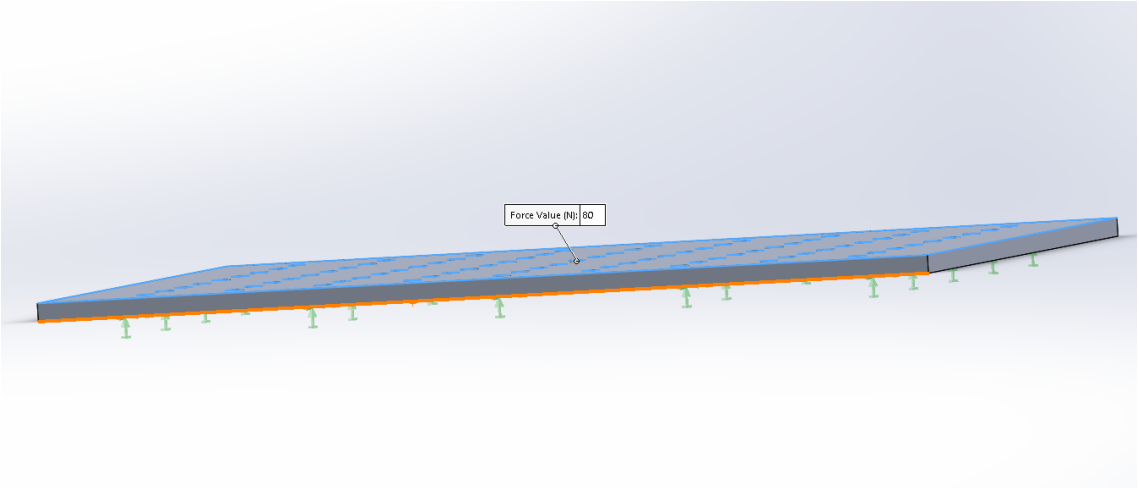

Figure B.1: Fixture and external load input

The analysis results are the following:

B.1.1.1. Stress simulation

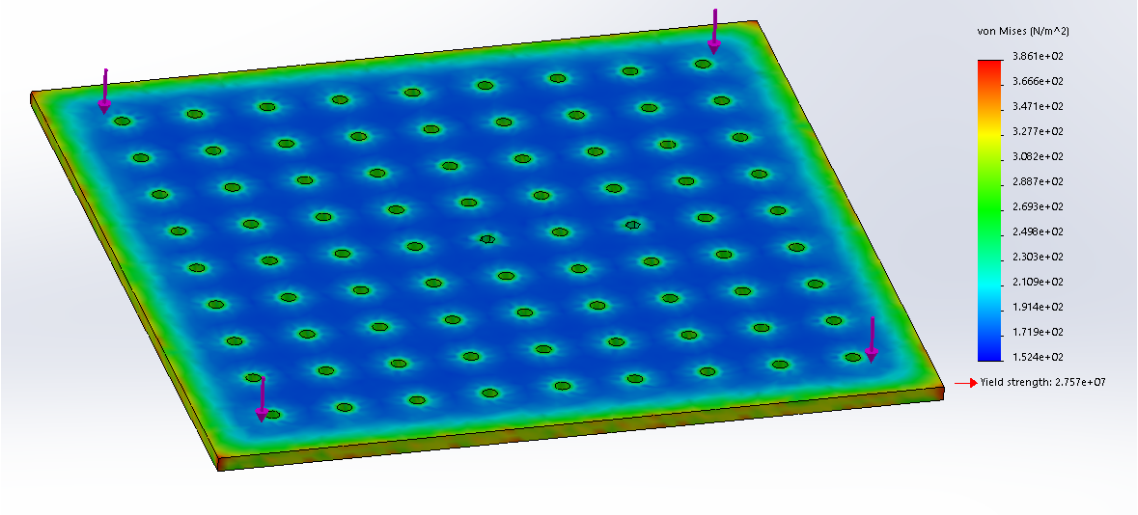

Figure B.2: Stress simulation

B.1.1.2. Displacement simulation

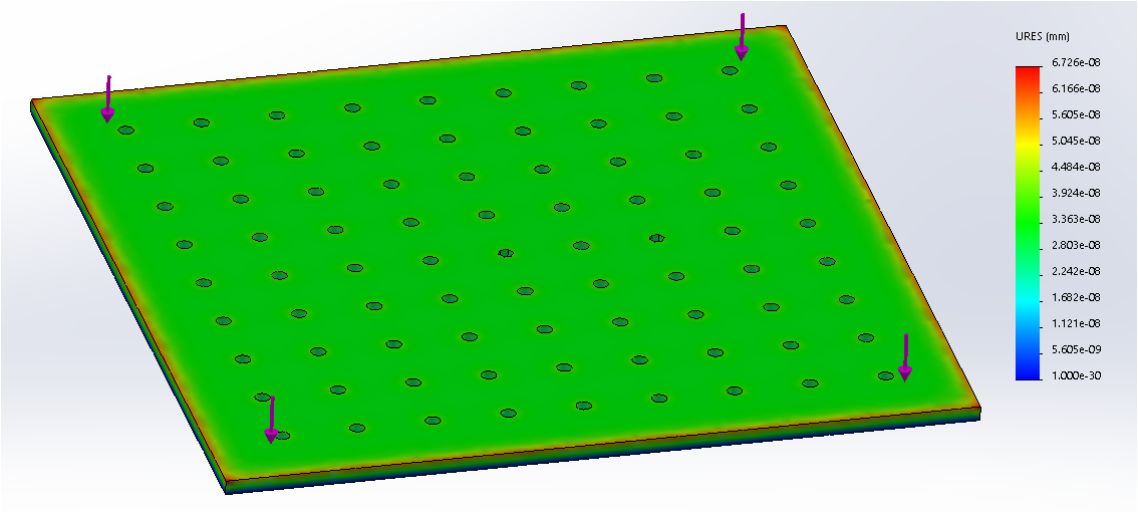

Figure B.3: Displacement simulation

B.1.1.3. Strain simulation

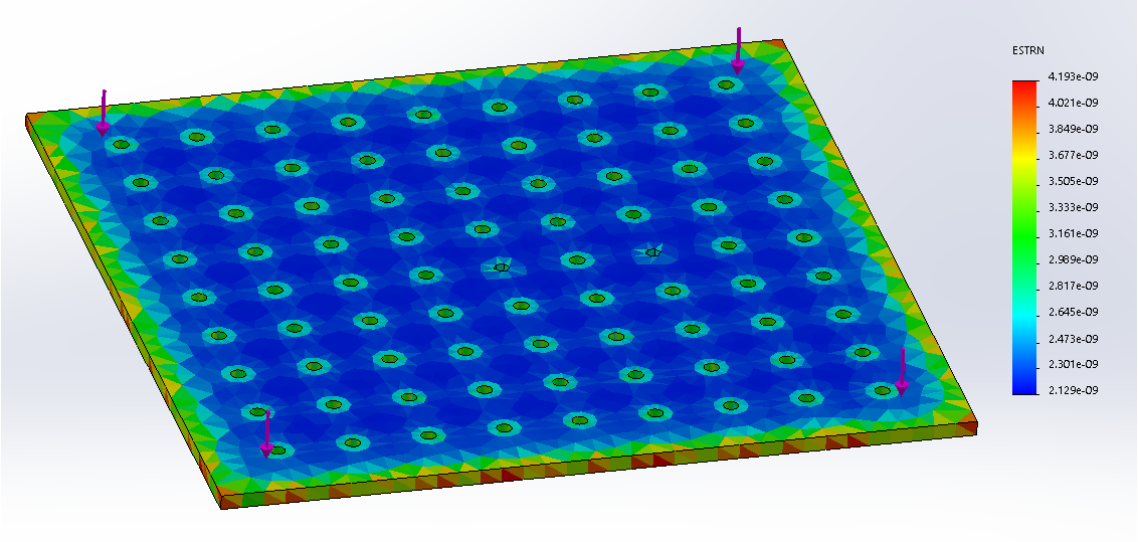

Figure B.4: Strain simulation

B.1.2. Second simulation

In this second simulation we choose as the fixture the center hexagonal hole and we apply the same external load of constant 80 N distributed throughout the base, as in the first simulation. The fixture (painted in green) and the external load (painted in purple) can be seen in Figure B.5.

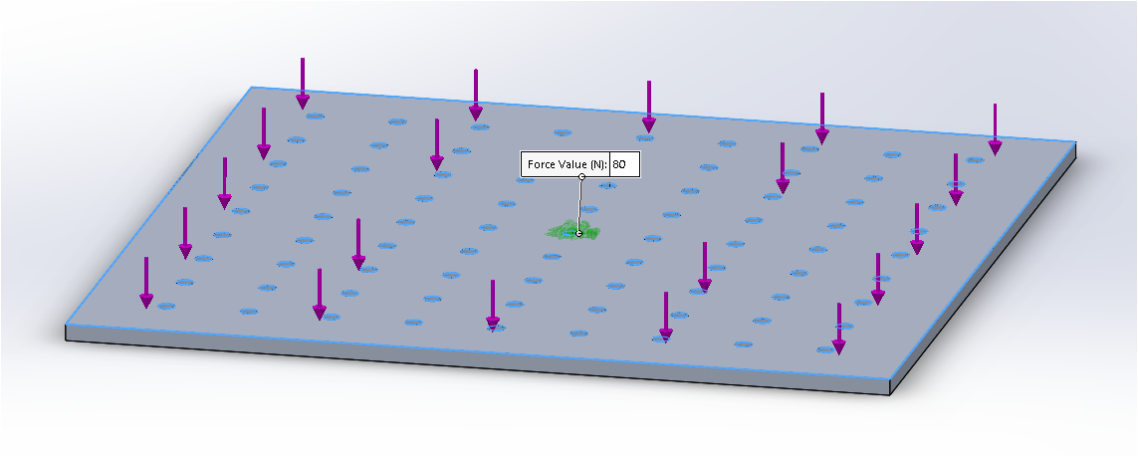

Figure B.5: Fixture and external load input

The analysis results are the following:

B.1.2.1. Stress simulation

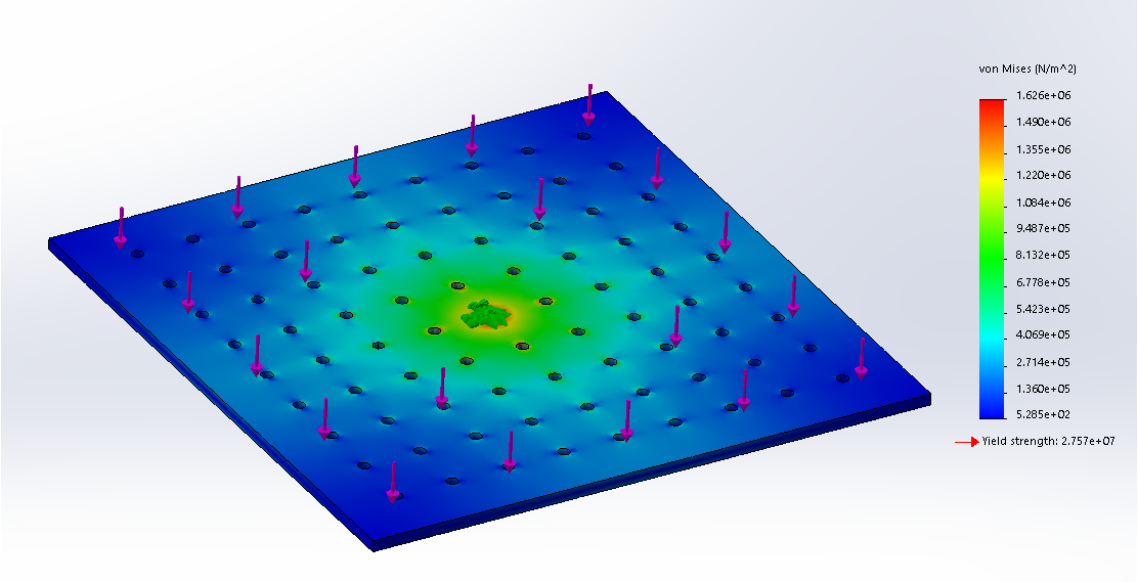

Figure B.6: Stress simulation

B.1.2.2. Displacement simulation

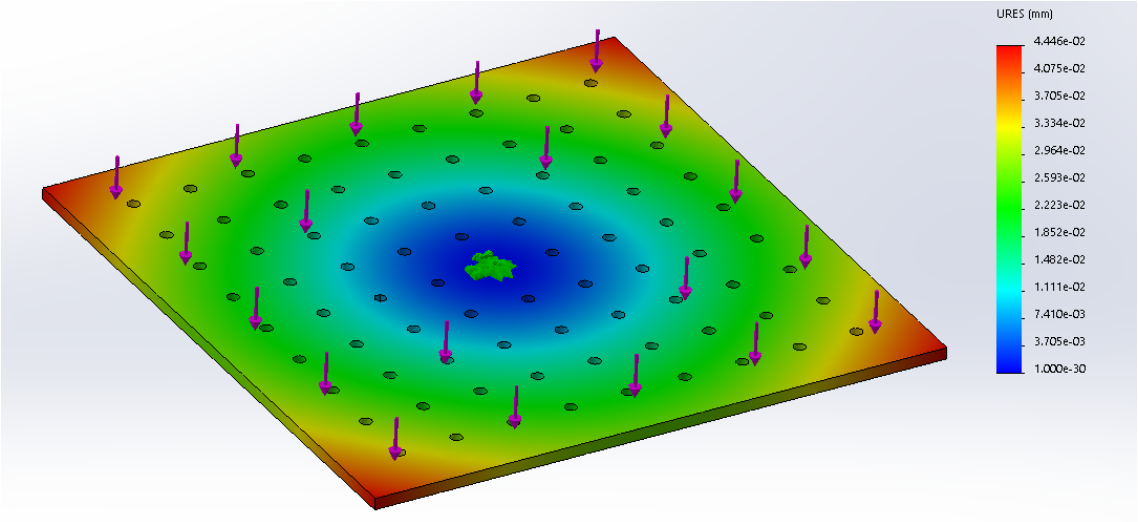

Figure B.7: Displacement simulation

B.1.2.3. Strain simulation

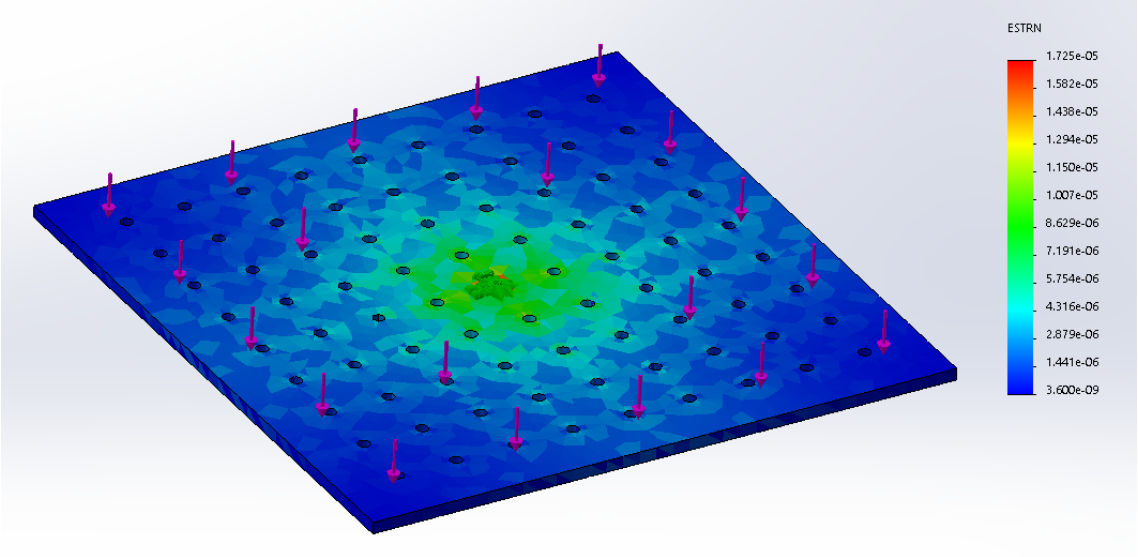

Figure B.8: Strain simulation

B.1.3. Third simulation

In this third simulation we choose as the fixture the hexagonal hole which is not centered (the one which is at 10 cm of the central, and colored in green) of the oscillating platform. Our input is again a constant 80 N load evenly distributed throughout the base (colored in purple). The simulation setup can be seen in Figure B.5.

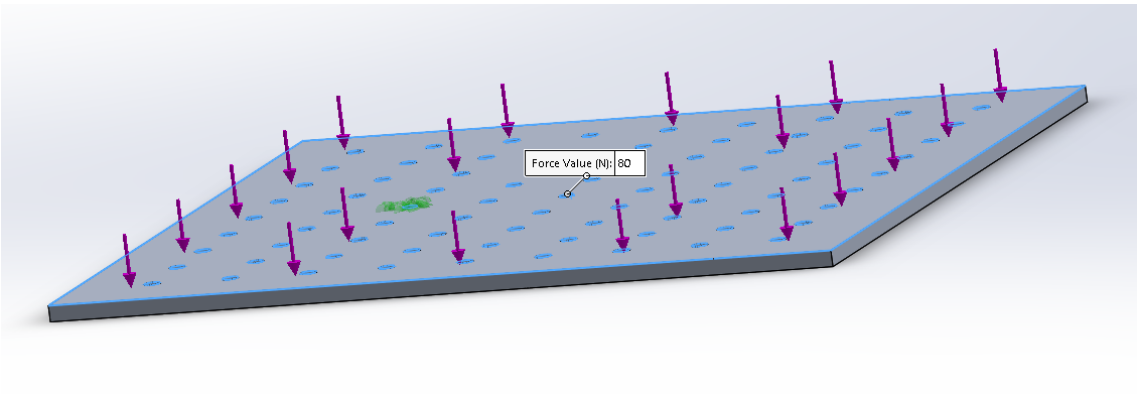

Figure B.9: Fixture and external load input

The analysis results are the following:

B.1.3.1. Stress simulation

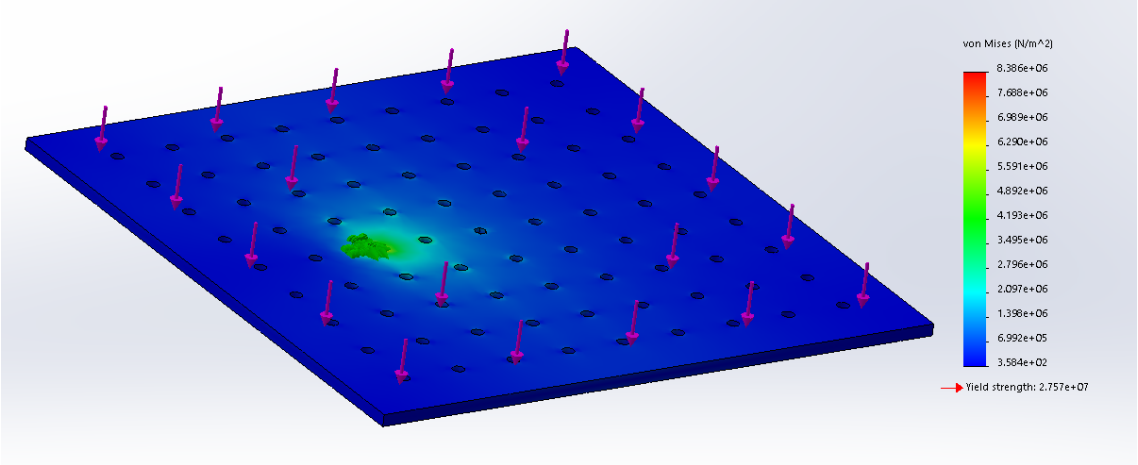

Figure B.10: Stress simulation

B.1.3.2. Displacement simulation

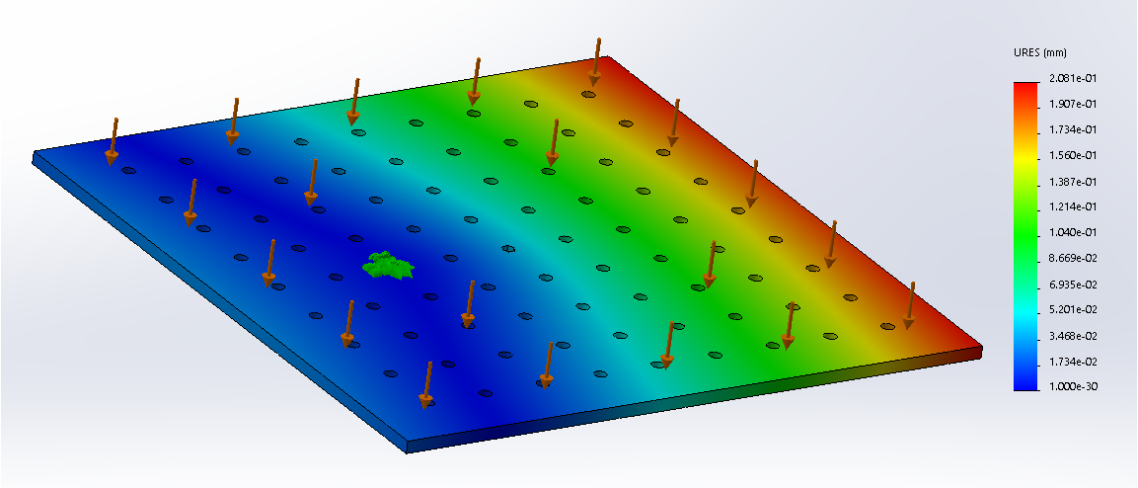

Figure B.11: Displacement simulation

B.1.3.3. Strain simulation

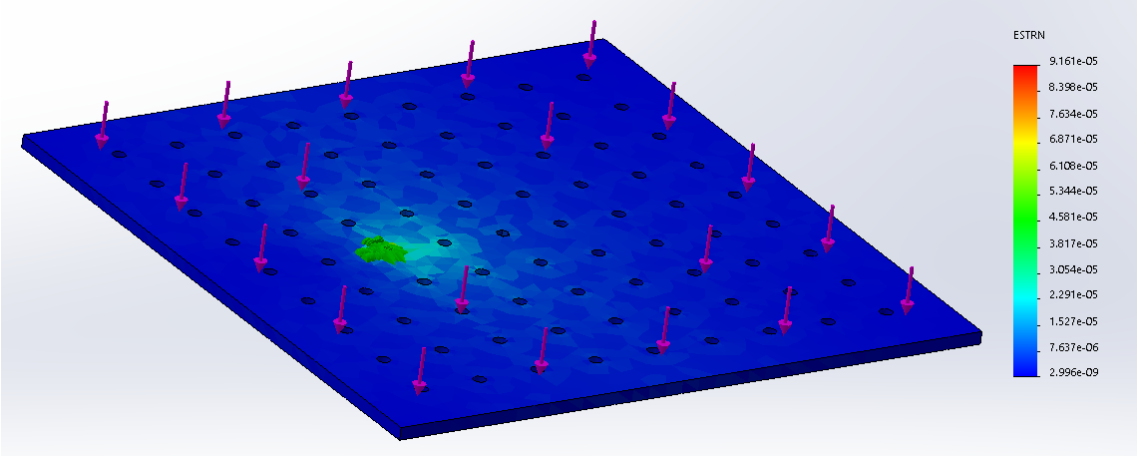

Figure B.12: Strain simulation

B.1.4. Fourth simulation

In this fourth and last simulation we consider the most extreme case: we choose as the fixture the hexagonal hole which is not centered and we apply a punctual external load of 80 N at one of two the farthest points from the fixture (that is, located in one of the two opposite diagonal), as can be seen in the figure B.5. Again the fixture is painted in green and the point of application of the external load is painted in purple. This is a worst, completely unrealistic case when using the torsion pendulum.

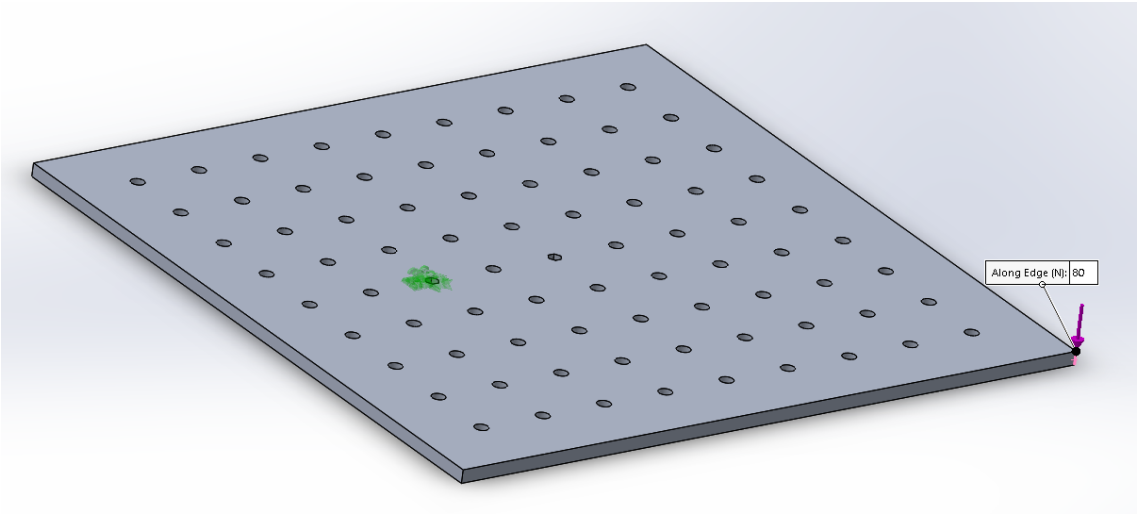

Figure B.13: Fixture and external load input

The analysis results are the following:

B.1.4.1. Stress simulation

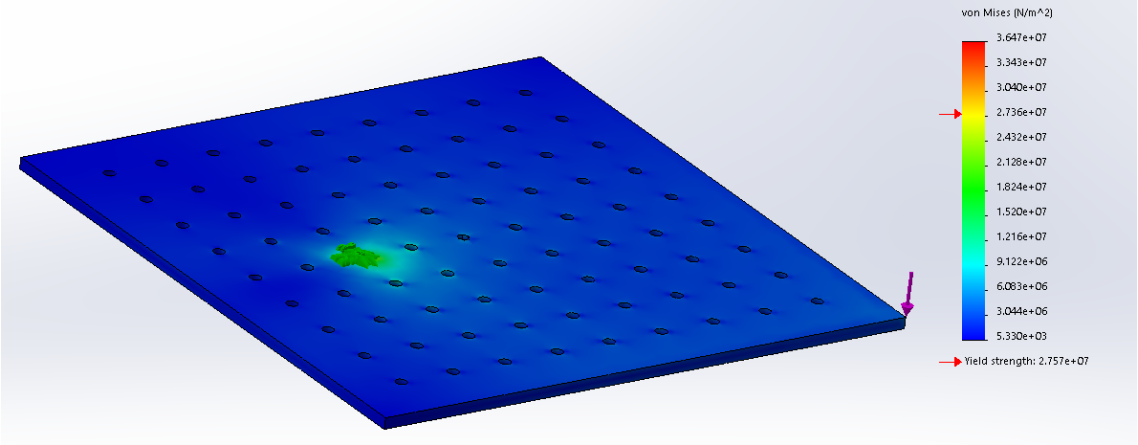

Figure B.14: Stress simulation

B.1.4.2. Displacement simulation

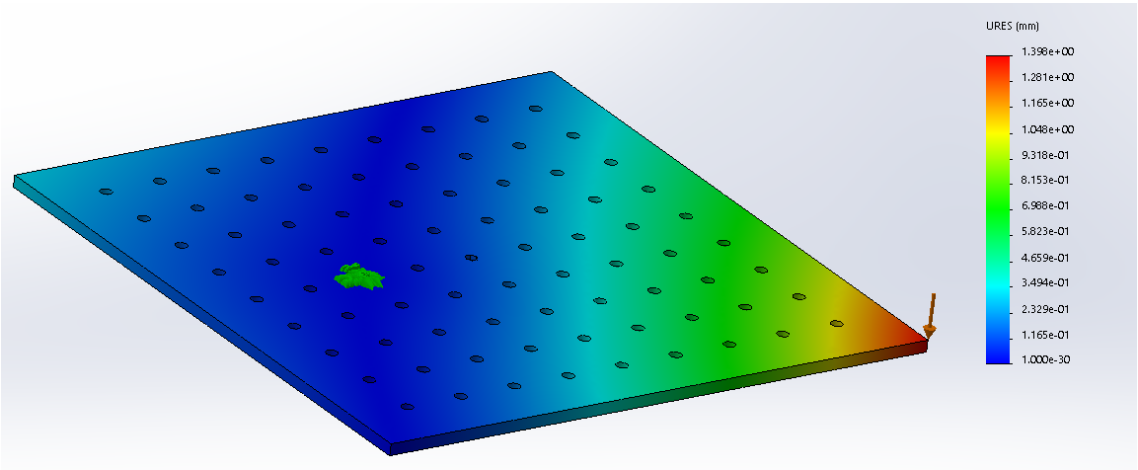

Figure B.15: Displacement simulation

B.1.4.3. Strain simulation

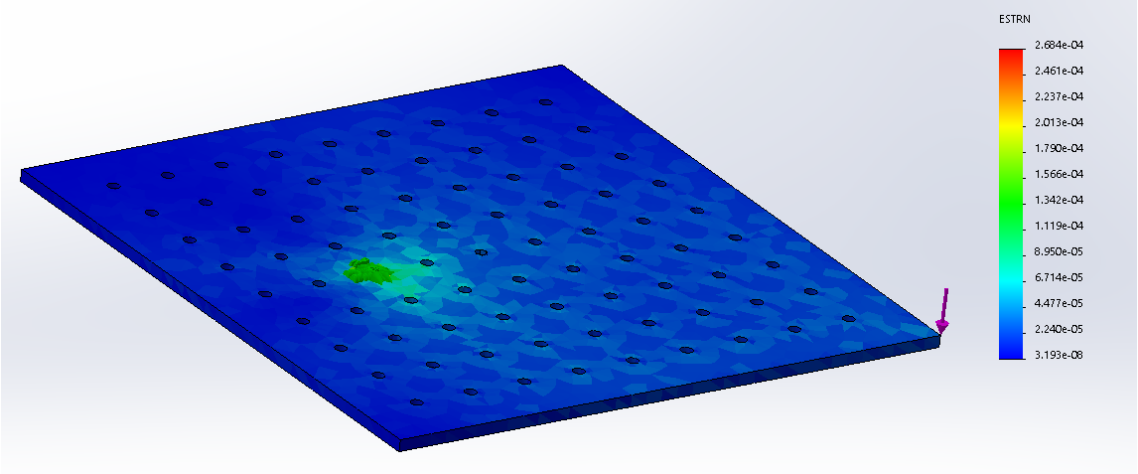

Figure B.16: Strain simulation

B.2. Pendulum Analysis

B.2.1. First Simulation

In this first simulation we choose as the fixture the full base of the pendulum base 3.2.1. (as if it was directly weld to the floor), and we apply an external load of constant 80 N evenly distributed throughout the base, as can be seen in Figure B.17.

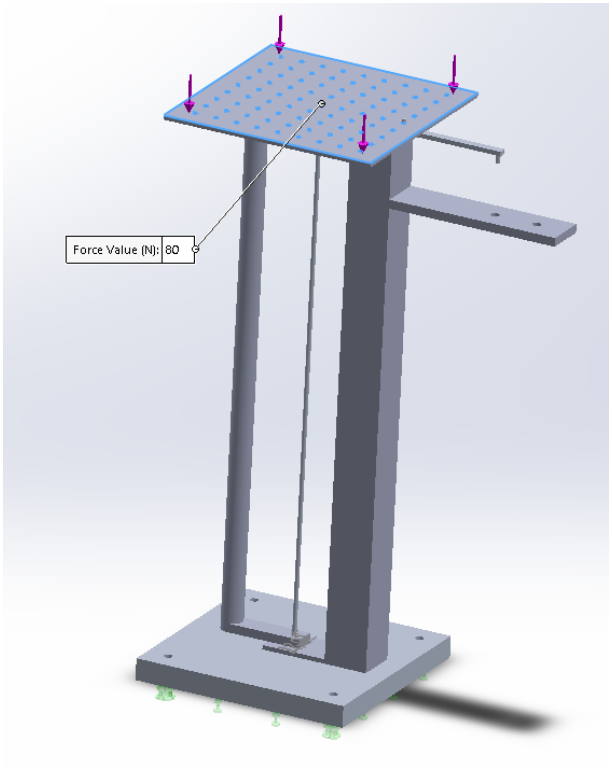

Figure B.17: Fixture and external load input

B.2.1.1. Stress simulation

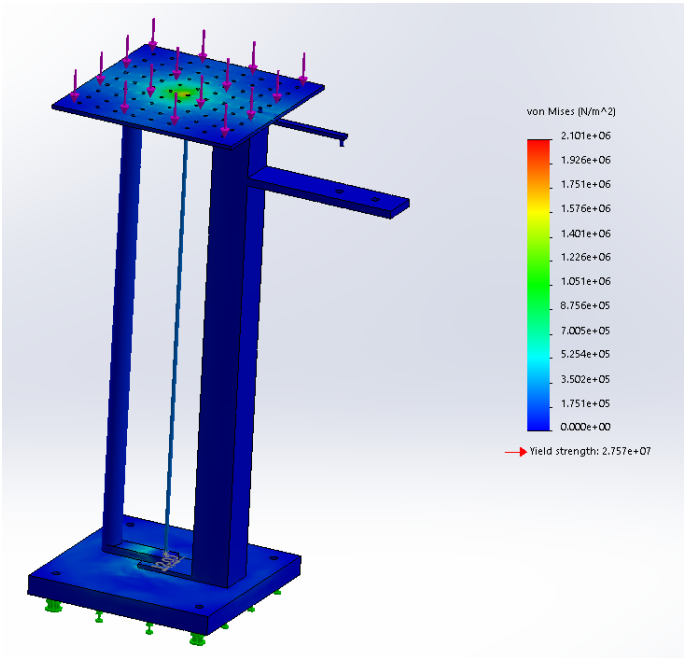

Figure B.18: Stress simulation

B.2.1.2. Displacement simulation

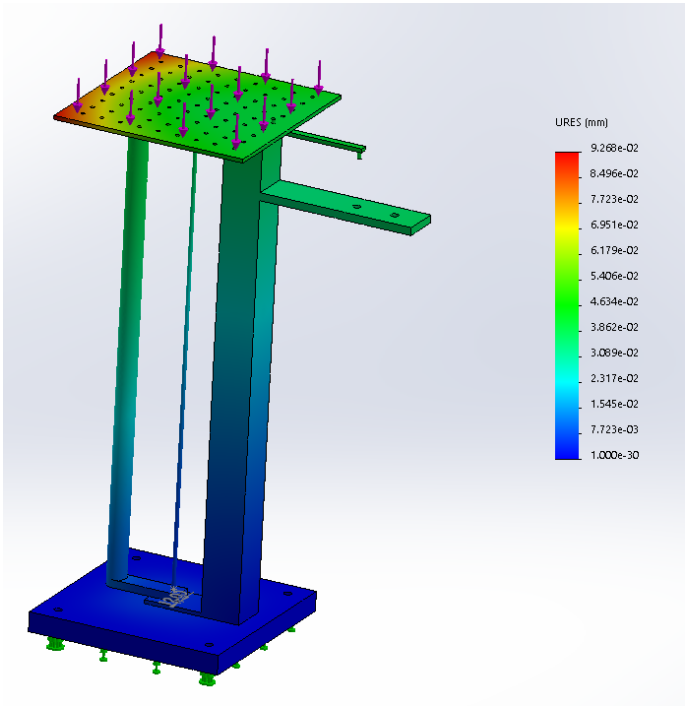

Figure B.19: Displacement simulation

B.2.1.3. Strain simulation

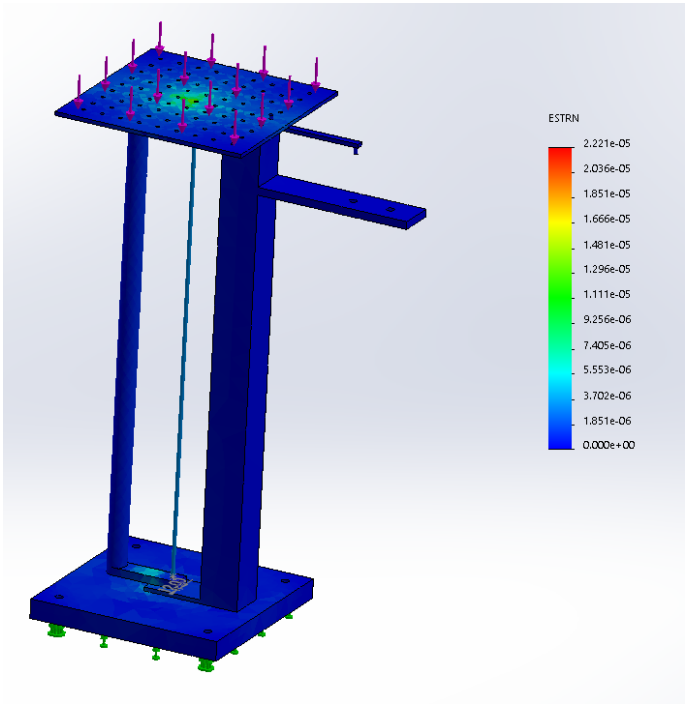

Figure B.20: Strain simulation

B.2.2. Second simulation

In this second simulation we consider the most extreme case we can perform to test the platform. We choose as the fixture the full base of the pendulum base 3.2.1. (as if it was directly weld to the floor) and we apply a punctual external load of 80 N at one of four farthest points from the center of the oscillatory satellite platform 3.2.2. as can be seen in Figure B.21. Again, this is a worst, completely unrealistic case when using the torsion pendulum.

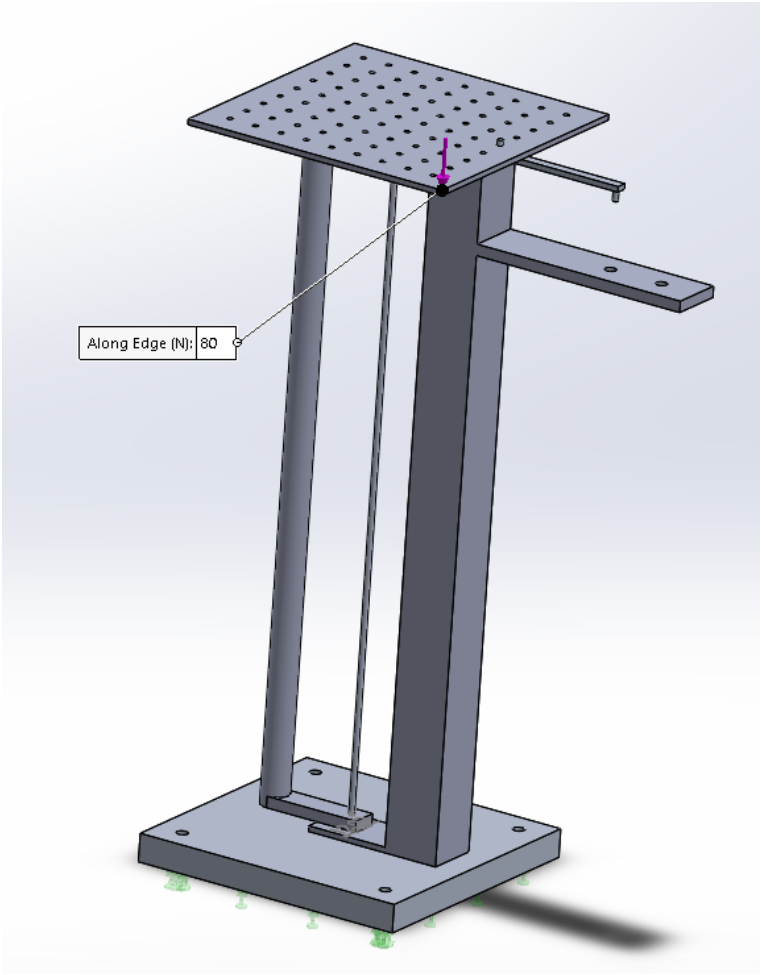

Figure B.21: Fixture and external load input

B.2.2.1. Stress simulation

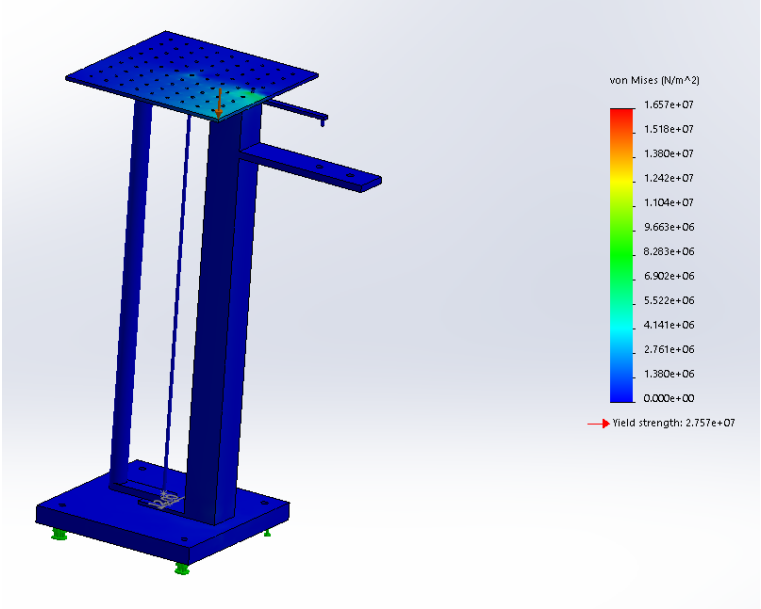

Figure B.22: Stress simulation

B.2.2.2. Displacement simulation

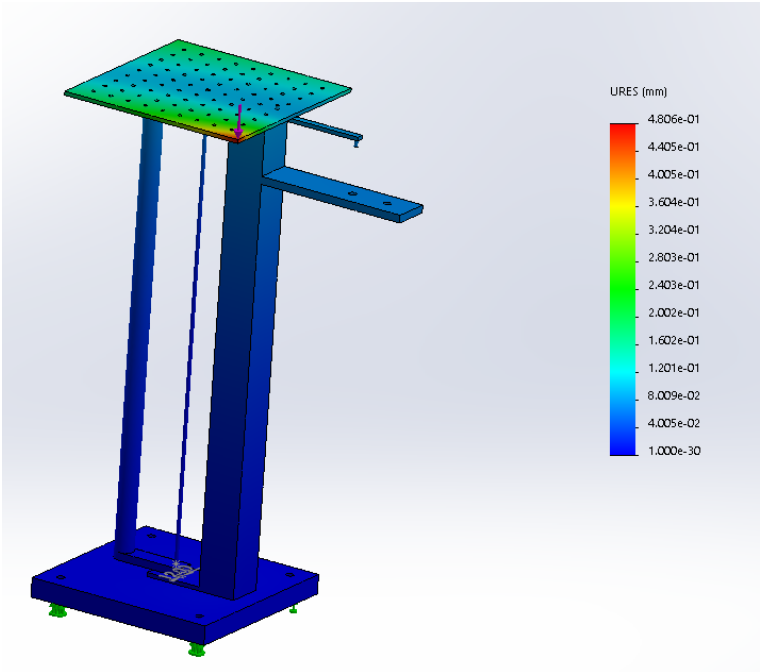

Figure B.23: Displacement simulation

B.2.2.3. Strain simulation

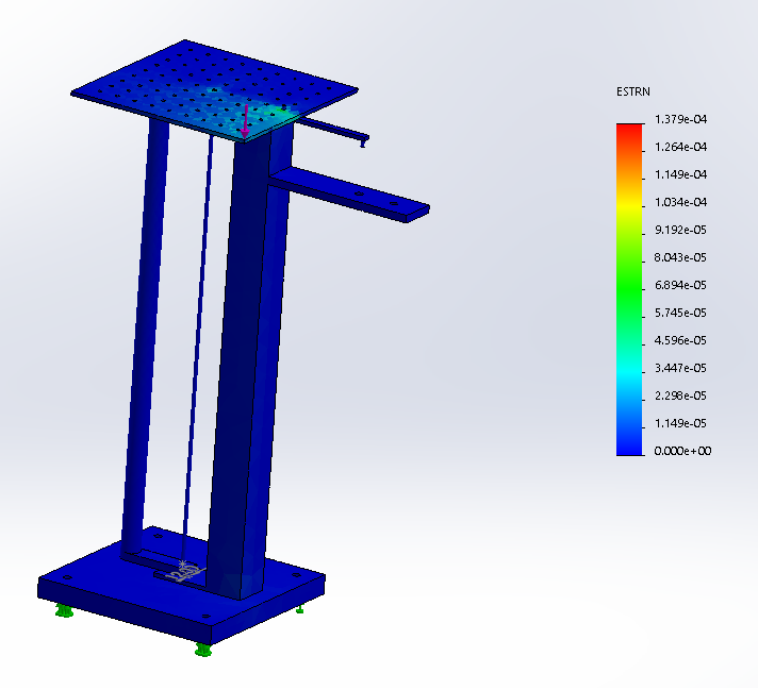

Figure B.24: Strain simulation

B.2.3. Third simulation

In this third simulation we choose as the fixture the full base of the pendulum base 3.2.1. (as if it was directly weld to the floor) and we apply an external load of constant 80 N evenly distributed throughout the base, as can be seen in Figure B.25.

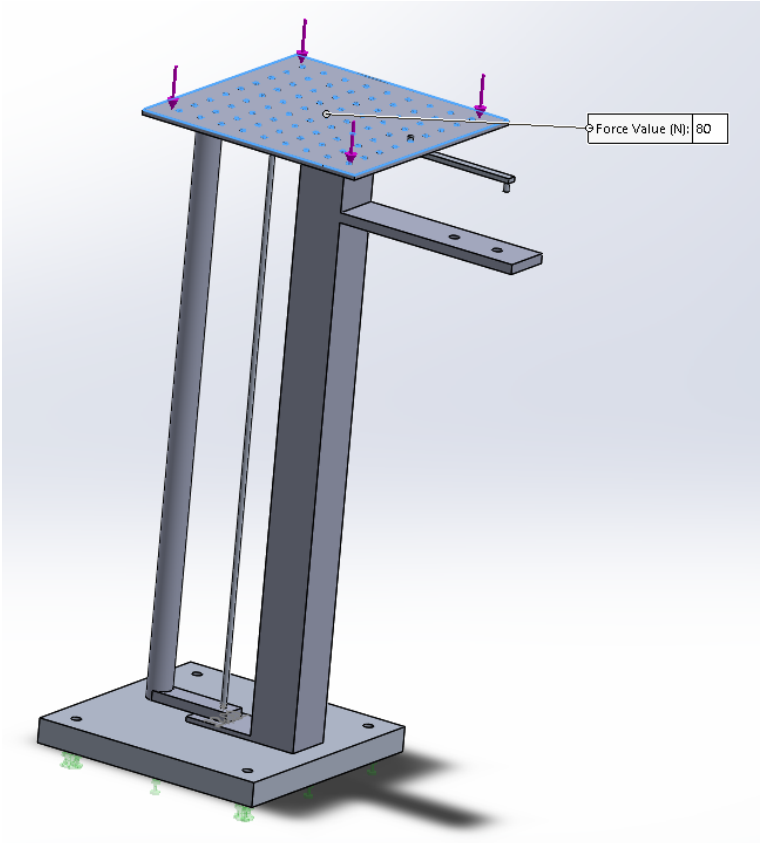

Figure B.25: Fixture and external load input

B.2.3.1. Stress simulation

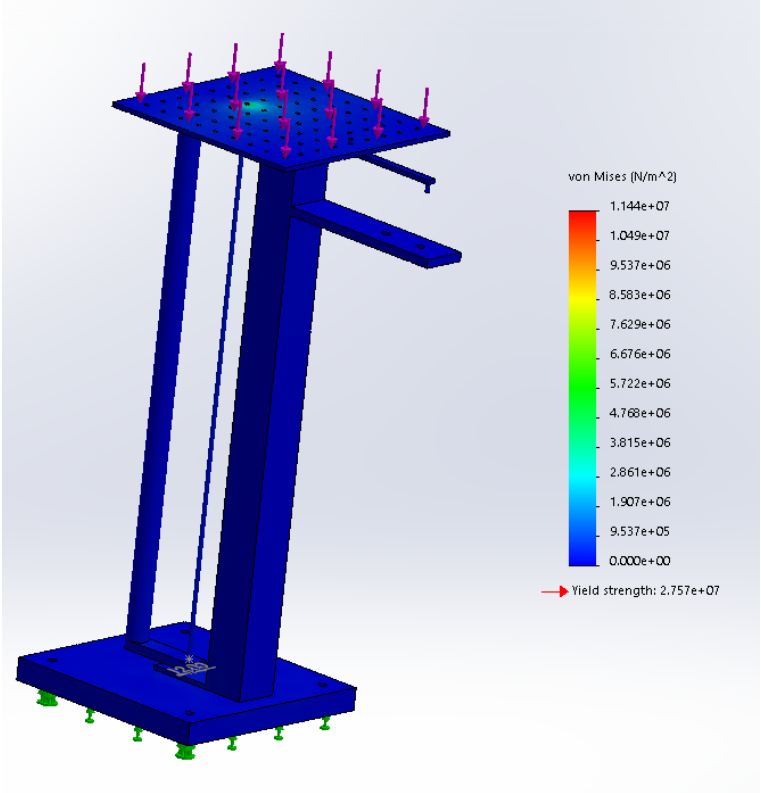

Figure B.26: Stress simulation

B.2.3.2. Displacement simulation

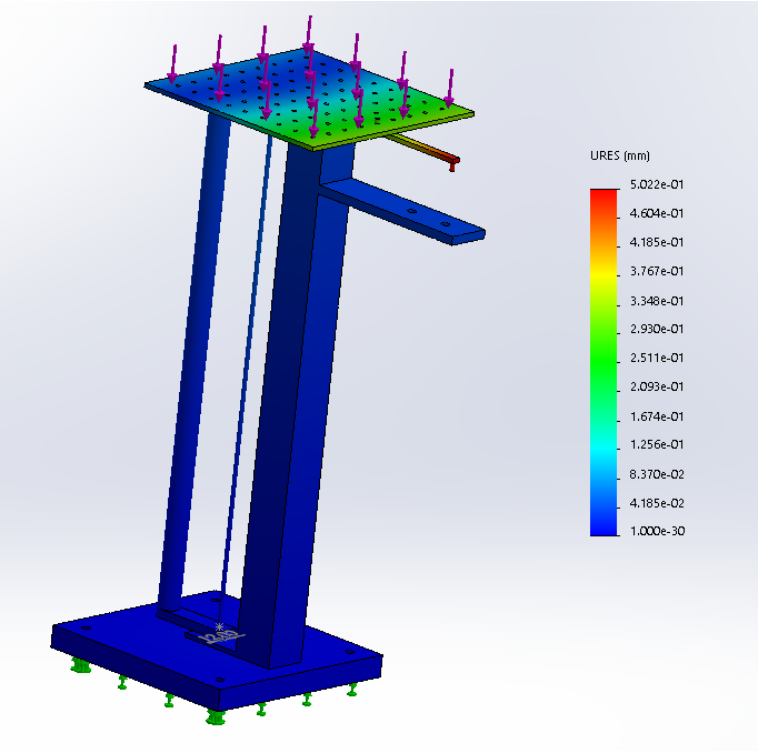

Figure B.27: Displacement simulation

B.2.3.3. Strain simulation

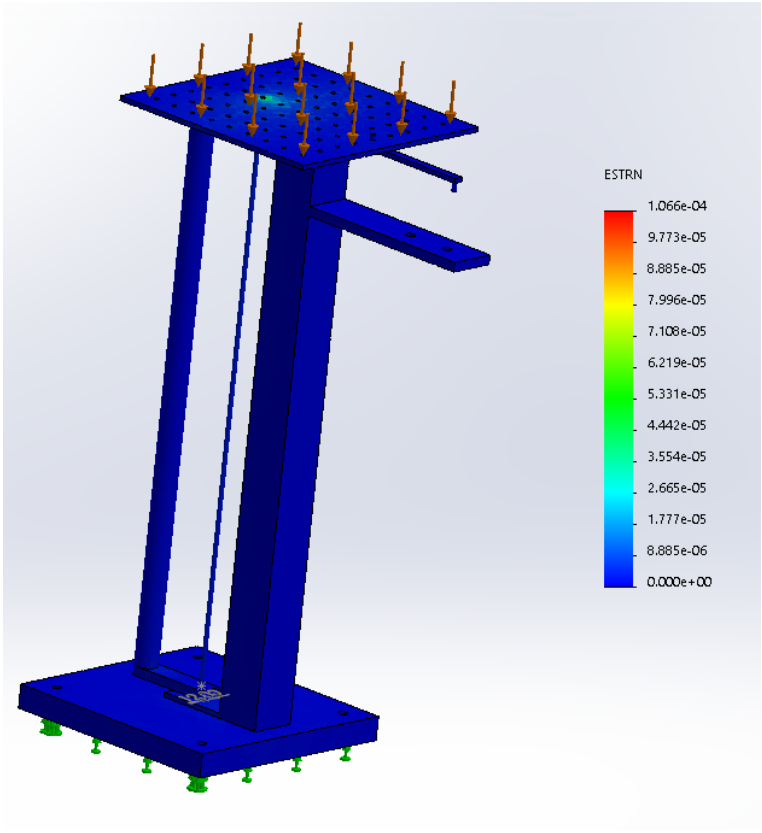

Figure B.28: Strain simulation

B.2.4. Fourth simulation

In this fourth simulation we consider the most extreme case we can perform to test the platform. We choose as the fixture the full base of the pendulum base 3.2.1. (as if it was directly weld to the floor) and we apply a point external load of 80 N at one of the four farthest points from the center of the oscillatory satellite platform 3.2.2., as can be seen in Figure B.29. Again, this is a worst, completely unrealistic case to when using the torsion pendulum.

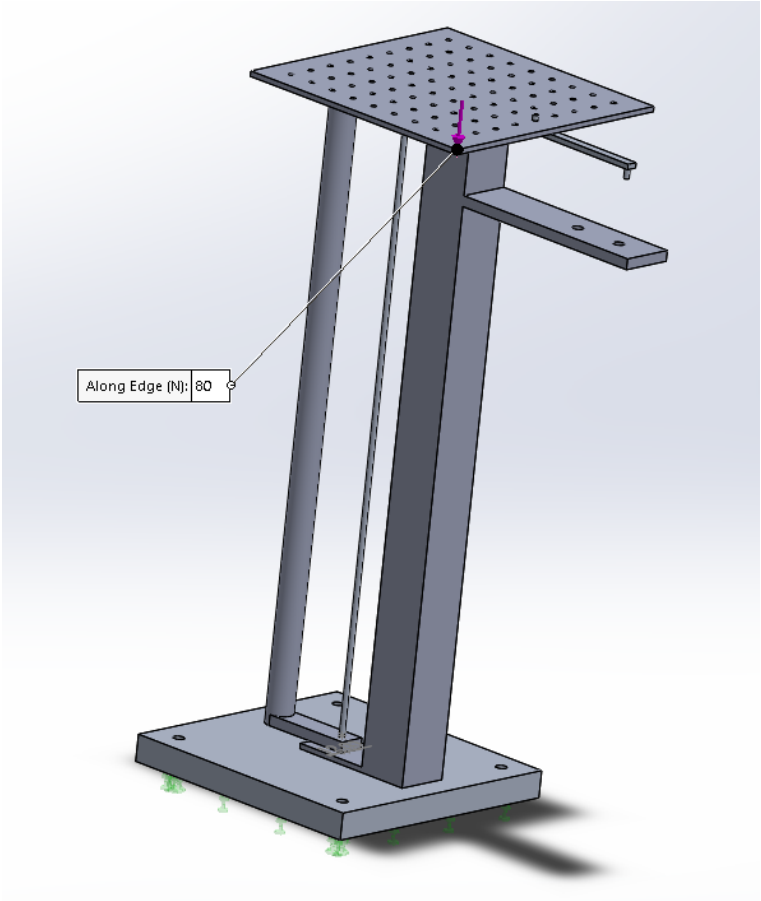

Figure B.29: Fixture and external load input

B.2.4.1. Stress simulation

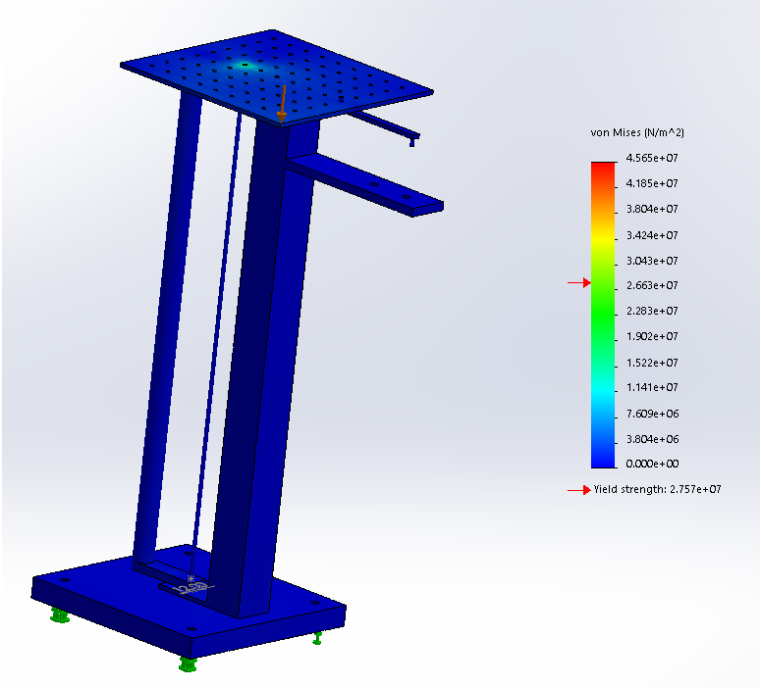

Figure B.30: Stress simulation

B.2.4.2. Displacement simulation

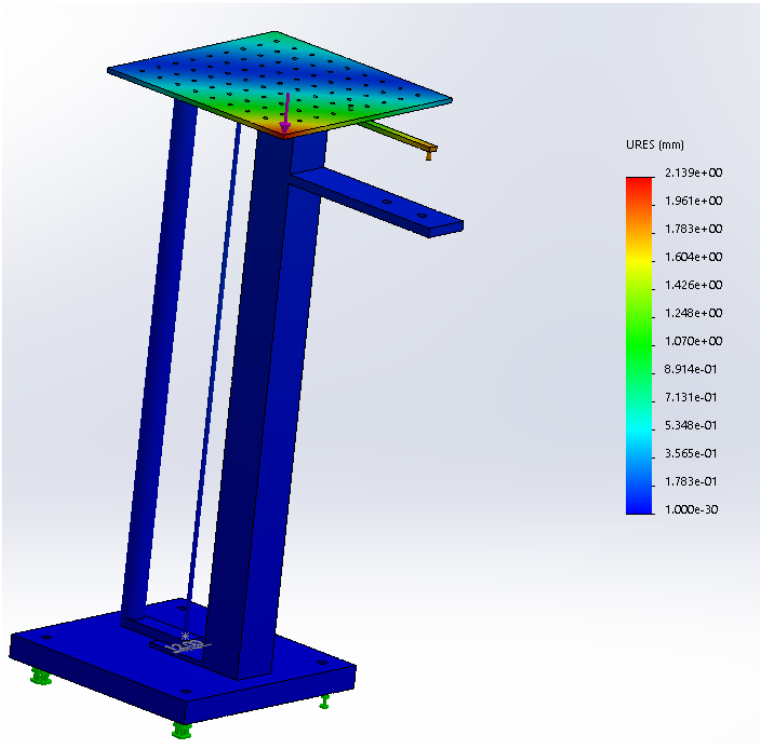

Figure B.31: Displacement simulation

B.2.4.3. Strain simulation

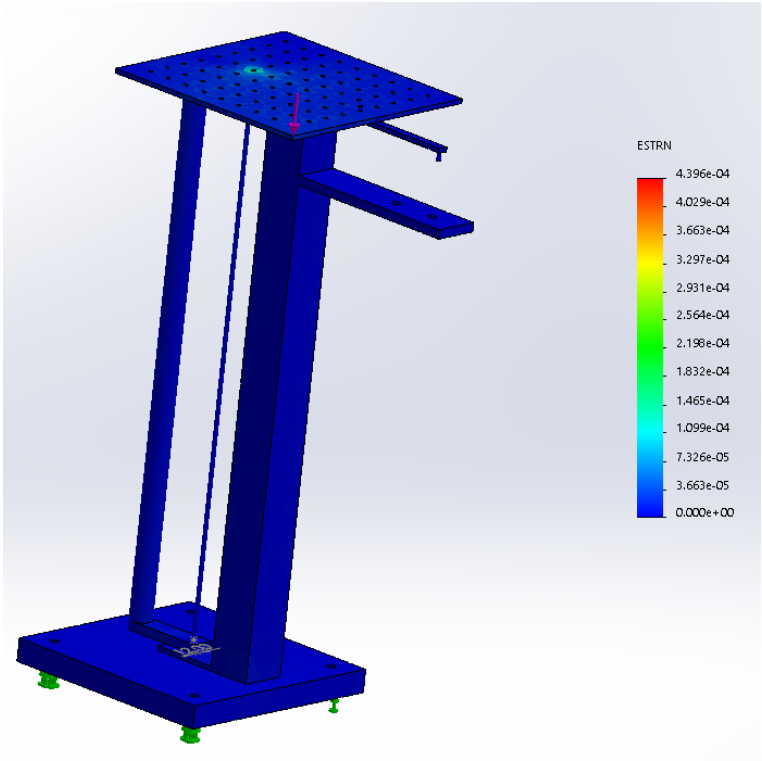

Figure B.32: Strain simulation

APPENDIX C. BASE ANALYSIS AND VALIDATION TESTS PER SHAPE

The present appendix shows the simulations performed for the study of the chapter 7. Where in the following sections, we will show the behavior of the different base shapes in resonance, random vibration qualification and acceptance testing environments with the maximum possible deformation that our bases would experience in case of resonance, a displacement higher than 1mm will be considered as unacceptable as it would modify the parameters introduced in order to calculate inertia tensors and the pendulum would be unusable.

We will design the base shapes in such a way that the dimensions of the final 3D volumes of the different solids is similar with one compared with the others, and at the same time trying to occupy the smallest floor area, so that the total volume of the pendulum is minimized and optimized.

For each 2D sketch we will let superimposed the previous shown design, so at the fourth base we have all the 2D sketches superimposed. Each sketch will be extruded 5cm vertically to produce a 3D solid. Then, the solids will be emptied 1cm using the shell feature with uniform thickness so that the mass and material use is reduced, as done with the pendulum design chapter 3.

Chosen Base Dimensions per Shape

The dimensions chosen for each of the base shapes for the pendulum study are:

- Square shape (the one used in our pendulum):

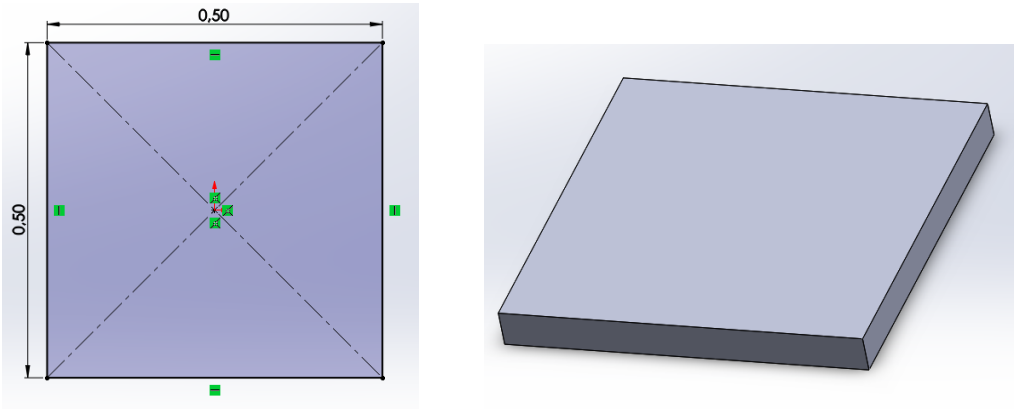

(a) 2D Sketch (b) 3D Extrude

Figure C.1: Square shape

- Round shape:

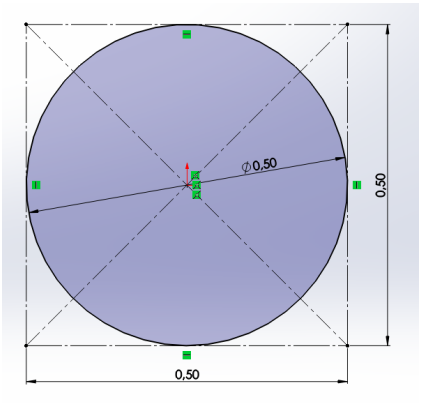

(a) 2D Sketch

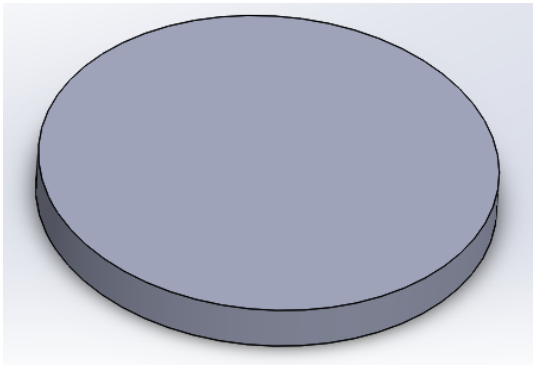

(b) 3D Extrude

Figure C.2: Round shape

- Hexagon shape:

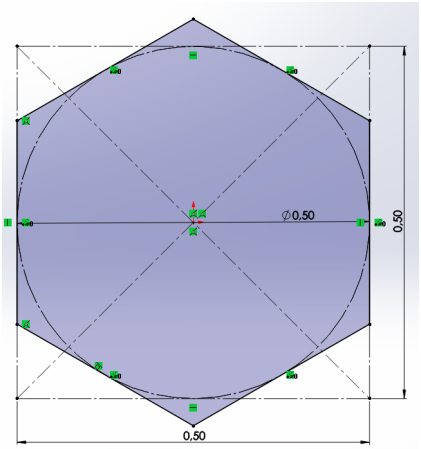

(a) 2D Sketch

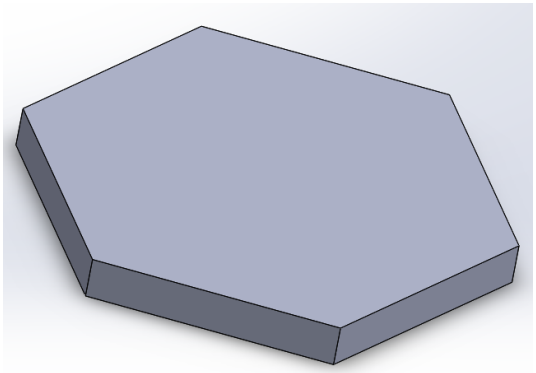

(b) 3D Extrude

Figure C.3: Hexagon shape

- Triangular shape:

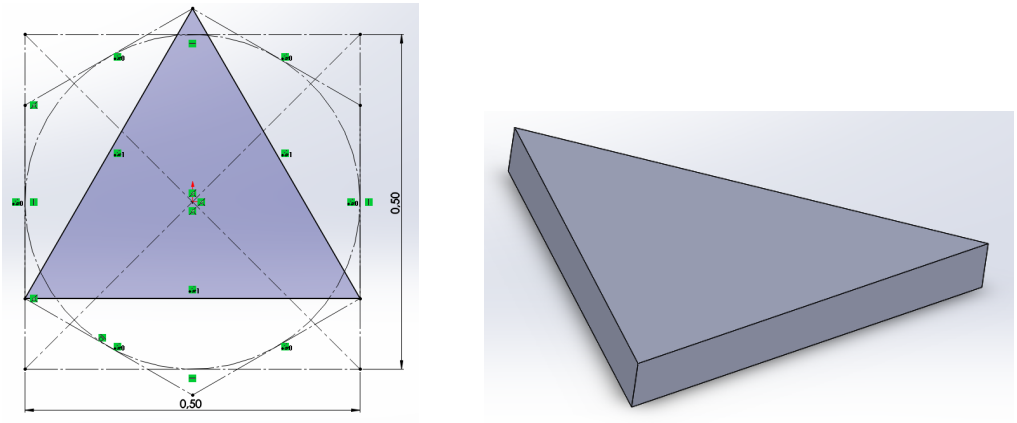

(a) 2D Sketch (b) 3D Extrude

Figure C.4: Triangular shape

Therefore, the first values to be considered in the analysis are the different masses of the bases, which will be studied in the following table C.1.

Table C.1: Base masses per shape

Square	Triangular	Round	Hexagon
15.09	7.02	11.85	13.07

In order to check the bases resistance to random vibrations, frequency perturbations, resonance and stress we will perform two different studies with the SolidWorks simulation package.

C.0.0.1. Frequency Analysis

Frequency analysis is the starting point for dynamic analysis. The analysis induce natural frequencies in five different modes of possible frequency perturbations to the different 3D bases. With the objective to check how the base of the pendulum would perform in reality and if induced vibrations or frequencies of the environment, in which the physic pendulum could be working, could modify the calculations of the tensor of inertia by means of introducing noise. It is studied in the following table C.2:

Table C.2: Resonant frequencies (Hz)

Mode	Square	Triangular	Round	Hexagon
1	359.69	966.45	399.83	377.91
2	719.83	1809.6	802.69	765.14
3	720.47	1814.1	805.04	766.52
4	1081	2860.5	1350.1	1268
5	1296	2999.5	1352	1269.6

As we can observe, all the natural frequencies are very high and they won't be a problem for our pendulum.

C.0.0.2. Random Vibration Analysis

The random vibration environment is expressed as a power spectral density (PSD) or acceleration spectral density in g^2/Hz. Looking at our resonant frequencies we will perform an analysis over a minimum frequency range from 20 to 6500Hz, in order to include all the resonant frequencies values in the study.

The curve of frequencies follows the following shape:

To perform the analysis SolidWorks asks us to introduce the phenomenon called damping. Damping is related with dynamics systems, in order to simulate the random vibration analysis as we are applying a complex phenomenon that dissipates energy by many mechanisms, if we apply some initial conditions to a dynamic system, the system vibrates with decreasing amplitudes until it comes to rest, for example, we could consider the possibility that the pendulum was affected by near steps, table moves or even earthquakes.

We will simulate Rayleigh Damping with a symmetric damping matrix C that is formulated as a linear combination of the stiffness K and the mass M matrices. We will perform the analysis with the recommended values provided by SolidWorks for each matrix:

$$\left[C\right] = \alpha \cdot \left[M\right] + \beta \cdot \left[K\right] \tag{C.1}$$

Where:

(i) Alpha Coefficient: Sets the mass proportional coefficient α of value 0.02

(ii) Beta Coefficient: Sets the stiffness proportional coefficient β of value 0.04

The system of equations of motion for a linear n degree-of-freedom system excited by a random time varying force, which is applied from below and simulated by SolidWorks, is defined by the following equation:

$$f(t) = \left[M\right] \cdot \ddot{u}(t) + \left[C\right] \cdot \dot{u}(t) + \left[K\right] \cdot u(t) \tag{C.2}$$

C.0.0.3. Stress Analysis

Once performed the analysis of the previous subsection C.0.0.2. SolidWorks provide us with a curve that includes the maximum provided stress that the base would face.

The different simulations with the maximum stress acceptance (N/m^2) for each type of studied base are the following:

We should consider the maximum predicted stress under the yield limit, which depends of the % of carbon in the cast alloy steel, in which depending of carbon percentage (always below the 0.75%) varies from 270 to 460 MPa, ensuring that in the worse possible imaginable conditions (earthquake) the structure will not experience permanent (plastic) deformation or even rupture. Therefore, we will simulate a power spectral density (PSD) acceleration of 1 g^2/Hz from the floor to all the bases

- Square shape

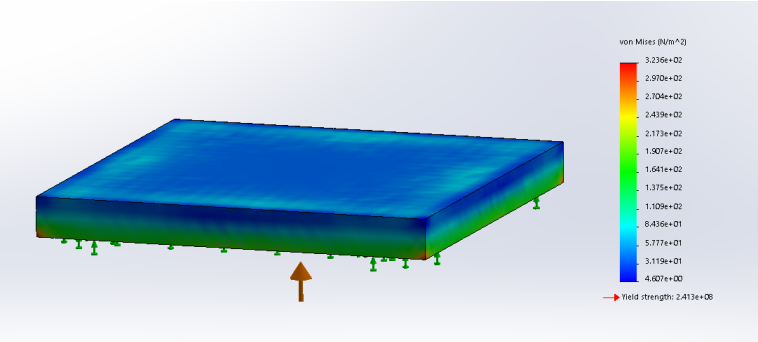

Figure C.5: Square shape maximum predicted stress

- Triangular shape

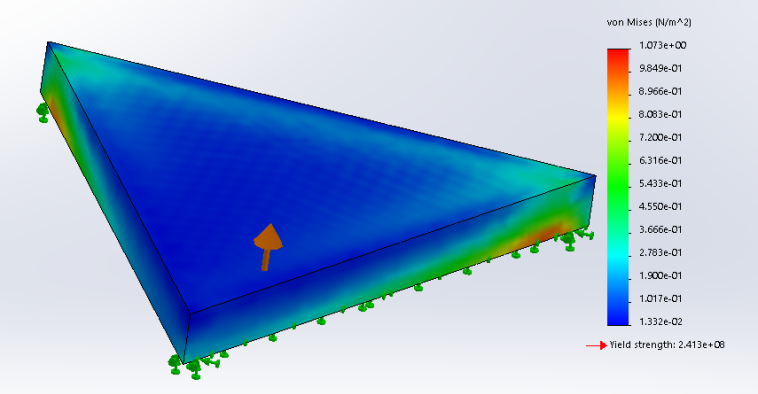

Figure C.6: Triangular shape maximum predicted stress

- Round shape

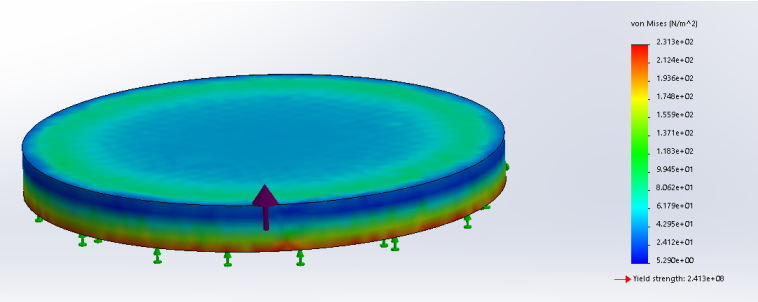

Figure C.7: Round shape maximum predicted stress

- Hexagon shape

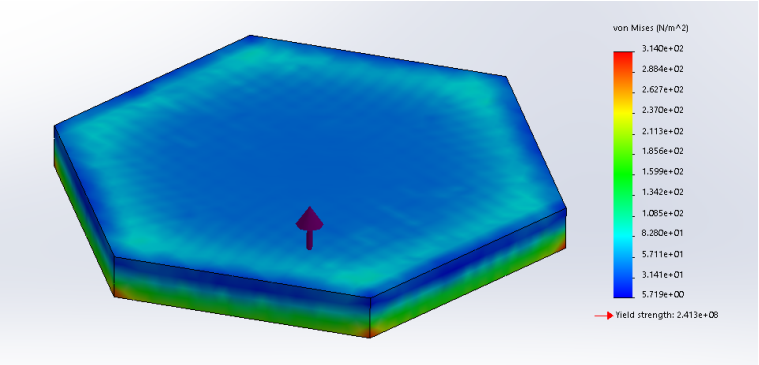

Figure C.8: Hexagon shape maximum predicted stress